كلية الهندسة- جامعة القاهرة
قسم هندسة القوى الميكانيكية
معمل التحكم الأوتوماتيكى

ACC Virtual Labs
Automatic Control Circuits &Virtual Labs
for Mechanical Power Systems
معمل التحكم الأوتوماتيكى و المعامل الإفتراضية لأنظمة القوى الميكانيكية

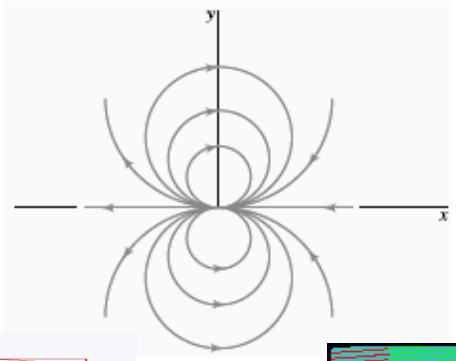

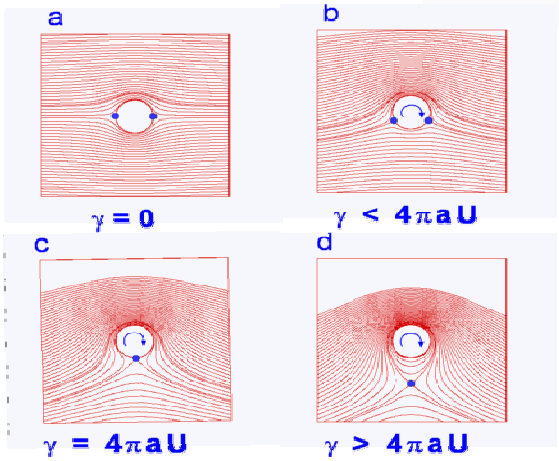

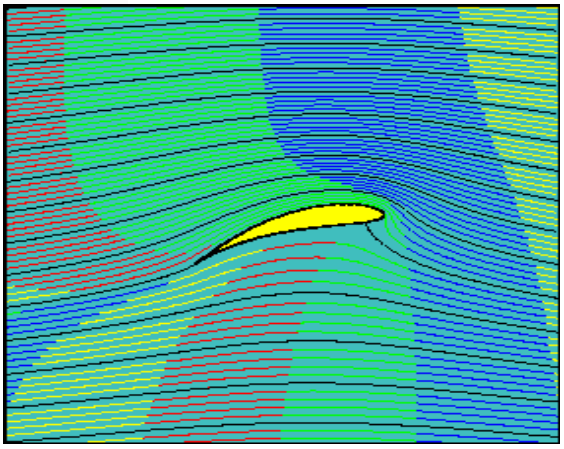

Notes on the course

Fluid Mechanics (3) - MEP 303A

For THRID YEAR MECHANICS (POWER)

Part (3)

Frictionless Incompressible Flow

Compiled and Edited by

Dr. Mohsen Soliman

2017/2018

Table of Contents of Part (3)

Part (3)*

Frictionless Incompressible Flow

Why Do we Study Frictionless Flow?:

The effect of viscosity can be neglected in many parts of most real viscous flow fields especially for external flow fields. It was found that viscous effects are important only near any solid boundaries in a small thin layer called the boundary layer.

3.1 Introduction and Review:

The purposes of the present chapter are:(1) to explore more examples of potential theory and (2) to indicate some flows which can be approximated by computational fluid dynamics (CFD). The combination of these two gives us a good picture of incompressible-flow theory and its relation to experiment. One of the most important applications of potential-flow theory is to aerodynamics and marine hydrodynamics. First, however, we will review and extend the concepts of frictionless flow given in Part 1.

Figure 3.1 reminds us of the problems to be faced. A free stream approaches two closely spaced bodies, creating an "internal" flow between them and "external" flows above and below them. The fronts of the bodies are regions of favorable gradient (decreasing pressure along the surface), and the boundary layers will be attached and thin: Inviscid theory will give excellent results for the outer flow if $Re > 10^4$. For the internal flow between bodies, the boundary layers will grow and eventually meet, and the inviscid core vanishes. Inviscid theory works well in a "short" duct $L/D < 10$, such as the nozzle of a wind tunnel. For longer ducts we must estimate boundary-layer growth and be cautious about using inviscid theory.

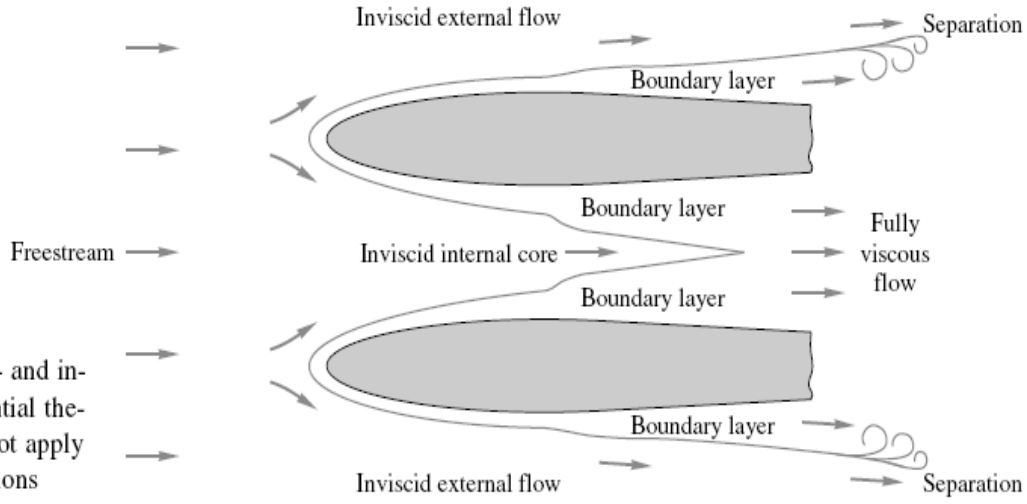

Fig. 3.1 Patching viscous- and inviscid-flow regions. Potential theory in this chapter does not apply to the boundary-layer regions

For the external flows above and below the bodies in Fig. 3.1, inviscid theory should work well for the outer flows, until the surface pressure gradient becomes adverse (increasing pressure) and the boundary layer separates or stalls. After the separation point, boundary-layer theory becomes inaccurate, and the outer flow streamlines are deflected and have a strong interaction with the viscous near-wall regions. The theoretical analysis of separated-flow regions is an active research area at present.

* Ref.:(1) Bruce R. Munson, Donald F. Young, Theodore H. Okiishi "Fundamental of Fluid Mechanics" 4th ed., John Wiley & Sons, Inc., 2002.
(2) Frank M. White "Fluid Mechanics", 4th ed. McGraw Hill, 2002.

3.1.1 Conservation of Mass:

From Part (1) we found the differential form of the mass conservation equation:

$$\frac{\partial \rho}{\partial t} + \frac{\partial (\rho u)}{\partial x} + \frac{\partial (\rho v)}{\partial y} + \frac{\partial (\rho w)}{\partial z} = 0 \qquad (3.1)$$

As previously mentioned, this equation is also commonly referred to as the continuity equation.

The continuity equation is one of the fundamental equations of fluid mechanics and, as expressed in Eq. 3.1 , is valid for steady or unsteady flow, and compressible or incompressible fluids. In vector notation, Eq. 3.1 can be written as

$$\frac{\partial \rho}{\partial t} + \nabla \cdot \rho \mathbf{V} = 0 \qquad (3.2)$$

Two special cases are of particular interest. For *steady* flow of *compressible* fluids

$$\nabla \cdot \rho \mathbf{V} = 0$$

$$\frac{\partial (\rho u)}{\partial x} + \frac{\partial (\rho v)}{\partial y} + \frac{\partial (\rho w)}{\partial z} = 0 \qquad (3.3)$$

This follows since by definition ρ is not a function of time for steady flow, but could be a function of position. For *incompressible* fluids the fluid density, ρ, is a constant throughout the flow field so that Eq. 3.2 becomes

$$\nabla \cdot \mathbf{V} = 0 \qquad (3.4)$$

or

$$\frac{\partial u}{\partial x} + \frac{\partial v}{\partial y} + \frac{\partial w}{\partial z} = 0 \qquad (3.5)$$

Equation 3.5 applies to both steady and unsteady flow of incompressible fluids. Note that Eq. 3.5 is the same as that obtained by setting the volumetric dilatation rate (Eq. 1.9) equal to zero. This result should not be surprising since both relationships are based on conservation of mass for incompressible fluids. However, the expression for the volumetric dilation rate was developed from a system approach, whereas Eq. 3.5 was developed from a control volume approach. In the former case the deformation of a particular differential mass of fluid was studied, and in the latter case mass flow through a fixed differential volume was studied.

The differential form of the continuity equation in cylindrical coordinates is

$$\frac{\partial \rho}{\partial t} + \frac{1}{r}\frac{\partial (r \rho v_r)}{\partial r} + \frac{1}{r}\frac{\partial (\rho v_\theta)}{\partial \theta} + \frac{\partial (\rho v_z)}{\partial z} = 0 \qquad (3.6)$$

This equation can be derived by following the same procedure used in the preceding section (see **Problem** 1.17). For steady, compressible flow

$$\frac{1}{r}\frac{\partial (r \rho v_r)}{\partial r} + \frac{1}{r}\frac{\partial (\rho v_\theta)}{\partial \theta} + \frac{\partial (\rho v_z)}{\partial z} = 0 \qquad (3.7)$$

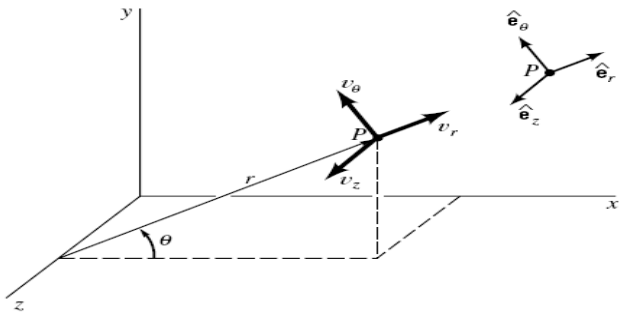

■ FIGURE 3.2 **The representation of velocity components in cylindrical polar coordinates.**

For incompressible fluids (for steady or unsteady flow)

$$\frac{1}{r}\frac{\partial(rv_r)}{\partial r} + \frac{1}{r}\frac{\partial v_\theta}{\partial \theta} + \frac{\partial v_z}{\partial z} = 0 \qquad (3.8)$$

3.1.2 Stream Function:

Also from Part (1) we defined the stream function, ψ, for 2-D flow only as:

The *stream function* ψ is a clever device which allows us to wipe out the continuity equation and solve the momentum equation directly for the single variable ψ.

The stream-function idea works only if the continuity equation (3.1) can be reduced to *two* terms. In general, we have *four* terms:

Cartesian:
$$\frac{\partial \rho}{\partial t} + \frac{\partial}{\partial x}(\rho u) + \frac{\partial}{\partial y}(\rho v) + \frac{\partial}{\partial z}(\rho w) = 0 \qquad (3.9\,a)$$

Cylindrical:
$$\frac{\partial \rho}{\partial t} + \frac{1}{r}\frac{\partial}{\partial r}(r\rho v_r) + \frac{1}{r}\frac{\partial}{\partial \theta}(\rho v_\theta) + \frac{\partial}{\partial z}(\rho v_z) = 0 \qquad (3.9\,b)$$

First, let us eliminate unsteady flow, which is a peculiar and unrealistic application of the stream-function idea. Reduce either of Eqs. (3.9) to any *two* terms. The most common application is incompressible flow in the xy plane

$$\frac{\partial u}{\partial x} + \frac{\partial v}{\partial y} = 0 \qquad (3.10)$$

This equation is satisfied *identically* if a function $\psi(x, y)$ is defined such that Eq. (3.10) becomes

$$\frac{\partial}{\partial x}\left(\frac{\partial \psi}{\partial y}\right) + \frac{\partial}{\partial y}\left(-\frac{\partial \psi}{\partial x}\right) \equiv 0 \qquad (3.11)$$

Comparison of (3.10) and (3.11) shows that this new function ψ must be defined such that

$$u = \frac{\partial \psi}{\partial y} \qquad v = -\frac{\partial \psi}{\partial x} \qquad (3.12)$$

or
$$\mathbf{V} = \mathbf{i}\frac{\partial \psi}{\partial y} - \mathbf{j}\frac{\partial \psi}{\partial x}$$

Is this legitimate? Yes, it is just a mathematical trick of replacing two variables (u and v) by a single higher-order function ψ. The vorticity, or curl $\mathbf{V}$, is an interesting function

$$\text{curl } \mathbf{V} = 2\mathbf{k}\omega_z = -\mathbf{k}\nabla^2\psi \qquad \text{where} \qquad \nabla^2\psi = \frac{\partial^2 \psi}{\partial x^2} + \frac{\partial^2 \psi}{\partial y^2} \qquad (3.13)$$

If we recall that the linear momentum equation is:

Momentum:
$$\rho\frac{d\mathbf{V}}{dt} = \rho\mathbf{g} - \nabla p + \mu\nabla^2\mathbf{V} \qquad (3.14)$$

Thus, if we take the curl of the momentum equation (3.14) and utilize Eq. (3.13), we obtain a single equation for ψ

$$\frac{\partial \psi}{\partial y}\frac{\partial}{\partial x}(\nabla^2\psi) - \frac{\partial \psi}{\partial x}\frac{\partial}{\partial y}(\nabla^2\psi) = \nu\nabla^2(\nabla^2\psi) \qquad (3.15)$$

where $\nu = \mu/\rho$ is the kinematic viscosity. This is partly a victory and partly a defeat: Eq. (3.15) is scalar and has only one variable, ψ, but it now contains *fourth*-order derivatives and probably will require computer analysis. There will be four boundary conditions required on ψ. For example, for the flow of a uniform stream in the x direction past a solid body, the four conditions would be

At infinity:
$$\frac{\partial \psi}{\partial y} = U_\infty \qquad \frac{\partial \psi}{\partial x} = 0$$

At the body:
$$\frac{\partial \psi}{\partial y} = \frac{\partial \psi}{\partial x} = 0 \qquad (3.16)$$

Many examples of numerical solution of Eqs. (3.15) and (3.16) are given in Ref. 1.

One important application is inviscid *irrotational* flow in the xy plane, where $\omega_z \equiv 0$. Equations (3.13) and (3.15) reduce to

$$\nabla^2 \psi = \frac{\partial^2 \psi}{\partial x^2} + \frac{\partial^2 \psi}{\partial y^2} = 0 \tag{3.17}$$

This is the second-order *Laplace equation* , for which many solutions and analytical techniques are known. Also, boundary conditions like Eq. (3.16) reduce to

At infinity: $$\psi = U_\infty y + \text{const} \tag{3.18}$$

At the body: $$\psi = \text{const}$$

It is well within our capability to find some useful solutions to Eqs. (3.17) and (3.18), which we shall do in the solved numerical examples given later.

3.1.3 The Geometric Meaning of ψ:

The fancy mathematics above would serve by itself to make the stream function immortal and always useful to engineers. Even better, though, ψ has a beautiful geometric interpretation: Lines of constant ψ are *streamlines* of the flow. This can be shown as follows. From the definition of a streamline in two-dimensional flow is

$$\frac{dx}{u} = \frac{dy}{v}$$

or $$u\,dy - v\,dx = 0 \qquad \text{streamline} \tag{3.19}$$

Introducing the stream function from Eq. (3.12), we have

$$\frac{\partial \psi}{\partial x}\,dx + \frac{\partial \psi}{\partial y}\,dy = 0 = d\psi \tag{3.20}$$

Thus the change in ψ is zero along a streamline, or

$$\psi = \text{const along a streamline} \tag{3.21}$$

Having found a given solution $\psi(x, y)$, we can plot lines of constant ψ to give the streamlines of the flow.

There is also a physical interpretation which relates ψ to volume flow. From Fig. 3.3, we can compute the volume flow dQ through an element ds of control surface of unit depth

$$dQ = (\mathbf{V} \cdot \mathbf{n})\,dA = \left(\mathbf{i}\frac{\partial \psi}{\partial y} - \mathbf{j}\frac{\partial \psi}{\partial x}\right) \cdot \left(\mathbf{i}\frac{dy}{ds} - \mathbf{j}\frac{dx}{ds}\right) ds(1)$$

$$= \frac{\partial \psi}{\partial x}\,dx + \frac{\partial \psi}{\partial y}\,dy = d\psi \tag{3.22}$$

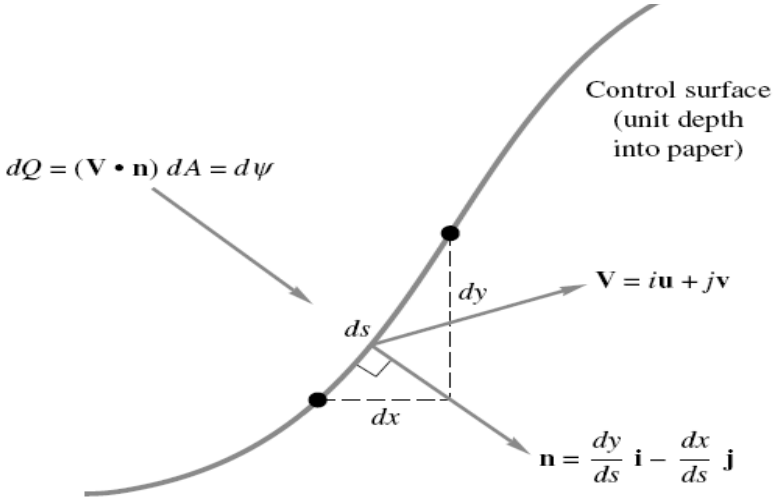

Fig. 3.3 Geometric interpretation of stream function: volume flow through a differential portion of a control surface.

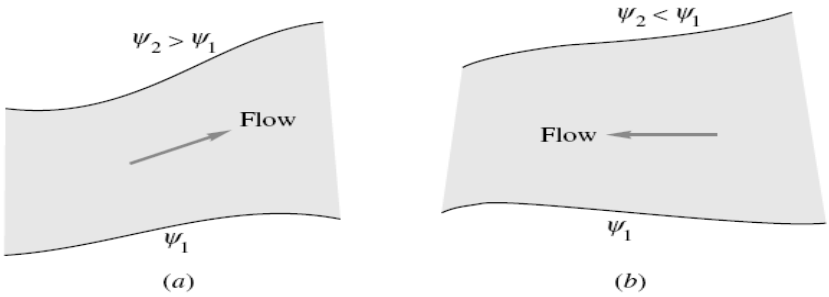

Fig. 3.4 Sign convention for flow in terms of change in stream function: (*a*) flow to the right if ψ_U is greater; (*b*) flow to the left if ψ_L is greater.

Thus the change in ψ across the element is numerically equal to the volume flow through the element. The volume flow between any two points in the flow field is equal to the change in stream function between those points:

$$Q_{1\to 2} = \int_1^2 (\mathbf{V} \cdot \mathbf{n})\, dA = \int_1^2 d\psi = \psi_2 - \psi_1 \qquad (3.23)$$

Further, the direction of the flow can be ascertained by noting whether ψ increases or decreases. As sketched in Fig. 3.4, the flow is to the right if ψ_U is greater than ψ_L, where the subscripts stand for upper and lower, as before; otherwise the flow is to the left.

Both the stream function and the velocity potential were invented by the French mathematician Joseph Louis Lagrange and published in his treatise on fluid mechanics in 1781.

Example 3.1:

If a stream function exists for the velocity field

$$u = a(x^2 - y^2) \quad v = -2axy \quad w = 0$$

find it, plot it, and interpret it.

Solution

Since this flow field was shown expressly to satisfy the equation of continuity, we are pretty sure that a stream function does exist. We can check again to see if

$$\frac{\partial u}{\partial x} + \frac{\partial v}{\partial y} = 0$$

Substitute: $2ax + (-2ax) = 0$ checks

Therefore we are certain that a stream function exists. To find ψ, we simply set

$$u = \frac{\partial \psi}{\partial y} = ax^2 - ay^2 \qquad (1)$$

$$v = -\frac{\partial \psi}{\partial x} = -2axy \qquad (2)$$

and work from either one toward the other. Integrate (1) partially

$$\psi = ax^2y - \frac{ay^3}{3} + f(x) \qquad (3)$$

Differentiate (3) with respect to x and compare with (2)

$$\frac{\partial \psi}{\partial x} = 2axy + f'(x) = 2axy \qquad (4)$$

Therefore $f'(x) = 0$, or $f =$ constant. The complete stream function is thus found

$$\psi = a\left(x^2y - \frac{y^3}{3}\right) + C \qquad Ans. \qquad (5)$$

To plot this, set $C = 0$ for convenience and plot the function

$$3x^2y - y^3 = \frac{3\psi}{a} \qquad (6)$$

for constant values of ψ. The result is shown in Fig. E3.1*a* to be six 60° wedges of circulating motion, each with identical flow patterns except for the arrows. Once the streamlines are labeled, the flow directions follow from the sign convention of Fig. 3.4. How can the flow be interpreted? Since there is slip along all streamlines, no streamline can truly represent a solid surface in a viscous flow. However, the flow could represent the impingement of three incoming streams at 60, 180, and 300°. This would be a rather unrealistic yet exact solution to the Navier-Stokes

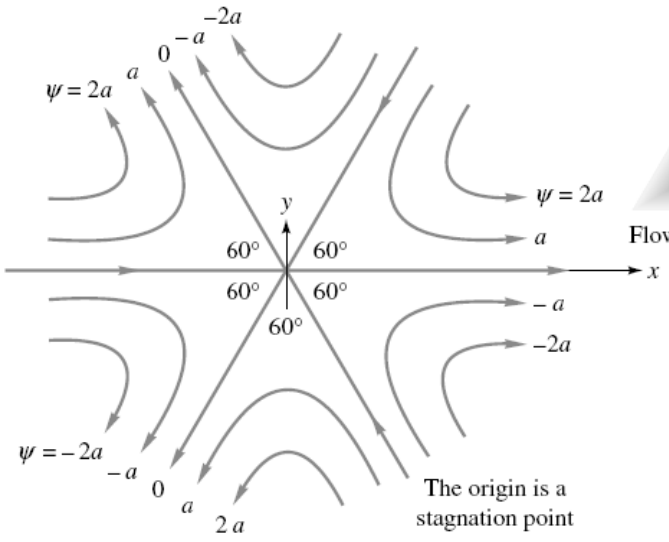

E 3.1a

Flow around a 60° corner

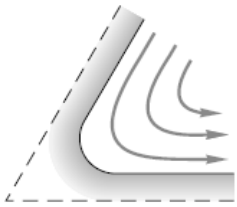

Flow around a rounded 60° corner

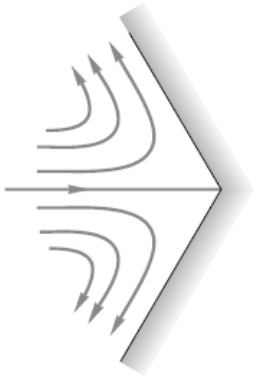

Incoming stream impinging against a 120° corner

E 3.1b

By allowing the flow to slip as a frictionless approximation, we could let any given streamline be a body shape. Some examples are shown in Fig. E3.1b

---

A stream function also exists in a variety of other physical situations where only two coordinates are needed to define the flow. Three examples are illustrated here.

Example 3.2:

The velocity components in a steady, incompressible, two-dimensional flow field are

$$u = 2y$$

$$v = 4x$$

Determine the corresponding stream function and show on a sketch several streamlines. Indicate the direction of flow along the streamlines.

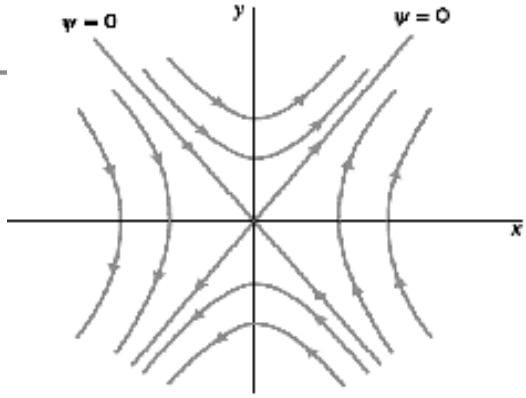

FIGURE E3.2

SOLUTION

From the definition of the stream function

$$u = \frac{\partial \psi}{\partial y} = 2y$$

and

$$v = -\frac{\partial \psi}{\partial x} = 4x$$

The first of these equations can be integrated to give

$$\psi = y^2 + f_1(x)$$

where $f_1(x)$ is an arbitrary function of x. Similarly from the second equation

$$\psi = -2x^2 + f_2(y)$$

where $f_2(y)$ is an arbitrary function of y. It now follows that in order to satisfy both expressions for the stream function

$$\psi = -2x^2 + y^2 + C \qquad \text{(Ans)}$$

where C is an arbitrary constant.

Since the velocities are related to the derivatives of the stream function, an arbitrary constant can always be added to the function, and the value of the constant is actually of no consequence. Usually, for simplicity, we set $C = 0$ so that for this particular example the simplest form for the stream function is

$$\psi = -2x^2 + y^2 \qquad \textbf{(1)} \quad \text{(Ans)}$$

Either answer indicated would be acceptable.

Streamlines can now be determined by setting ψ = constant and plotting the resulting curve. With the above expression for ψ (with $C = 0$) the value of ψ at the origin is zero so

that the equation of the streamline passing through the origin (the $\psi = 0$ streamline) is

$$0 = -2x^2 + y^2$$

or

$$y = \pm\sqrt{2}x$$

Other streamlines can be obtained by setting ψ equal to various constants. It follows from Eq. 1 that the equations of these streamlines (for $\psi \neq 0$) can be expressed in the form

$$\frac{y^2}{\psi} - \frac{x^2}{\psi/2} = 1$$

which we recognize as the equation of a hyperbola. Thus, the streamlines are a family of hyperbolas with the $\psi = 0$ streamlines as asymptotes. Several of the streamlines are plotted in Fig. E3.2. Since the velocities can be calculated at any point, the direction of flow along a given streamline can be easily deduced. For example, $v = -\partial\psi/\partial x = 4x$ so that $v > 0$ if $x > 0$ and $v < 0$ if $x < 0$. The direction of flow is indicated on the figure.

3.1.4 Stream function for Steady Plane Compressible Flow:

Suppose now that the density is variable but that $w = 0$, so that the flow is in the xy plane. Then the equation of continuity becomes

$$\frac{\partial}{\partial x}(\rho u) + \frac{\partial}{\partial y}(\rho v) = 0 \qquad (3.24)$$

We see that this is in exactly the same form as Eq. (3.11). Therefore a compressible-flow stream function can be defined such that

$$\rho u = \frac{\partial \psi}{\partial y} \qquad \rho v = -\frac{\partial \psi}{\partial x} \qquad (3.25)$$

Again lines of constant ψ are streamlines of the flow, but the change in ψ is now equal to the *mass* flow, not the volume flow

$$d\dot{m} = \rho(\mathbf{V} \cdot \mathbf{n})\, dA = d\psi$$

or

$$\dot{m}_{1\to 2} = \int_1^2 \rho(\mathbf{V} \cdot \mathbf{n})\, dA = \psi_2 - \psi_1 \qquad (3.26)$$

The sign convention on flow direction is the same as in Fig. 3.4. This particular stream function combines density with velocity and must be substituted into not only momentum but also the energy and state relations as given in part 1 with pressure and temperature as companion variables. Thus the compressible stream function is not a great victory, and further assumptions must be made to effect an analytical solution to a typical problem (see, e.g., Ref. 5).

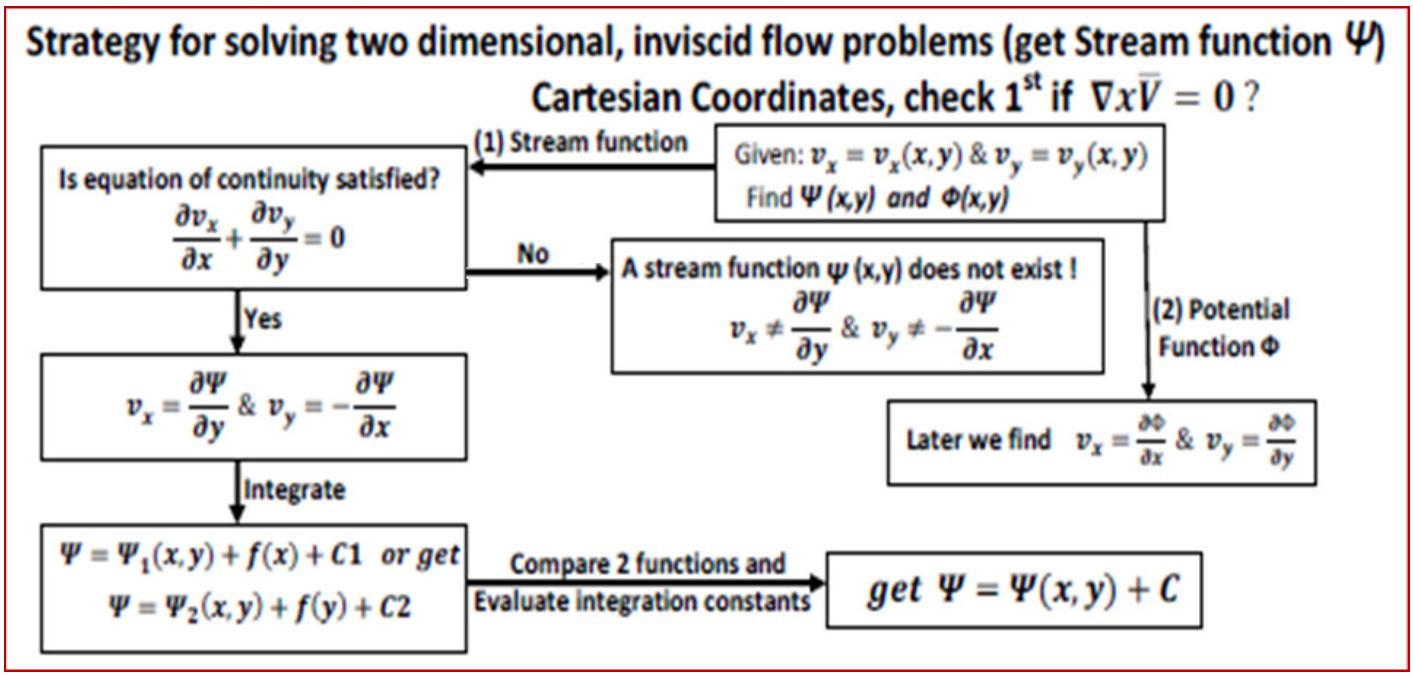

3.1.5 Stream function for Incompressible Plane Flow in Polar Coordinates:

Suppose that the important coordinates are r and θ, with $v_z = 0$, and that the density is constant. Then Eq. (3.9 b) reduces to

$$\frac{1}{r}\frac{\partial}{\partial r}(rv_r) + \frac{1}{r}\frac{\partial}{\partial \theta}(v_\theta) = 0 \qquad (3.27)$$

After multiplying through by r, we see that this is the same as the analogous form of Eq. (3.11)

$$\frac{\partial}{\partial r}\left(\frac{\partial \psi}{\partial \theta}\right) + \frac{\partial}{\partial \theta}\left(-\frac{\partial \psi}{\partial r}\right) = 0 \qquad (3.28)$$

By comparison of (3.27) and (3.28) we deduce the form of the incompressible polar-coordinate stream function

$$v_r = \frac{1}{r}\frac{\partial \psi}{\partial \theta} \qquad v_\theta = -\frac{\partial \psi}{\partial r} \qquad (3.29)$$

Once again lines of constant ψ are streamlines, and the change in ψ is the *volume flow* $Q_{1\to 2} = \psi_2 - \psi_1$. The sign convention is the same as in Fig. 3.4 . This type of stream function is very useful in analyzing flows with cylinders, vortices, sources, and sinks (as shown later).

3.1.6 Stream function for Incompressible Axisymmetric Flow:

As a final example, suppose that the flow is three-dimensional (v_r, v_z) but with no circumferential variations, $v_\theta = \partial/\partial\theta = 0$ (see Fig. 3.2 for definition of coordinates). Such a flow is termed *axisymmetric*, and the flow pattern is the same when viewed on any meridional plane through the axis of revolution z. For incompressible flow, Eq. (3.9 b) becomes

$$\frac{1}{r}\frac{\partial}{\partial r}(rv_r) + \frac{\partial}{\partial z}(v_z) = 0 \qquad (3.30)$$

This doesn't seem to work: Can't we get rid of the one r outside? But when we realize that r and z are independent coordinates, Eq. (3.30) can be rewritten as

$$\frac{\partial}{\partial r}(rv_r) + \frac{\partial}{\partial z}(rv_z) = 0 \qquad (3.31)$$

By analogy with Eq. (3.11), this has the form

$$\frac{\partial}{\partial r}\left(-\frac{\partial \psi}{\partial z}\right) + \frac{\partial}{\partial z}\left(\frac{\partial \psi}{\partial r}\right) = 0 \qquad (3.32)$$

By comparing (3.31) and (3.32), we deduce the form of an incompressible axisymmetric stream function $\psi(r, z)$

$$v_r = -\frac{1}{r}\frac{\partial \psi}{\partial z} \qquad v_z = \frac{1}{r}\frac{\partial \psi}{\partial r} \qquad (3.33)$$

Here again lines of constant ψ are streamlines, but there is a factor (2π) in the volume flow: $Q_{1\to 2} = 2\pi(\psi_2 - \psi_1)$. The sign convention on flow is the same as in Fig. 3.4 .

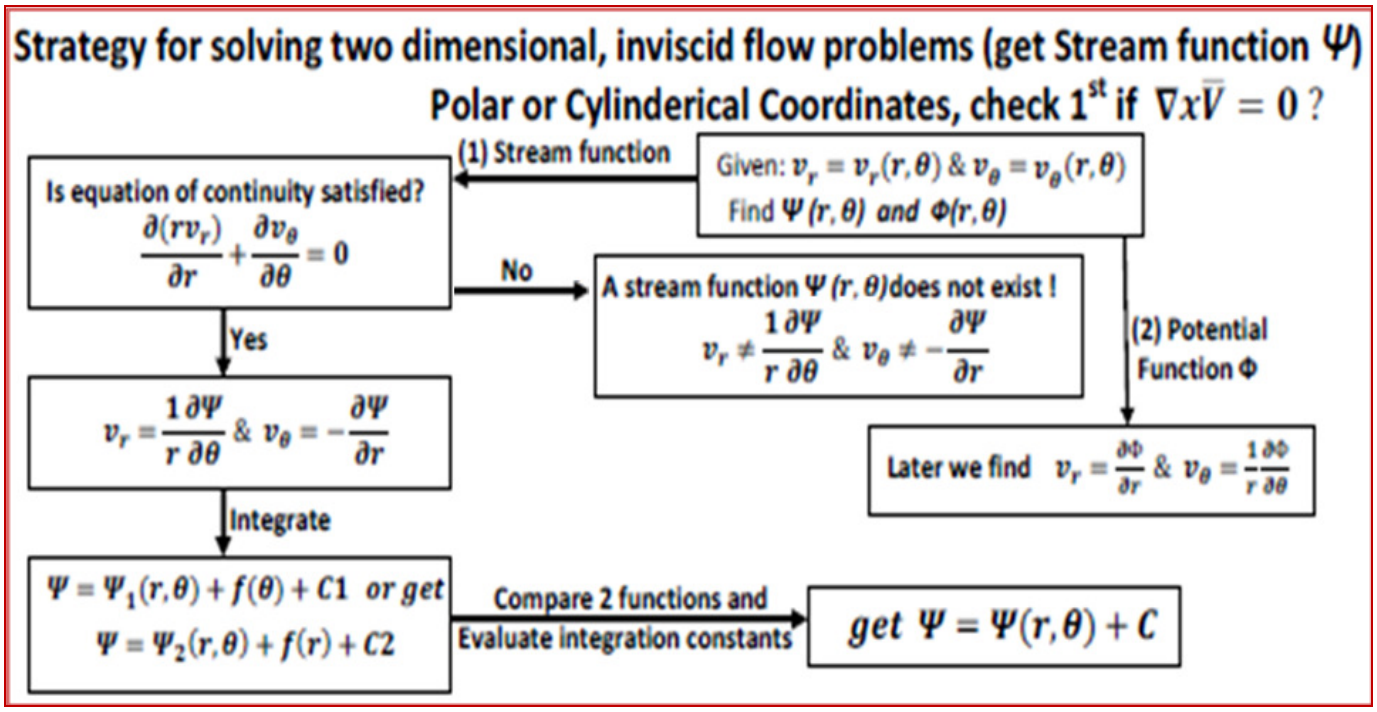

Example 3.3:

Investigate the stream function in polar coordinates

$$\psi = U \sin\theta\left(r - \frac{R^2}{r}\right) \tag{1}$$

where U and R are constants, a velocity and a length, respectively. Plot the streamlines. What does the flow represent? Is it a realistic solution to the basic equations?

Solution

The streamlines are lines of constant ψ, which has units of square meters per second. Note that $\psi/(UR)$ is dimensionless. Rewrite Eq. (1) in dimensionless form

$$\frac{\psi}{UR} = \sin\theta\left(\eta - \frac{1}{\eta}\right) \qquad \eta = \frac{r}{R} \tag{2}$$

Of particular interest is the special line $\psi = 0$. From Eq. (1) or (2) this occurs when (a) $\theta = 0$ or 180° and (b) $r = R$. Case (a) is the x-axis, and case (b) is a circle of radius R, both of which are plotted in Fig. E3.3.

For any other nonzero value of ψ it is easiest to pick a value of r and solve for θ:

$$\sin\theta = \frac{\psi/(UR)}{r/R - R/r} \tag{3}$$

In general, there will be two solutions for θ because of the symmetry about the y-axis. For example take $\psi/(UR) = +1.0$:

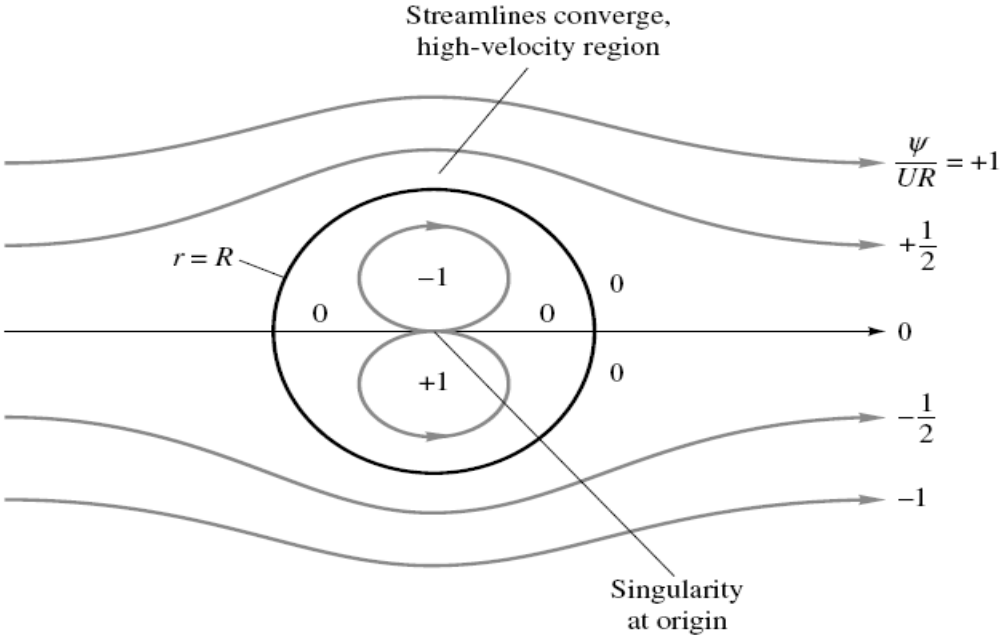

E 3.3

Guess r/R	3.0	2.5	2.0	1.8	1.7	1.618
Compute θ	22° 158°	28° 152°	42° 138°	54° 156°	64° 116°	90°

This line is plotted in Fig. E3.3 and passes over the circle $r = R$. You have to watch it, though, because there is a second curve for $\psi/(UR) = +1.0$ for small $r < R$ below the x-axis:

Guess r/R	0.618	0.6	0.5	0.4	0.3	0.2	0.1
Compute θ	−90°	−70° −110°	−42° −138°	−28° −152°	−19° −161°	−12° −168°	−6° −174°

This second curve plots as a closed curve inside the circle $r = R$. There is a singularity of infinite velocity and indeterminate flow direction at the origin. Figure E3.3 shows the full pattern.

The given stream function, Eq. (1), is an exact and classic solution to the momentum equation for frictionless flow. Outside the circle $r = R$ it represents two-dimensional inviscid flow of a uniform stream past a circular cylinder . Inside the circle it represents a rather unrealistic trapped circulating motion of what is called a *line doublet*.

3.1.7 Graphical Superposition of Stream Functions of Plane Flows:

We can now form a variety of interesting potential flows by summing the velocity-potential and stream functions of a uniform stream, source or sink, and vortex. Most of the results are classic, of course, needing only a brief treatment here.

A simple means of accomplishing $\psi_{tot} = \sum \psi_i$ graphically is to plot the individual stream functions separately and then look at their intersections. The value of ψ_{tot} at each intersection is the sum of the individual values ψ_i which cross there. Connecting intersections with the same value of ψ_{tot} creates the desired superimposed flow streamlines.

A simple example is shown in Fig. 3.5 , summing two families of streamlines ψ_a and ψ_b. The individual components are plotted separately, and four typical intersections are shown. Dashed lines are then drawn through intersections representing the same sum of $\psi_a + \psi_b$. These dashed lines are the desired solution. Often this graphical method is a quick means of evaluating the proposed superposition before a full-blown numerical plot routine is executed.

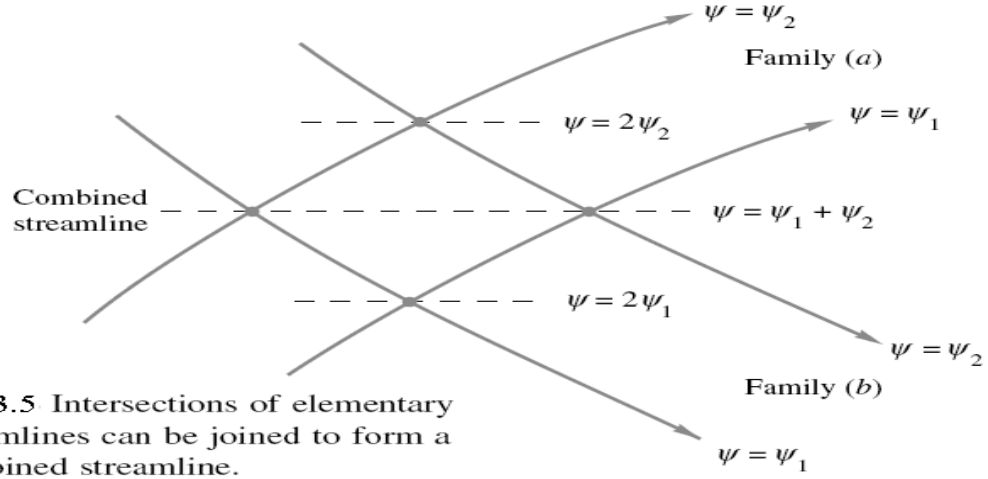

Fig. 3.5 Intersections of elementary streamlines can be joined to form a combined streamline.

3.1.8 Vorticity and Irrotationality:

The assumption of zero fluid angular velocity, or irrotationality, is a very useful simplification. Here we show that angular velocity is associated with the curl of the local-velocity vector.

The differential relations for deformation of a fluid element can be derived by examining Fig. 3.6 . Two fluid lines AB and BC, initially perpendicular at time t, move and deform so that at $t + dt$ they have slightly different lengths $A'B'$ and $B'C'$ and are slightly off the perpendicular by angles $d\alpha$ and $d\beta$. Such deformation occurs kinematically because A, B, and C have slightly different velocities when the velocity field $\mathbf{V}$

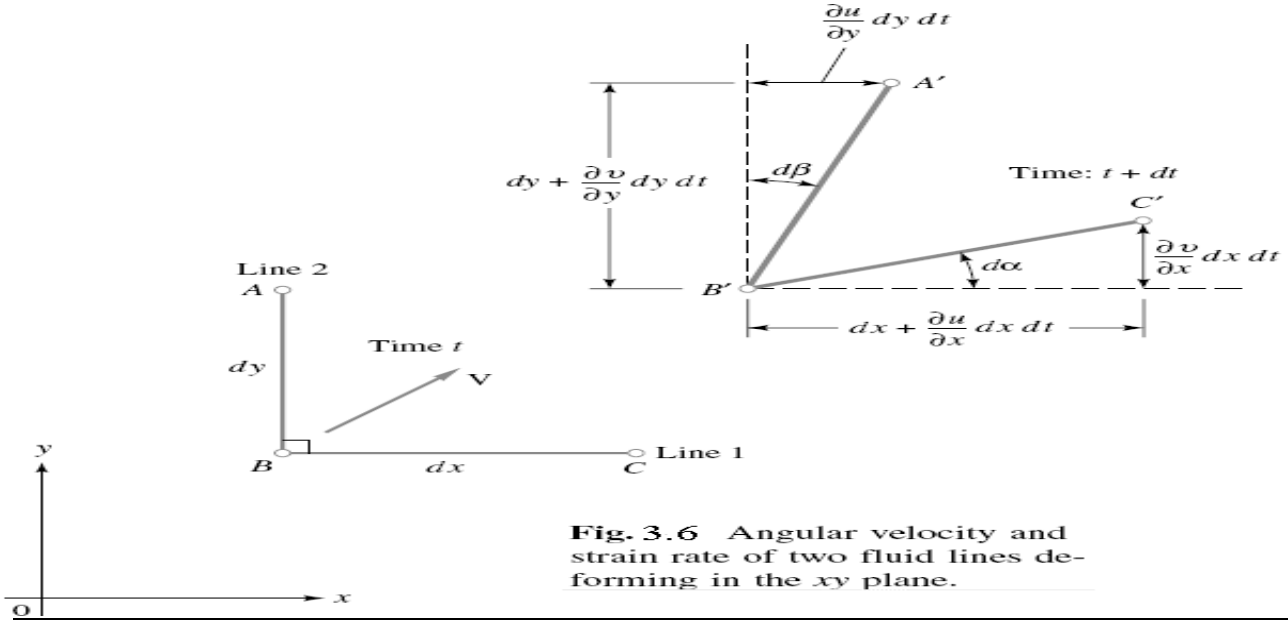

Fig. 3.6 Angular velocity and strain rate of two fluid lines deforming in the xy plane.

has spatial gradients. All these differential changes in the motion of A, B, and C are noted in Fig. 3.6 .

We define the angular velocity ω_z about the z axis as the average rate of counter-clockwise turning of the two lines

$$\omega_z = \frac{1}{2}\left(\frac{d\alpha}{dt} - \frac{d\beta}{dt}\right) \qquad (3.34)$$

But from Fig. 3.6 , $d\alpha$ and $d\beta$ are each directly related to velocity derivatives in the limit of small dt

$$d\alpha = \lim_{dt\to 0}\left[\tan^{-1}\frac{(\partial v/\partial x)\,dx\,dt}{dx + (\partial u/\partial x)\,dx\,dt}\right] = \frac{\partial v}{\partial x}\,dt$$
$$d\beta = \lim_{dt\to 0}\left[\tan^{-1}\frac{(\partial u/\partial y)\,dy\,dt}{dy + (\partial v/\partial y)\,dy\,dt}\right] = \frac{\partial u}{\partial y}\,dt \qquad (3.35)$$

Combining Eqs. (3.34) and (3.35) gives the desired result:

$$\omega_z = \frac{1}{2}\left(\frac{\partial v}{\partial x} - \frac{\partial u}{\partial y}\right) \qquad (3.36)$$

In exactly similar manner we determine the other two rates:

$$\omega_x = \frac{1}{2}\left(\frac{\partial w}{\partial y} - \frac{\partial v}{\partial z}\right) \qquad \omega_y = \frac{1}{2}\left(\frac{\partial u}{\partial z} - \frac{\partial w}{\partial x}\right) \qquad (3.37)$$

The vector $\omega = \mathbf{i}\omega_x + \mathbf{j}\omega_y + \mathbf{k}\omega_z$ is thus one-half the curl of the velocity vector

$$\omega = \frac{1}{2}(\text{curl } \mathbf{V}) = \frac{1}{2}\begin{vmatrix} \mathbf{i} & \mathbf{j} & \mathbf{k} \\ \frac{\partial}{\partial x} & \frac{\partial}{\partial y} & \frac{\partial}{\partial z} \\ u & v & w \end{vmatrix} \qquad (3.38)$$

Since the factor of $\frac{1}{2}$ is annoying, many workers prefer to use a vector twice as large, called the *vorticity*:

$$\zeta = 2\omega = \text{curl } \mathbf{V} \qquad (3.39)$$

Many flows have negligible or zero vorticity and are called *irrotational*

$$\text{curl } \mathbf{V} \equiv 0 \qquad (3.40)$$

The next section expands on this idea. Such flows can be incompressible or compressible, steady or unsteady.

We may also note that Fig. 3.6 demonstrates the *shear-strain rate* of the element, which is defined as the rate of closure of the initially perpendicular lines

$$\dot{\epsilon}_{xy} = \frac{d\alpha}{dt} + \frac{d\beta}{dt} = \frac{\partial v}{\partial x} + \frac{\partial u}{\partial y} \qquad (3.41)$$

When multiplied by viscosity μ, this equals the shear stress τ_{xy} in a newtonian fluid,

3.2 Conservation of Linear Momentum (Navier-Stokes Equations):

Also from Part (1) we defined the Conservation of Linear Momentum as:

The basic differential momentum equation for an infinitesimal element

$$\rho\mathbf{g} - \nabla p + \nabla \cdot \tau_{ij} = \rho\,\frac{d\mathbf{V}}{dt} \qquad (3.42)$$

where
$$\frac{d\mathbf{V}}{dt} = \frac{\partial \mathbf{V}}{\partial t} + u\frac{\partial \mathbf{V}}{\partial x} + v\frac{\partial \mathbf{V}}{\partial y} + w\frac{\partial \mathbf{V}}{\partial z} \qquad (3.43)$$

We can also express Eq. (3.42) in words:

Gravity force per unit volume + pressure force per unit volume

+ viscous force per unit volume = density × acceleration (3.44)

Equation (3.42) is so brief and compact that its inherent complexity is almost invisible. It is a *vector* equation, each of whose component equations contains nine terms. Let us therefore write out the component equations in full to illustrate the mathematical difficulties inherent in the momentum equation:

$$\rho g_x - \frac{\partial p}{\partial x} + \frac{\partial \tau_{xx}}{\partial x} + \frac{\partial \tau_{yx}}{\partial y} + \frac{\partial \tau_{zx}}{\partial z} = \rho\left(\frac{\partial u}{\partial t} + u\frac{\partial u}{\partial x} + v\frac{\partial u}{\partial y} + w\frac{\partial u}{\partial z}\right)$$

$$\rho g_y - \frac{\partial p}{\partial y} + \frac{\partial \tau_{xy}}{\partial x} + \frac{\partial \tau_{yy}}{\partial y} + \frac{\partial \tau_{zy}}{\partial z} = \rho\left(\frac{\partial v}{\partial t} + u\frac{\partial v}{\partial x} + v\frac{\partial v}{\partial y} + w\frac{\partial v}{\partial z}\right) \qquad (3.45)$$

$$\rho g_z - \frac{\partial p}{\partial z} + \frac{\partial \tau_{xz}}{\partial x} + \frac{\partial \tau_{yz}}{\partial y} + \frac{\partial \tau_{zz}}{\partial z} = \rho\left(\frac{\partial w}{\partial t} + u\frac{\partial w}{\partial x} + v\frac{\partial w}{\partial y} + w\frac{\partial w}{\partial z}\right)$$

This is the differential momentum equation in its full glory, and it is valid for any fluid in any general motion, particular fluids being characterized by particular viscous-stress terms. Note that the last three "convective" terms on the right-hand side of each component equation in (3.45) are nonlinear, which complicates the general mathematical analysis.

The stresses as defined in the preceding section can be substituted into the differential equations of motion (Eqs. 3.45) and simplified by using the continuity equation (Eq. 3.5) to obtain (x direction):

$$\rho\left(\frac{\partial u}{\partial t} + u\frac{\partial u}{\partial x} + v\frac{\partial u}{\partial y} + w\frac{\partial u}{\partial z}\right) = -\frac{\partial p}{\partial x} + \rho g_x + \mu\left(\frac{\partial^2 u}{\partial x^2} + \frac{\partial^2 u}{\partial y^2} + \frac{\partial^2 u}{\partial z^2}\right) \qquad (3.46\ \mathbf{a})$$

(y direction)

$$\rho\left(\frac{\partial v}{\partial t} + u\frac{\partial v}{\partial x} + v\frac{\partial v}{\partial y} + w\frac{\partial v}{\partial z}\right) = -\frac{\partial p}{\partial y} + \rho g_y + \mu\left(\frac{\partial^2 v}{\partial x^2} + \frac{\partial^2 v}{\partial y^2} + \frac{\partial^2 v}{\partial z^2}\right) \qquad (3.46\ \mathbf{b})$$

(z direction)

$$\rho\left(\frac{\partial w}{\partial t} + u\frac{\partial w}{\partial x} + v\frac{\partial w}{\partial y} + w\frac{\partial w}{\partial z}\right) = -\frac{\partial p}{\partial z} + \rho g_z + \mu\left(\frac{\partial^2 w}{\partial x^2} + \frac{\partial^2 w}{\partial y^2} + \frac{\partial^2 w}{\partial z^2}\right) \qquad (3.46\ \mathbf{c})$$

where we have rearranged the equations so the acceleration terms are on the left side and the force terms are on the right. These equations are commonly called the *Navier–Stokes* equations, named in honor of the French mathematician **L. M. H. Navier** (1758–1836) and the English mechanician **Sir G. G. Stokes** (1819–1903), who were responsible for their formulation. These three equations of motion, when combined with the conservation of mass equation (Eq. 3.5), provide a complete mathematical description of the flow of incompressible Newtonian fluids. We have four equations and four unknowns (u, v, w, and p), and therefore the problem is "well-posed" in mathematical terms. Unfortunately, because of the general complexity of the Navier–Stokes equations (they are nonlinear, second-order, partial differential equations), they are not amenable to exact mathematical solutions except in a few instances. However, in those few instances in which solutions have been obtained and compared with experimental results, the results have been in close agreement. Thus, the Navier–Stokes equations are considered to be the governing differential equations of motion for incompressible Newtonian fluids.

In terms of cylindrical polar coordinates (see **Fig. 3.2**), the Navier–Stokes equation can be written as

(r direction)

$$\rho\left(\frac{\partial v_r}{\partial t} + v_r\frac{\partial v_r}{\partial r} + \frac{v_\theta}{r}\frac{\partial v_r}{\partial \theta} - \frac{v_\theta^2}{r} + v_z\frac{\partial v_r}{\partial z}\right)$$
$$= -\frac{\partial p}{\partial r} + \rho g_r + \mu\left[\frac{1}{r}\frac{\partial}{\partial r}\left(r\frac{\partial v_r}{\partial r}\right) - \frac{v_r}{r^2} + \frac{1}{r^2}\frac{\partial^2 v_r}{\partial \theta^2} - \frac{2}{r^2}\frac{\partial v_\theta}{\partial \theta} + \frac{\partial^2 v_r}{\partial z^2}\right] \qquad (3.47\ \mathbf{a})$$

(θ direction)

$$\rho\left(\frac{\partial v_\theta}{\partial t} + v_r\frac{\partial v_\theta}{\partial r} + \frac{v_\theta}{r}\frac{\partial v_\theta}{\partial \theta} + \frac{v_r v_\theta}{r} + v_z\frac{\partial v_\theta}{\partial z}\right)$$
$$= -\frac{1}{r}\frac{\partial p}{\partial \theta} + \rho g_\theta + \mu\left[\frac{1}{r}\frac{\partial}{\partial r}\left(r\frac{\partial v_\theta}{\partial r}\right) - \frac{v_\theta}{r^2} + \frac{1}{r^2}\frac{\partial^2 v_\theta}{\partial \theta^2} + \frac{2}{r^2}\frac{\partial v_r}{\partial \theta} + \frac{\partial^2 v_\theta}{\partial z^2}\right] \qquad (3.47\ \mathbf{b})$$

(z direction)

$$\rho\left(\frac{\partial v_z}{\partial t} + v_r\frac{\partial v_z}{\partial r} + \frac{v_\theta}{r}\frac{\partial v_z}{\partial \theta} + v_z\frac{\partial v_z}{\partial z}\right)$$

$$= -\frac{\partial p}{\partial z} + \rho g_z + \mu\left[\frac{1}{r}\frac{\partial}{\partial r}\left(r\frac{\partial v_z}{\partial r}\right) + \frac{1}{r^2}\frac{\partial^2 v_z}{\partial \theta^2} + \frac{\partial^2 v_z}{\partial z^2}\right] \quad (3.47\,c)$$

3.2.1 Irrotational Flow Fields:

If we make one additional assumption—that the flow is *irrotational*—the analysis of inviscid flow problems is further simplified. Recall from part (1) sec. 1.3 that the rotation of a fluid element is equal to $\frac{1}{2}(\nabla \times \mathbf{V})$, and an irrotational flow field is one for which $\nabla \times \mathbf{V} = 0$. Since the vorticity, ζ, is defined as $\nabla \times \mathbf{V}$, it also follows that in an irrotational flow field the vorticity is zero. The concept of irrotationality may seem to be a rather strange condition for a flow field. Why would a flow field be irrotational? To answer this question we note that if $\frac{1}{2}(\nabla \times \mathbf{V}) = 0$, then each of the components of this vector, must be equal to zero. Since these components include the various velocity gradients in the flow field, the condition of irrotationality imposes specific relationships among these velocity gradients. For example, for rotation about the z axis to be zero, it follows that

$$\omega_z = \frac{1}{2}\left(\frac{\partial v}{\partial x} - \frac{\partial u}{\partial y}\right) = 0$$

and, therefore,

$$\frac{\partial v}{\partial x} = \frac{\partial u}{\partial y} \qquad (3.a)$$

Similarly from the conditions for zero rotation about the x-axis and the y-axis

$$\frac{\partial w}{\partial y} = \frac{\partial v}{\partial z} \qquad (3.b)$$

and

$$\frac{\partial u}{\partial z} = \frac{\partial w}{\partial x} \qquad (3.c)$$

A general flow field would not satisfy these three equations. However, a uniform flow as is illustrated in Fig. 3.i does. Since $u = U$ (a constant), $v = 0$, and $w = 0$, it follows that Eqs. 3.a , 3.b , and 3.c are all satisfied. Therefore, a uniform flow field (in which there are no velocity gradients) is certainly an example of an irrotational flow.

Uniform flows by themselves are not very interesting. However, many interesting and important flow problems include uniform flow in some part of the flow field. Two examples are shown in Fig. 3.ii . In Fig.(3.ii a) a solid body is placed in a uniform stream of fluid. Far away from the body the flow remains uniform, and in this far region the flow is irrotational. In Fig.(3.ii b), flow from a large reservoir enters a pipe through a streamlined entrance where the velocity distribution is essentially uniform. Thus, at the entrance the flow is irrotational.

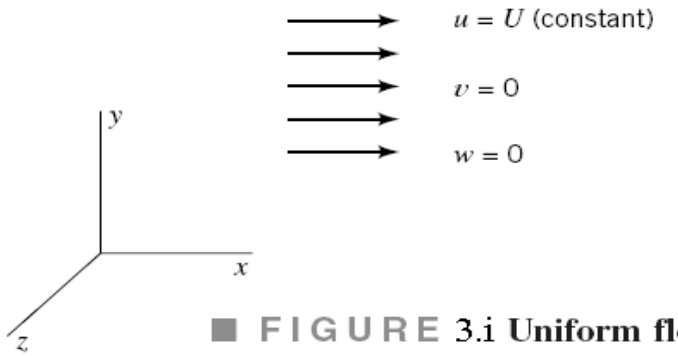

■ FIGURE 3.i **Uniform flow in the x direction.**

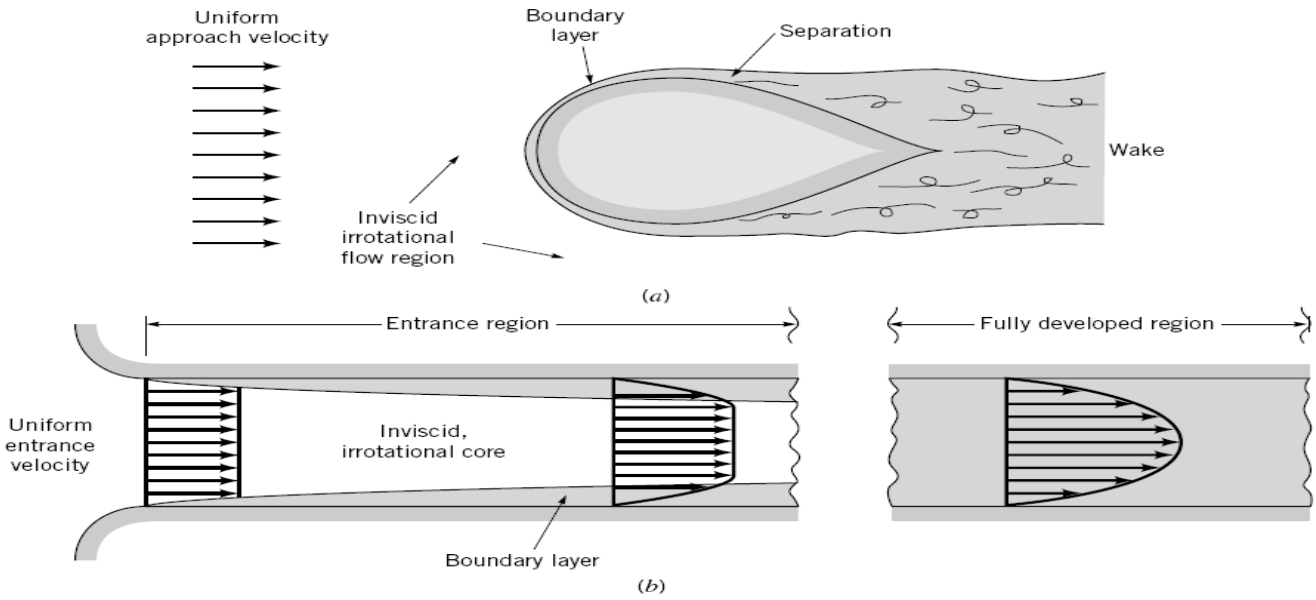

■ FIGURE 3.ii **Various regions of flow: (*a*) around bodies; (*b*) through channels.**

For an inviscid fluid there are no shearing stresses—the only forces acting on a fluid element are its weight and pressure forces. Since the weight acts through the element center of gravity, and the pressure acts in a direction normal to the element surface, neither of these forces can cause the element to rotate. Therefore, for an inviscid fluid, if some part of the flow field is irrotational, the fluid elements emanating from this region will not take on any rotation as they progress through the flow field. This phenomenon is illustrated in Fig. 3.ii a in which fluid elements flowing far away from the body have irrotational motion, and as they flow around the body the motion remains irrotational except very near the boundary. Near the boundary the velocity changes rapidly from zero at the boundary (no-slip condition) to some relatively large value in a short distance from the boundary. This rapid change in velocity gives rise to a large velocity gradient normal to the boundary and produces significant shearing stresses, even though the viscosity is small. Of course if we had a truly inviscid fluid, the fluid would simply "slide" past the boundary and the flow would be irrotational everywhere. But this is not the case for real fluids, so we will typically have a layer (usually very thin) near any fixed surface in a moving stream in which shearing stresses are not negligible. This layer is called the *boundary layer*. Outside the boundary layer the flow can be treated as an irrotational flow. Another possible consequence of the boundary layer is that the main stream may "separate" from the surface and form a *wake* downstream from the body.The wake would include a region of slow, randomly moving fluid.

To completely analyze this type of problem it is necessary to consider both the inviscid, irrotational flow outside the boundary layer, and the viscous, rotational flow within the boundary layer and to somehow "match" these two regions.

As is illustrated in Fig. 3.ii *b*, the flow in the entrance to a pipe may be uniform (if the entrance is streamlined), and thus will be irrotational. In the central core of the pipe the flow remains irrotational for some distance. However, a boundary layer will develop along the wall and grow in thickness until it fills the pipe. Thus, for this type of internal flow there will be an *entrance region* in which there is a central irrotational core, followed by a so-called *fully developed region* in which viscous forces are dominant. The concept of irrotationality is completely invalid in the fully developed region. This type of internal flow problem is considered in detail in Part (2).

The two preceding examples are intended to illustrate the possible applicability of irrotational flow to some "real fluid" flow problems and to indicate some limitations of the irrotationality concept. We proceed to develop some useful equations based on the assumptions of inviscid, incompressible, irrotational flow, with the admonition to use caution when applying the equations.

3.2.2 Case of Frictionless and Irrotational Flow (Euler's Equations):

When a flow is both frictionless and irrotational, pleasant things happen. First, the momentum equation (3.46) reduces to Euler's equation

$$\rho \frac{d\mathbf{V}}{dt} = \rho\mathbf{g} - \nabla p \qquad (3.48)$$

Second, there is a great simplification in the acceleration term. Recall from Part 1 that acceleration has two terms

$$\frac{d\mathbf{V}}{dt} = \frac{\partial \mathbf{V}}{\partial t} + (\mathbf{V} \cdot \nabla)\mathbf{V}$$

A beautiful vector identity exists for the second term [11]:

$$(\mathbf{V} \cdot \nabla)\mathbf{V} \equiv \nabla(\tfrac{1}{2}V^2) + \boldsymbol{\zeta} \times \mathbf{V} \qquad (3.49)$$

where ζ = curl $\mathbf{V}$ from Eq. (3.39) is the fluid vorticity.

Now combine (3.48) and (3.49), divide by ρ, and rearrange on the left-hand side. Dot the entire equation into an arbitrary vector displacement $d\mathbf{r}$:

$$\left[\frac{\partial \mathbf{V}}{\partial t} + \nabla\left(\frac{1}{2}\,V^2\right) + \boldsymbol{\zeta} \times \mathbf{V} + \frac{1}{\rho}\,\nabla p - \mathbf{g}\right] \cdot d\mathbf{r} = 0 \qquad (3.50)$$

Nothing works right unless we can get rid of the third term. We want

$$(\boldsymbol{\zeta} \times \mathbf{V}) \cdot (d\mathbf{r}) \equiv 0 \qquad (3.51)$$

This will be true under various conditions:

1. $\mathbf{V}$ is zero; trivial, no flow (hydrostatics).
2. $\boldsymbol{\zeta}$ is zero; irrotational flow.
3. $d\mathbf{r}$ is perpendicular to $\boldsymbol{\zeta} \times \mathbf{V}$; this is rather specialized and rare.
4. $d\mathbf{r}$ is parallel to $\mathbf{V}$; we integrate *along a streamline*

Condition 4 is the common assumption. If we integrate along a streamline in frictionless compressible flow and take, for convenience, $\mathbf{g} = -g\mathbf{k}$, Eq. (3.50) reduces to

$$\frac{\partial \mathbf{V}}{\partial t} \cdot d\mathbf{r} + d\left(\frac{1}{2}\,V^2\right) + \frac{dp}{\rho} + g\,dz = 0 \qquad (3.52)$$

Except for the first term, these are exact differentials. Integrate between any two points 1 and 2 along the streamline:

$$\int_1^2 \frac{\partial V}{\partial t}\,ds + \int_1^2 \frac{dp}{\rho} + \frac{1}{2}\,(V_2^2 - V_1^2) + g(z_2 - z_1) = 0 \qquad (3.53)$$

where ds is the arc length along the streamline. Equation (3.53) is Bernoulli's equation for frictionless unsteady flow along a streamline. For incompressible steady flow, it reduces to

$$\frac{p}{\rho} + \frac{1}{2}\,V^2 + gz = \text{constant along streamline} \qquad (3.54)$$

The constant may vary from streamline to streamline unless the flow is also irrotational (assumption 2). For irrotational flow $\zeta = 0$, the offending term Eq. (3.51) vanishes regardless of the direction of $d\mathbf{r}$, and Eq. (3.54) then holds all over the flow field with the same constant.

3.2.3 The Velocity Potential, Φ :

Irrotationality gives rise to a scalar function ϕ similar and complementary to the stream function ψ. From a theorem in vector analysis [11], a vector with zero curl must be the gradient of a scalar function

$$\text{If} \qquad \nabla \times \mathbf{V} \equiv 0 \qquad \text{then} \qquad \mathbf{V} = \nabla\phi \tag{3.55}$$

where $\phi = \phi(x, y, z, t)$ is called the *velocity potential function*. Knowledge of ϕ thus immediately gives the velocity components

$$u = \frac{\partial\phi}{\partial x} \qquad v = \frac{\partial\phi}{\partial y} \qquad w = \frac{\partial\phi}{\partial z} \tag{3.56}$$

Lines of constant ϕ are called the *potential lines* of the flow.

Note that ϕ, unlike the stream function, is fully three-dimensional and not limited to two coordinates. It reduces a velocity problem with three unknowns u, v, and w to a single unknown potential ϕ; many examples are given in this part of the study. The velocity potential also simplifies the unsteady Bernoulli equation (3.52) because if ϕ exists, we obtain

$$\frac{\partial \mathbf{V}}{\partial t} \cdot d\mathbf{r} = \frac{\partial}{\partial t}(\nabla\phi) \cdot d\mathbf{r} = d\left(\frac{\partial\phi}{\partial t}\right) \tag{3.57}$$

Equation (3.52) then becomes a relation between ϕ and p

$$\frac{\partial\phi}{\partial t} + \int \frac{dp}{\rho} + \frac{1}{2}|\nabla\phi|^2 + gz = \text{const} \tag{3.58}$$

This is the unsteady irrotational Bernoulli equation. It is very important in the analysis of accelerating flow fields (see, e.g., Refs. 10 and 15), but the only application in this text will be for steady flow.

3.2.4 The Orthogonality of Stream Lines and Potential Lines:

If a flow is both irrotational and described by only two coordinates, ψ and ϕ both exist and the streamlines and potential lines are everywhere mutually perpendicular except at a stagnation point. For example, for incompressible flow in the xy plane, we would have

$$u = \frac{\partial\psi}{\partial y} = \frac{\partial\phi}{\partial x} \tag{3.59}$$

$$v = -\frac{\partial\psi}{\partial x} = \frac{\partial\phi}{\partial y} \tag{3.60}$$

Can you tell by inspection not only that these relations imply orthogonality but also that ϕ and ψ satisfy Laplace's equation?[10] A line of constant ϕ would be such that the change in ϕ is zero

$$d\phi = \frac{\partial\phi}{\partial x}dx + \frac{\partial\phi}{\partial y}dy = 0 = u\,dx + v\,dy \tag{3.61}$$

Solving, we have

$$\left(\frac{dy}{dx}\right)_{\phi=\text{const}} = -\frac{u}{v} = -\frac{1}{(dy/dx)_{\psi=\text{const}}} \tag{3.62}$$

Equation (3.62) is the mathematical condition that lines of constant ϕ and ψ be mutually orthogonal. It may not be true at a stagnation point, where both u and v are zero, so that their ratio in Eq. (3.62) is indeterminate.

3.2.5 The Generation of Rotationality:

This is the second time we have discussed Bernoulli's equation under different circumstances (the first was in Part 1). Such reinforcement is useful, since this is probably the most widely used equation in fluid mechanics. It requires frictionless flow with no shaft work or heat transfer between sections 1 and 2. The flow may or may not be irrotational, the latter being an easier condition, allowing a universal Bernoulli constant.

The only remaining question is: *When* is a flow irrotational? In other words, when does a flow have negligible angular velocity? The exact analysis of fluid rotationality under arbitrary conditions is a topic for advanced study, e.g., Ref. 10, sec. 8.5; Ref. 9, sec. 5.2; and Ref. 5, sec. 2.10. We shall simply state those results here without proof.

A fluid flow which is initially irrotational may become rotational if

1. There are significant viscous forces induced by jets, wakes, or solid boundaries. In this case Bernoulli's equation will not be valid in such viscous regions.

[10] Equations (3.59) and (3.60) are called the *Cauchy-Riemann equations* and are studied in complex-variable theory.

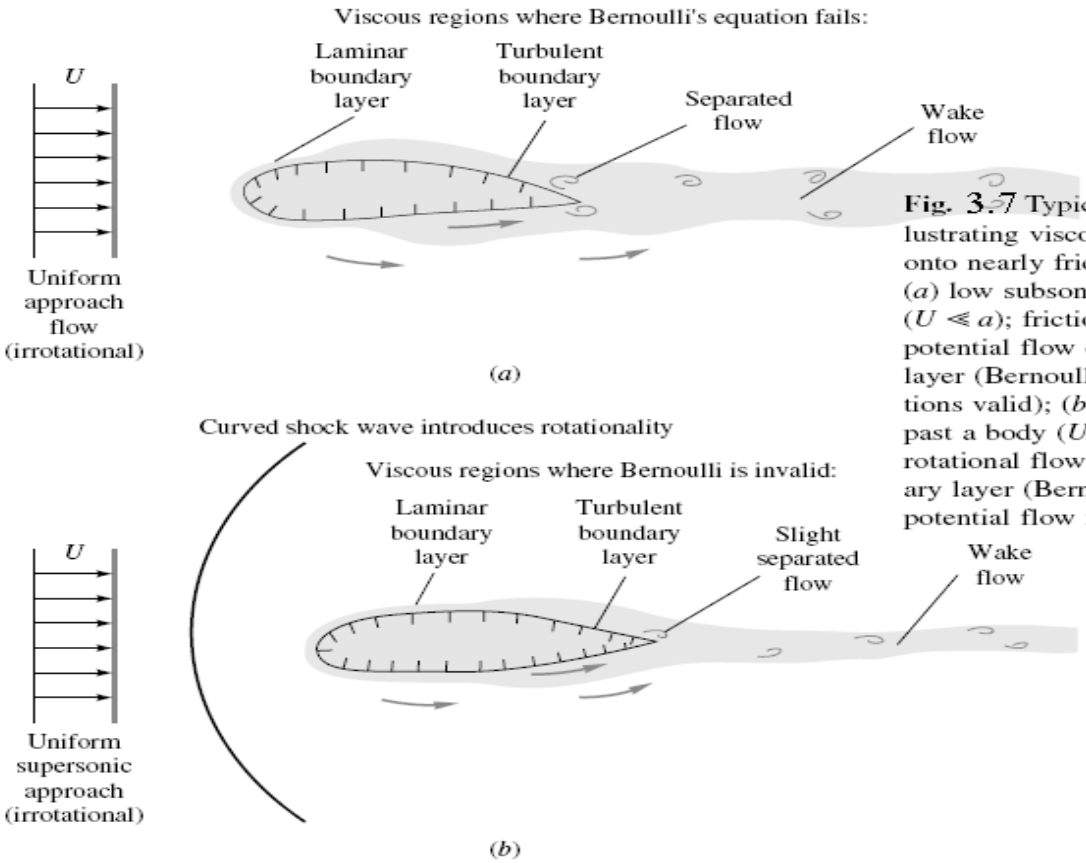

Fig. 3.7 Typical flow patterns illustrating viscous regions patched onto nearly frictionless regions: (*a*) low subsonic flow past a body ($U \ll a$); frictionless, irrotational potential flow outside the boundary layer (Bernoulli and Laplace equations valid); (*b*) supersonic flow past a body ($U > a$); frictionless, rotational flow outside the boundary layer (Bernoulli equation valid, potential flow invalid).

2. There are entropy gradients caused by curved shock waves (see Fig. 3.7 *b*).
3. There are density gradients caused by *stratification* (uneven heating) rather than by pressure gradients.
4. There are significant *noninertial* effects such as the earth's rotation (the Coriolis acceleration).

In cases 2 to 4, Bernoulli's equation still holds along a streamline if friction is negligible. We shall not study cases 3 and 4 in this book. Case 2 will be treated briefly in Chap. 9 on gas dynamics. Primarily we are concerned with case 1, where rotation is induced by viscous stresses. This occurs near solid surfaces, where the no-slip condition creates a boundary layer through which the stream velocity drops to zero, and in jets and wakes, where streams of different velocities meet in a region of high shear.

Internal flows, such as pipes and ducts, are mostly viscous, and the wall layers grow to meet in the core of the duct. Bernoulli's equation does not hold in such flows unless it is modified for viscous losses.

External flows, such as a body immersed in a stream, are partly viscous and partly inviscid, the two regions being patched together at the edge of the shear layer or boundary layer. Two examples are shown in Fig. 3.7 . Figure 3.7 *a* shows a low-speed

subsonic flow past a body. The approach stream is irrotational; i.e., the curl of a constant is zero, but viscous stresses create a rotational shear layer beside and downstream of the body. Generally speaking (see **part 2**), the shear layer is laminar, or smooth, near the front of the body and turbulent, or disorderly, toward the rear. A separated, or deadwater, region usually occurs near the trailing edge, followed by an unsteady turbulent wake extending far downstream. Some sort of laminar or turbulent viscous theory must be applied to these viscous regions; they are then patched onto the outer flow, which is frictionless and irrotational. If the stream Mach number is less than about 0.3, we can combine Eq. (3.56) with the incompressible continuity equation

$$\nabla \cdot \mathbf{V} = \nabla \cdot (\nabla \phi) = 0$$

or

$$\nabla^2 \phi = 0 = \frac{\partial^2 \phi}{\partial x^2} + \frac{\partial^2 \phi}{\partial y^2} + \frac{\partial^2 \phi}{\partial z^2} \qquad (3.63)$$

This is Laplace's equation in three dimensions, there being no restraint on the number of coordinates in potential flow. A great deal of **part 3** will be concerned with solving Eq. (3.63) for practical engineering problems; it holds in the entire region of Fig. 3.7*a* outside the shear layer.

Figure 3.7*b* shows a supersonic flow past a body. A curved shock wave generally forms in front, and the flow downstream is *rotational* due to entropy gradients (case 2). We can use Euler's equation (3.48) in this frictionless region but not potential theory. The shear layers have the same general character as in Fig. 3.7 *a* except that the separation zone is slight or often absent and the wake is usually thinner. Theory of separated flow is presently qualitative, but we can make quantitative estimates of laminar and turbulent boundary layers and wakes.

Example 3.4:

If a velocity potential exists for the velocity field

$$u = a(x^2 - y^2) \qquad v = -2axy \qquad w = 0$$

find it, plot it, and compare with Example 3.1 .

Solution

Since $w = 0$, the curl of $\mathbf{V}$ has only one z component, and we must show that it is zero:

$$(\nabla \times \mathbf{V})_z = 2\omega_z = \frac{\partial v}{\partial x} - \frac{\partial u}{\partial y} = \frac{\partial}{\partial x}(-2axy) - \frac{\partial}{\partial y}(ax^2 - ay^2)$$

$$= -2ay + 2ay = 0 \qquad \text{checks} \qquad \textit{Ans.}$$

The flow is indeed irrotational. A potential exists.

To find $\phi(x, y)$, set

$$u = \frac{\partial \phi}{\partial x} = ax^2 - ay^2 \qquad (1)$$

$$v = \frac{\partial \phi}{\partial y} = -2axy \qquad (2)$$

Integrate (1)

$$\phi = \frac{ax^3}{3} - axy^2 + f(y) \qquad (3)$$

Differentiate (3) and compare with (2)

$$\frac{\partial \phi}{\partial y} = -2axy + f'(y) = -2axy \qquad (4)$$

Therefore $f' = 0$, or $f =$ constant.

The velocity potential is

$$\phi = \frac{ax^3}{3} - axy^2 + C \qquad \textit{Ans.}$$

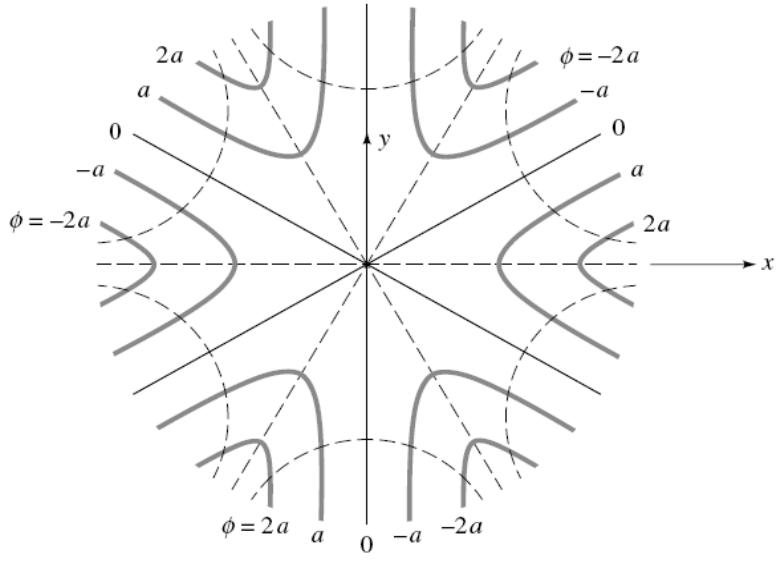

E3.4

Letting $C = 0$, we can plot the ϕ lines in the same fashion as in Example 3.1 . The result is shown in Fig. E3.4 (no arrows on ϕ). For this particular problem, the ϕ lines form the same pattern as the ψ lines of Example3.1 (which are shown here as dashed lines) but are displaced 30°. The ϕ and ψ lines are everywhere perpendicular except at the origin, a stagnation point, where they are 30° apart. We expected trouble at the stagnation point, and there is no general rule for determining the behavior of the lines at that point.

Example 3.5:

The two-dimensional flow of a nonviscous, incompressible fluid in the vicinity of the 90° corner of Fig. E3.5 a is described by the stream function

$$\psi = 2r^2 \sin 2\theta$$

where ψ has units of m^2/s when r is in meters. (a) Determine, if possible, the corresponding velocity potential. (b) If the pressure at point (1) on the wall is 30 kPa, what is the pressure at point (2)? Assume the fluid density is 10^3 kg/m^3 and the x–y plane is horizontal—that is, there is no difference in elevation between points (1) and (2).

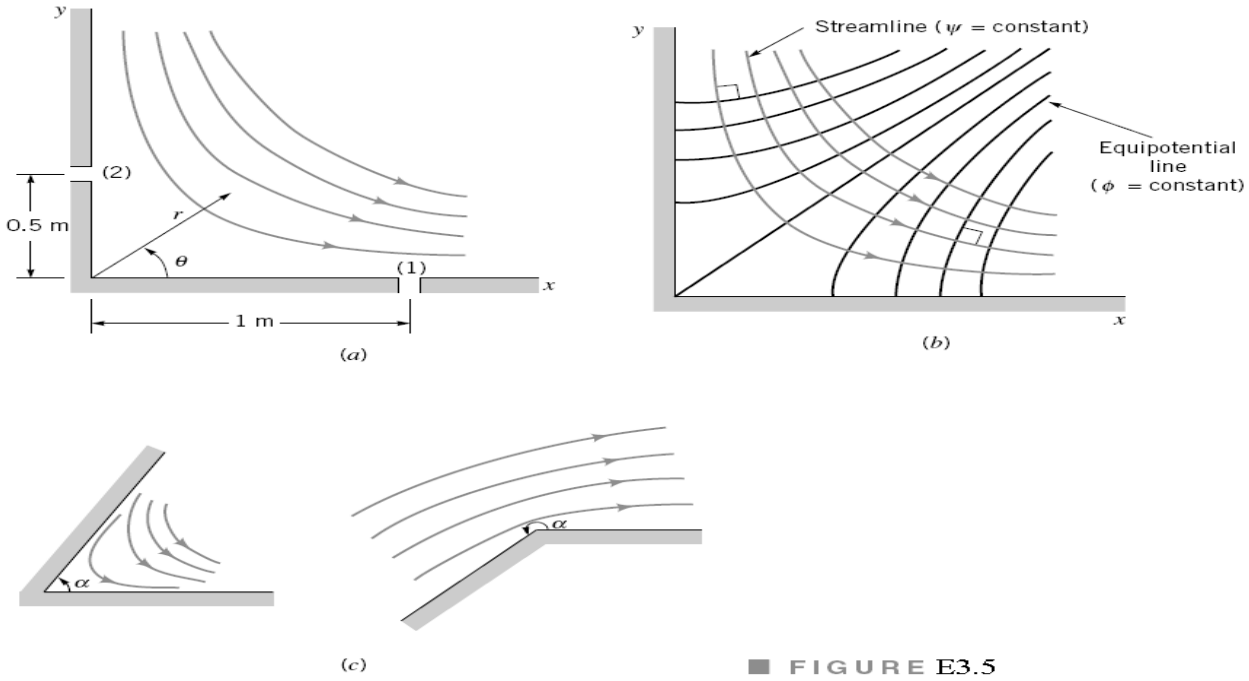

FIGURE E3.5

Solution

(a) The radial and tangential velocity components can be obtained from the stream function as

$$v_r = \frac{1}{r}\frac{\partial \psi}{\partial \theta} = 4r \cos 2\theta$$

and

$$v_\theta = -\frac{\partial \psi}{\partial r} = -4r \sin 2\theta$$

Since

$$v_r = \frac{\partial \phi}{\partial r}$$

it follows that

$$\frac{\partial \phi}{\partial r} = 4r \cos 2\theta$$

and therefore by integration $\phi = 2r^2 \cos 2\theta + f_1(\theta)$ **(1)**

where $f_1(\theta)$ is an arbitrary function of θ. Similarly

$$v_\theta = \frac{1}{r}\frac{\partial \phi}{\partial \theta} = -4r \sin 2\theta$$

and integration yields $\phi = 2r^2 \cos 2\theta + f_2(r)$ **(2)**

where $f_2(r)$ is an arbitrary function of r. To satisfy both Eqs. 1 and 2, the velocity potential must have the form

$$\phi = 2r^2 \cos 2\theta + C \quad \text{(Ans)}$$

where C is an arbitrary constant. As is the case for stream functions, the specific value of C is not important, and it is customary to let $C = 0$ so that the velocity potential for this corner flow is

$$\phi = 2r^2 \cos 2\theta \qquad \textbf{(Ans)}$$

In the statement of this problem it was implied by the wording "if possible" that we might not be able to find a corresponding velocity potential. The reason for this concern is that we can always define a stream function for two-dimensional flow, but the flow must be *irrotational* if there is a corresponding velocity potential. Thus, the fact that we were able to determine a velocity potential means that the flow is irrotational. Several streamlines and lines of constant ϕ are plotted in Fig. E3.5 b. These two sets of lines are *orthogonal*. The reason why streamlines and lines of constant ϕ are always orthogonal is explained in next sections.

(b) Since we have an irrotational flow of a nonviscous, incompressible fluid, the Bernoulli equation can be applied between any two points. Thus, between points (1) and (2) with no elevation change

$$\frac{p_1}{\gamma} + \frac{V_1^2}{2g} = \frac{p_2}{\gamma} + \frac{V_2^2}{2g}$$

or

$$p_2 = p_1 + \frac{\rho}{2}(V_1^2 - V_2^2) \qquad \textbf{(3)}$$

Since

$$V^2 = v_r^2 + v_\theta^2$$

it follows that for any point within the flow field

$$\begin{aligned} V^2 &= (4r \cos 2\theta)^2 + (-4r \sin 2\theta)^2 \\ &= 16r^2(\cos^2 2\theta + \sin^2 2\theta) \\ &= 16r^2 \end{aligned}$$

This result indicates that the square of the velocity at any point depends only on the radial distance, r, to the point. Note that the constant, 16, has units of s^{-2}. Thus,

and

$$V_1^2 = (16\ s^{-2})(1\ m)^2 = 16\ m^2/s^2$$
$$V_2^2 = (16\ s^{-2})(0.5\ m)^2 = 4\ m^2/s^2$$

Substitution of these velocities into Eq. 3 gives

$$p_2 = 30 \times 10^3\ N/m^2 + \frac{10^3 kg/m^3}{2}(16\ m^2/s^2 - 4\ m^2/s^2) = 36\ kPa \qquad \textbf{(Ans)}$$

The stream function used in this example could also be expressed in Cartesian coordinates as

$$\psi = 2r^2 \sin 2\theta = 4r^2 \sin\theta \cos\theta$$

or

$$\psi = 4xy$$

since $x = r\cos\theta$ and $y = r\sin\theta$. However, in the cylindrical polar form the results can be generalized to describe flow in the vicinity of a corner of angle α (see Fig. E3.5*c*) with the equations

$$\psi = Ar^{\pi/\alpha} \sin\frac{\pi\theta}{\alpha}$$

and

$$\phi = Ar^{\pi/\alpha} \cos\frac{\pi\theta}{\alpha}$$

where A is a constant.

3.3 Some Illustrative Plane Potential Flows:

A major advantage of Laplace's equation is that it is a linear partial differential equation. Since it is linear, various solutions can be added to obtain other solutions—that is, if $\phi_1(x, y, z)$ and $\phi_2(x, y, z)$ are two solutions to Laplace's equation, then $\phi_3 = \phi_1 + \phi_2$ is also a solution. The practical implication of this result is that if we have certain basic solutions we can combine them to obtain more complicated and interesting solutions. In this section several basic velocity potentials, which describe some relatively simple flows, will be determined. In the next section these basic potentials will be combined to represent complicated flows.

For simplicity, only plane (two-dimensional) flows will be considered. In this case, by using Cartesian coordinates

$$u = \frac{\partial\phi}{\partial x} \qquad v = \frac{\partial\phi}{\partial y} \qquad (3.64)$$

or by using cylindrical coordinates

$$v_r = \frac{\partial\phi}{\partial r} \qquad v_\theta = \frac{1}{r}\frac{\partial\phi}{\partial\theta} \qquad (3.65)$$

Since we can define a stream function for plane flow, we can also let

$$u = \frac{\partial \psi}{\partial y} \qquad v = -\frac{\partial \psi}{\partial x} \tag{3.66}$$

or

$$v_r = \frac{1}{r}\frac{\partial \psi}{\partial \theta} \qquad v_\theta = -\frac{\partial \psi}{\partial r} \tag{3.67}$$

where the stream function was previously defined in last sections. We know that by defining the velocities in terms of the stream function, conservation of mass is identically satisfied. If we now impose the condition of irrotationality, $W_Z = 0.0$, it follows that

$$\frac{\partial u}{\partial y} = \frac{\partial v}{\partial x}$$

and in terms of the stream function

$$\frac{\partial}{\partial y}\left(\frac{\partial \psi}{\partial y}\right) = \frac{\partial}{\partial x}\left(-\frac{\partial \psi}{\partial x}\right)$$

or

$$\frac{\partial^2 \psi}{\partial x^2} + \frac{\partial^2 \psi}{\partial y^2} = 0$$

Thus, for a plane irrotational flow we can use either the velocity potential or the stream function—both must satisfy Laplace's equation in two dimensions. It is apparent from these results that the velocity potential and the stream function are somehow related. We have previously shown that lines of constant ψ are streamlines; that is,

$$\left.\frac{dy}{dx}\right|_{\text{along } \psi = \text{constant}} = \frac{v}{u} \tag{3.68}$$

The change in ϕ as we move from one point (x, y) to a nearby point $(x + dx, y + dy)$ is given by the relationship

$$d\phi = \frac{\partial \phi}{\partial x}dx + \frac{\partial \phi}{\partial y}dy = u\,dx + v\,dy$$

Along a line of constant ϕ we have $d\phi = 0$ so that

$$\left.\frac{dy}{dx}\right|_{\text{along } \phi = \text{constant}} = -\frac{u}{v} \tag{3.69}$$

A comparison of Eqs. 3.68 and 3.69 shows that lines of constant ϕ (called *equipotential lines*) are orthogonal to lines of constant ψ (streamlines) at all points where they intersect. (Recall that two lines are orthogonal if the product of their slopes is minus one.) For any potential flow field a "*flow net*" can be drawn that consists of a family of streamlines and equipotential lines. The flow net is useful in visualizing flow patterns and can be used to obtain graphical solutions by sketching in streamlines and equipotential lines and adjusting the lines until the lines are approximately orthogonal at all points where they intersect. An example of a flow net is shown in Fig. 3.8 . Velocities can be estimated from the flow net, since the velocity is inversely proportional to the streamline spacing. Thus, for example, from Fig. 3.8 we can see that the velocity near the inside corner will be higher than the velocity along the outer part of the bend.

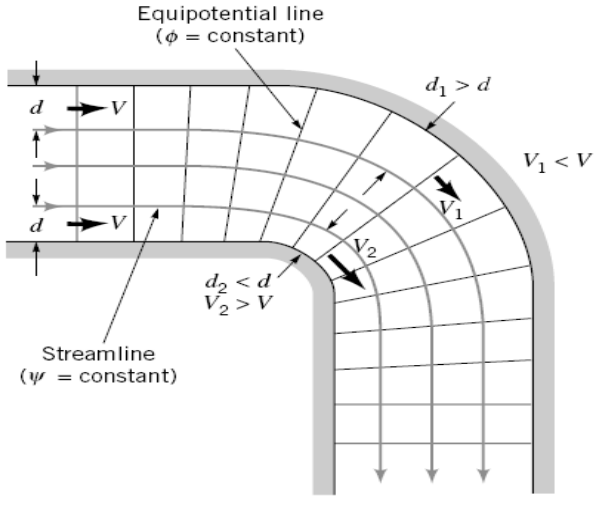

■ FIGURE 3.8 **Flow net for a 90° bend. (From Ref. 3, used by permission.)**

3.3.1 Uniform Flow:

The simplest plane flow is one for which the streamlines are all straight and parallel, and the magnitude of the velocity is constant. This type of flow is called a *uniform flow*. For example, consider a uniform flow in the positive x direction as is illustrated in Fig. 3.9 a . In this instance, $u = U$ and $v = 0$, and in terms of the velocity potential

$$\frac{\partial \phi}{\partial x} = U \qquad \frac{\partial \phi}{\partial y} = 0$$

These two equations can be integrated to yield

$$\phi = Ux + C$$

where C is an arbitrary constant, which can be set equal to zero. Thus, for a uniform flow in the positive x direction

$$\phi = Ux \tag{3.70}$$

The corresponding stream function can be obtained in a similar manner, since

$$\frac{\partial \psi}{\partial y} = U \qquad \frac{\partial \psi}{\partial x} = 0$$

and, therefore,

$$\psi = Uy \tag{3.71}$$

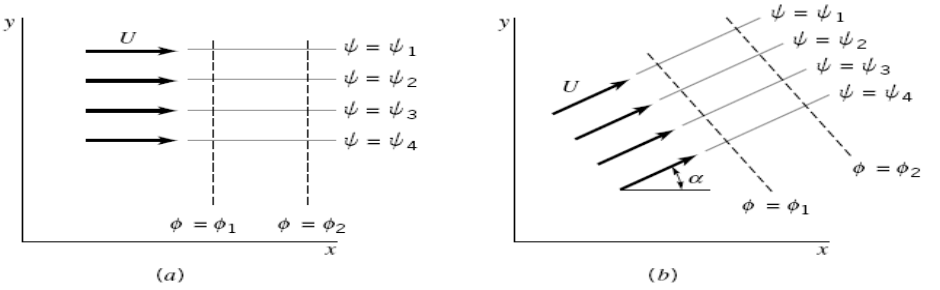

■ **FIGURE 3.9**
Uniform flow: (*a*) in the x direction; (*b*) in an arbitrary direction, α.

These results can be generalized to provide the velocity potential and stream function for a uniform flow at an angle α with the x axis, as in Fig. 6.16*b*. For this case

$$\phi = U(x \cos \alpha + y \sin \alpha) \tag{3.72}$$

and

$$\psi = U(y \cos \alpha - x \sin \alpha) \tag{3.73}$$

3.3.2 Source and Sink:

Consider a fluid flowing radially outward from a line through the origin perpendicular to the x–y plane as is shown in Fig. 3.10 . Let m be the volume rate of flow emanating from the line (per unit length), and therefore to satisfy conservation of mass

or

$$(2\pi r)v_r = m$$
$$v_r = \frac{m}{2\pi r}$$

Also, since the flow is a purely radial flow, $v_\theta = 0$, the corresponding velocity potential can be obtained by integrating the equations

$$\frac{\partial \phi}{\partial r} = \frac{m}{2\pi r} \qquad \frac{1}{r}\frac{\partial \phi}{\partial \theta} = 0$$

It follows that

$$\phi = \frac{m}{2\pi} \ln r \tag{3.74}$$

If m is positive, the flow is radially outward, and the flow is considered to be a *source* flow. If m is negative, the flow is toward the origin, and the flow is considered to be a *sink* flow. The flowrate, m, is the *strength* of the source or sink.

We note that at the origin where $r = 0$ the velocity becomes infinite, which is of course physically impossible. Thus, sources and sinks do not really exist in real flow fields, and the line representing the source or sink is a mathematical *singularity* in the flow field. However, some real flows can be approximated at points away from the origin by using sources or sinks. Also, the velocity potential representing this hypothetical flow can be combined with other basic velocity potentials to describe approximately some real flow fields. This idea is further discussed in Section 3.4 .

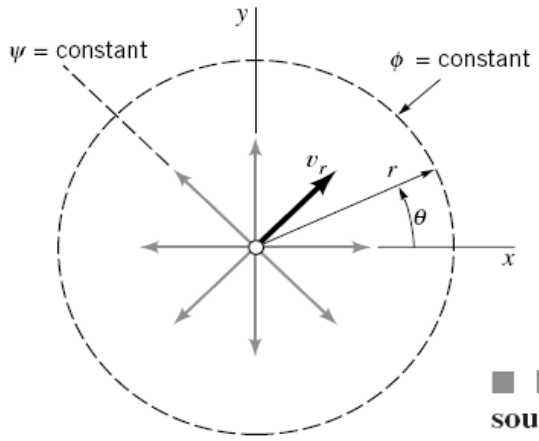

■ FIGURE 3.10 **The streamline pattern for a source.**

The stream function for the source can be obtained by integrating the relationships

$$\frac{1}{r}\frac{\partial \psi}{\partial \theta} = \frac{m}{2\pi r} \qquad \frac{\partial \psi}{\partial r} = 0$$

to yield

$$\psi = \frac{m}{2\pi}\theta \tag{3.75}$$

It is apparent from Eq. 3.75 that the streamlines (lines of ψ = constant) are radial lines, and from Eq. 3.74 the equipotential lines (lines of ϕ = constant) are concentric circles centered at the origin.

Example 3.6:

A nonviscous, incompressible fluid flows between wedge-shaped walls into a small opening as shown in Fig. E3.6. The velocity potential (in ft^2/s), which approximately describes this flow is $\phi = -2 \ln r$

Determine the volume rate of flow (per unit length) into the opening.

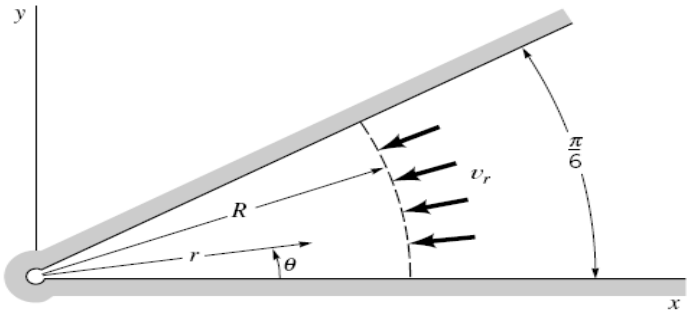

■ FIGURE E3.6

Solution

The components of velocity are

$$v_r = \frac{\partial \phi}{\partial r} = -\frac{2}{r} \qquad v_\theta = \frac{1}{r}\frac{\partial \phi}{\partial \theta} = 0$$

which indicates we have a purely radial flow. The flowrate per unit width, q, crossing the arc of length $R\pi/6$ can thus be obtained by integrating the expression

$$q = \int_0^{\pi/6} v_r R\, d\theta = -\int_0^{\pi/6} \left(\frac{2}{R}\right) R\, d\theta = -\frac{\pi}{3} = -1.05 \text{ ft}^2/\text{s} \qquad \text{(Ans)}$$

Note that the radius R is arbitrary since the flowrate crossing any curve between the two walls must be the same. The negative sign indicates that the flow is toward the opening, that is, in the negative radial direction.

3.3.3 Vortex:

We next consider a flow field in which the streamlines are concentric circles—that is, we interchange the velocity potential and stream function for the source. Thus, let

$$\phi = K\theta \tag{3.76}$$

and

$$\psi = -K \ln r \tag{3.77}$$

where K is a constant. In this case the streamlines are concentric circles as are illustrated in Fig. 3.11 , with $v_r = 0$ and

$$v_\theta = \frac{1}{r}\frac{\partial \phi}{\partial \theta} = -\frac{\partial \psi}{\partial r} = \frac{K}{r} \tag{3.78}$$

This result indicates that the tangential velocity varies inversely with the distance from the origin, with a singularity occurring at $r = 0$ (where the velocity becomes infinite).

It may seem strange that this *vortex* motion is irrotational (and it is since the flow field is described by a velocity potential). However, it must be recalled that rotation refers to the orientation of a fluid element and not the path followed by the element. Thus, for an irrotational vortex, if a pair of small sticks were placed in the flow field at location A, as indicated in Fig. 3.12 a, the sticks would rotate as they move to location B. One of the sticks, the one that is aligned along the streamline, would follow a circular path and rotate in a counterclockwise direction. The other stick would rotate in a clockwise direction due to the nature of the flow field—that is, the part of the stick nearest the origin moves faster than the opposite end. Although both sticks are rotating, the average angular velocity of the two sticks is zero since the flow is irrotational.

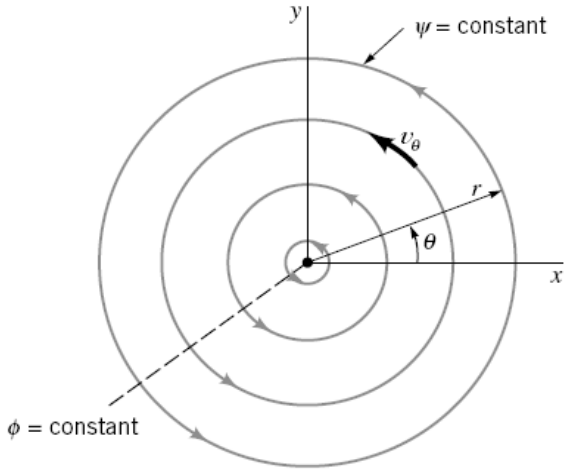

■ FIGURE 3.11 **The streamline pattern for a vortex.**

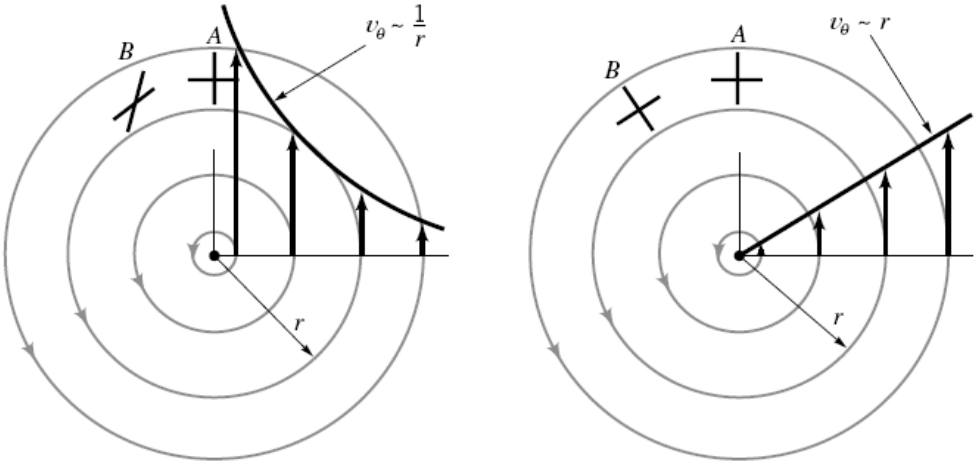

■ FIGURE 3.12 **Motion of fluid element from A to B: (a) for irrotational (free) vortex; (b) for rotational (forced) vortex.**

If the fluid were rotating as a rigid body, such that $v_\theta = K_1 r$ where K_1 is a constant, then sticks similarly placed in the flow field would rotate as is illustrated in Fig. 3.12 b. This type of vortex motion is *rotational* and cannot be described with a velocity potential. The rotational vortex is commonly called a *forced vortex*, whereas the irrotational vortex is usually called a *free vortex*. The swirling motion of the water as it drains from a bathtub is similar to that of a free vortex, whereas the motion of a liquid contained in a tank that is rotated about its axis with angular velocity ω corresponds to a forced vortex.

A *combined vortex* is one with a forced vortex as a central core and a velocity distribution corresponding to that of a free vortex outside the core. Thus, for a combined vortex

$$v_\theta = \omega r \qquad r \leq r_0 \tag{3.79}$$

and

$$v_\theta = \frac{K}{r} \qquad r > r_0 \tag{3.80}$$

where K and ω are constants and r_0 corresponds to the radius of the central core.

Circulation:

A mathematical concept commonly associated with vortex motion is that of *circulation*. The circulation, Γ, is defined as the line integral of the tangential component of the velocity taken around a closed curve in the flow field. In equation form, Γ can be expressed as

$$\Gamma = \oint_C \mathbf{V} \cdot d\mathbf{s} \tag{3.81}$$

where the integral sign means that the integration is taken around a closed curve, C, in the counterclockwise direction, and $d\mathbf{s}$ is a differential length along the curve as is illustrated in Fig.3.13 . For an irrotational flow, $\mathbf{V} = \nabla\phi$ so that $\mathbf{V} \cdot d\mathbf{s} = \nabla\phi \cdot d\mathbf{s} = d\phi$ and, therefore,

$$\Gamma = \oint_C d\phi = 0$$

This result indicates that for an irrotational flow the circulation will generally be zero. However, if there are singularities enclosed within the curve the circulation may not be zero. For example, for the free vortex with $v_\theta = K/r$ the circulation around the circular path of radius r shown in Fig. 3.14 is

$$\Gamma = \int_0^{2\pi} \frac{K}{r}(r\, d\theta) = 2\pi K$$

which shows that the circulation is nonzero and the constant $K = \Gamma/2\pi$. However, the circulation around any path that does not include the singular point at the origin will be zero.

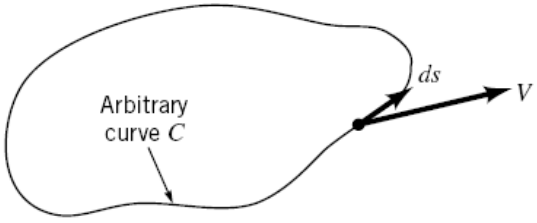

■ FIGURE 3.19 **The notation for determining circulation around closed curve *C*.**

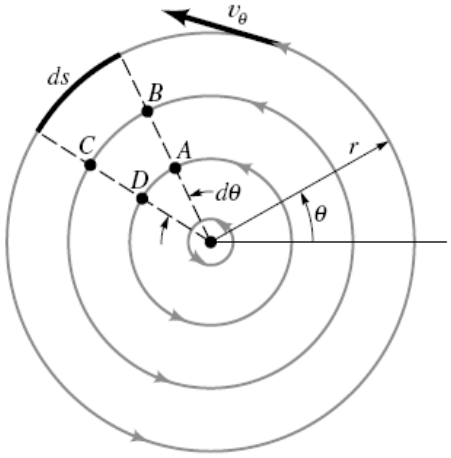

■ FIGURE 3.14 **Circulation around various paths in a free vortex.**

This can be easily confirmed by evaluating the circulation around a closed path such as *ABCD* of Fig. 3.14 , which does not include the origin.

The velocity potential and stream function for the free vortex are commonly expressed in terms of the circulation as

$$\phi = \frac{\Gamma}{2\pi}\theta \tag{3.82}$$

and

$$\psi = -\frac{\Gamma}{2\pi}\ln r \tag{3.83}$$

The concept of circulation is often useful when evaluating the forces developed on bodies immersed in moving fluids. This application is used in studying a uniform flow around a cylinder

Example 3.7:

A liquid drains from a large tank through a small opening as illustrated in Fig. E 3.7. A vortex forms whose velocity distribution away from the tank opening can be approximated as that of a free vortex having a velocity potential $\phi = \frac{\Gamma}{2\pi}\theta$

Determine an expression relating the surface shape to the strength of the vortex as specified by the circulation Γ.

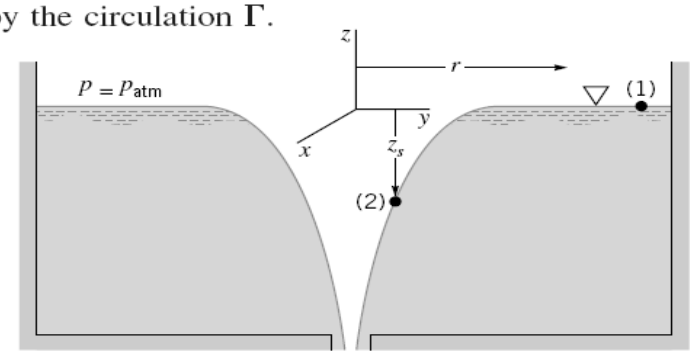

■ FIGURE E 3.7

Solution:

Since the free vortex represents an irrotational flow field, the Bernoulli equation

$$\frac{p_1}{\gamma} + \frac{V_1^2}{2g} + z_1 = \frac{p_2}{\gamma} + \frac{V_2^2}{2g} + z_2$$

can be written between any two points. If the points are selected at the free surface, $p_1 = p_2 = 0$, so that

$$\frac{V_1^2}{2g} = z_s + \frac{V_2^2}{2g} \qquad (1)$$

where the free surface elevation, z_s, is measured relative to a datum passing through point (1).

The velocity is given by the equation $v_\theta = \frac{1}{r}\frac{\partial \phi}{\partial \theta} = \frac{\Gamma}{2\pi r}$

We note that far from the origin at point (1), $V_1 = v_\theta \approx 0$ so that Eq. 1 becomes

$$z_s = -\frac{\Gamma^2}{8\pi^2 r^2 g} \qquad \text{(Ans)}$$

which is the desired equation for the surface profile. The negative sign indicates that the surface falls as the origin is approached as shown in Fig. E 3.7. This solution is not valid very near the origin since the predicted velocity becomes excessively large as the origin is approached.

3.3.4 Doublet:

The final, basic potential flow to be considered is one that is formed by combining a source and sink in a special way. Consider the equal strength, source-sink pair of Fig. 3.15 . The combined stream function for the pair is $\psi = -\frac{m}{2\pi}(\theta_1 - \theta_2)$

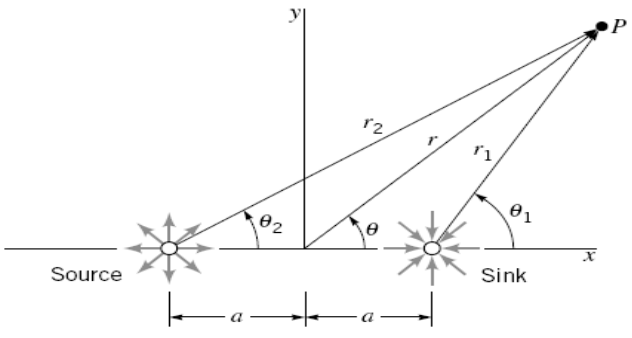

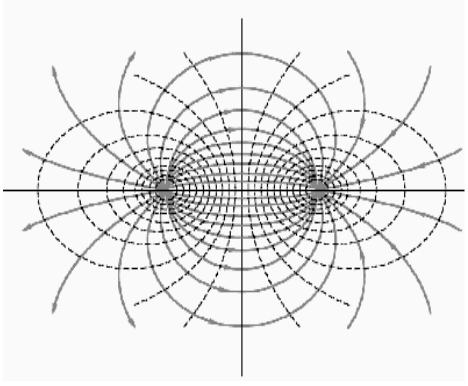

■ FIGURE 3.15 **The combination of a source and sink of equal strength located along the x axis.**

which can be rewritten as

$$\tan\left(-\frac{2\pi\psi}{m}\right) = \tan(\theta_1 - \theta_2) = \frac{\tan\theta_1 - \tan\theta_2}{1 + \tan\theta_1 \tan\theta_2} \tag{3.84}$$

From Fig. 3.15 it follows that $\tan\theta_1 = \dfrac{r\sin\theta}{r\cos\theta - a}$

and $\tan\theta_2 = \dfrac{r\sin\theta}{r\cos\theta + a}$

These results substituted into Eq. 3.84 give

$$\tan\left(-\frac{2\pi\psi}{m}\right) = \frac{2ar\sin\theta}{r^2 - a^2}$$

so that

$$\psi = -\frac{m}{2\pi}\tan^{-1}\left(\frac{2ar\sin\theta}{r^2 - a^2}\right) \tag{3.85}$$

For small values of a

$$\psi = -\frac{m}{2\pi}\frac{2ar\sin\theta}{r^2 - a^2} = -\frac{mar\sin\theta}{\pi(r^2 - a^2)} \tag{3.86}$$

since the tangent of an angle approaches the value of the angle for small angles.

The so-called *doublet* is formed by letting the source and sink approach one another ($a \to 0$) while increasing the strength m ($m \to \infty$) so that the product ma/π remains constant. In this case, since $r/(r^2 - a^2) \to 1/r$, Eq. 3.86 reduces to

$$\psi = -\frac{K\sin\theta}{r} \tag{3.87}$$

where K, a constant equal to ma/π, is called the *strength* of the doublet. The corresponding velocity potential for the doublet is

$$\phi = \frac{K\cos\theta}{r} \tag{3.88}$$

Plots of lines of constant ψ reveal that the streamlines for a doublet are circles through the origin tangent to the x axis as shown in Fig. 3.16 . Just as sources and sinks are not physically realistic entities, neither are doublets. However, the doublet when combined with other basic potential flows provides a useful representation of some flow fields of practical interest. For example, we will determine in Section 3.4 that the combination of a uniform flow and a doublet can be used to represent the flow around a circular cylinder. Table 3.1 provides a summary of the pertinent equations for the basic, plane potential flows considered in the preceding sections.

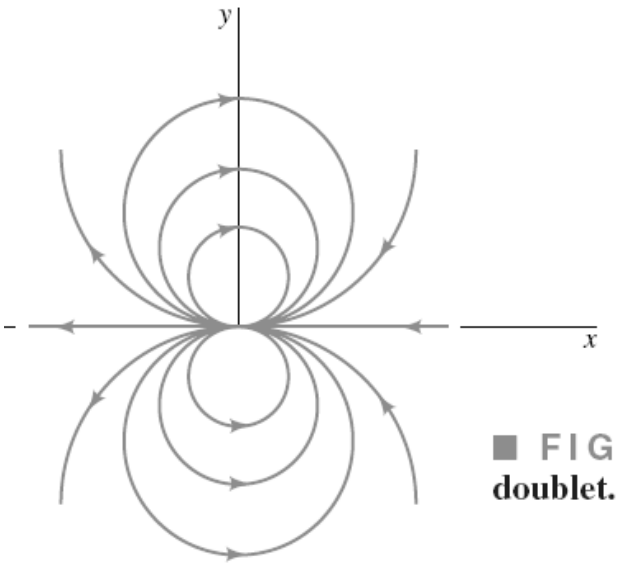

■ FIGURE 3.16 **Streamlines for a doublet.**

TABLE 3.1
Summary of Basic, Plane Potential Flows.

Description of Flow Field	Velocity Potential	Stream Function	Velocity Components[a]
Uniform flow at angle α with the x axis (see fig.3.9 b)	$\phi = U(x\cos\alpha + y\sin\alpha)$	$\psi = U(y\cos\alpha - x\sin\alpha)$	$u = U\cos\alpha$ $v = U\sin\alpha$
Source or sink (see fig.3.10) $m > 0$ source $m < 0$ sink	$\phi = \frac{m}{2\pi}\ln r$	$\psi = \frac{m}{2\pi}\theta$	$v_r = \frac{m}{2\pi r}$ $v_\theta = 0$
Free vortex (see fig. 3.11) $\Gamma > 0$ counterclockwise motion $\Gamma < 0$ clockwise motion	$\phi = \frac{\Gamma}{2\pi}\theta$	$\psi = -\frac{\Gamma}{2\pi}\ln r$	$v_r = 0$ $v_\theta = \frac{\Gamma}{2\pi r}$
Doublet (see fig.3.16)	$\phi = \frac{K\cos\theta}{r}$	$\psi = -\frac{K\sin\theta}{r}$	$v_r = -\frac{K\cos\theta}{r^2}$ $v_\theta = -\frac{K\sin\theta}{r^2}$

[a]Velocity components are related to the velocity potential and stream function through the relationships:

$$u = \frac{\partial\phi}{\partial x} = \frac{\partial\psi}{\partial y} \qquad v = \frac{\partial\phi}{\partial y} = -\frac{\partial\psi}{\partial x} \qquad v_r = \frac{\partial\phi}{\partial r} = \frac{1}{r}\frac{\partial\psi}{\partial\theta} \qquad v_\theta = \frac{1}{r}\frac{\partial\phi}{\partial\theta} = -\frac{\partial\psi}{\partial r}$$

3.4 Superposition of Basic, Plane Potential Flows

As was discussed in the previous section, potential flows are governed by Laplace's equation, which is a linear partial differential equation. It therefore follows that the various basic velocity potentials and stream functions can be combined to form new potentials and stream functions. (Why is this true?) Whether such combinations yield useful results remains to be seen. It is to be noted that *any streamline in an inviscid flow field can be considered as a solid boundary*, since the conditions along a solid boundary and a streamline are the same—that is, there is no flow through the boundary or the streamline. Thus, if we can combine some of the basic velocity potentials or stream functions to yield a streamline that corresponds to a particular body shape of interest, that combination can be used to describe in detail the flow around that body. This method of solving some interesting flow problems, commonly called the *method of superposition*, is illustrated in the following three sections.

3.4.1 Source in a Uniform Stream—Half-Body

Consider the superposition of a source and a uniform flow as shown in Fig. 3.17 a . The resulting stream function is

$$\psi = \psi_{\text{uniform flow}} + \psi_{\text{source}}$$
$$= Ur\sin\theta + \frac{m}{2\pi}\theta \qquad (3.89)$$

and the corresponding velocity potential is

$$\phi = Ur\cos\theta + \frac{m}{2\pi}\ln r \qquad (3.90)$$

It is clear that at some point along the negative x axis the velocity due to the source will just cancel that due to the uniform flow and a stagnation point will be created. For the source alone

$$v_r = \frac{m}{2\pi r}$$

so that the stagnation point will occur at $x = -b$ where $U = \frac{m}{2\pi b}$

or

$$b = \frac{m}{2\pi U} \qquad (3.91)$$

The value of the stream function at the stagnation point can be obtained by evaluating ψ at $r = b$ and $\theta = \pi$, which yields from Eq. 3.89

$$\psi_{\text{stagnation}} = \frac{m}{2}$$

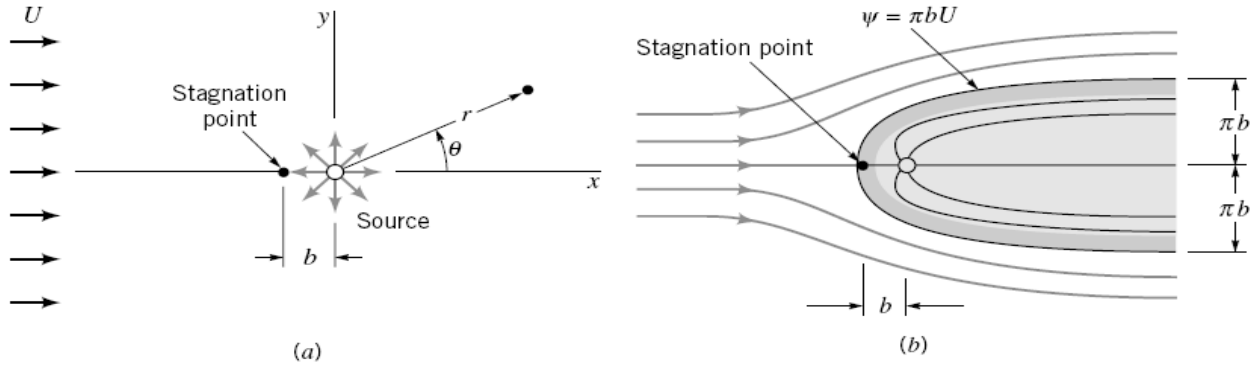

■ **FIGURE 3.17 The flow around a half-body: (*a*) superposition of a source and a uniform flow; (*b*) replacement of streamline $\psi = \pi bU$ with solid boundary to form half-body.**

Since $m/2 = \pi bU$ (from Eq. 3.91) it follows that the equation of the streamline passing through the stagnation point is

$$\pi bU = Ur \sin\theta + bU\theta$$

or

$$r = \frac{b(\pi - \theta)}{\sin\theta} \qquad (3.92)$$

where θ can vary between 0 and 2π. A plot of this streamline is shown in Fig. 3.17 b. If we replace this streamline with a solid boundary, as indicated in the figure, then it is clear that this combination of a uniform flow and a source can be used to describe the flow around a streamlined body placed in a uniform stream. The body is open at the downstream end, and thus is called a *half-body*. Other streamlines in the flow field can be obtained by setting $\psi =$ constant in Eq. 3.89 and plotting the resulting equation. A number of these streamlines are shown in Fig. 3.17 *b*. Although the streamlines inside the body are shown, they are actually of no interest in this case, since we are concerned with the flow field outside the body. It should be noted that the singularity in the flow field (the source) occurs inside the body, and there are no singularities in the flow field of interest (outside the body).

The width of the half-body asymptotically approaches $2\pi b$. This follows from Eq. 3.92 , which can be written as

$$y = b(\pi - \theta)$$

so that as $\theta \to 0$ or $\theta \to 2\pi$ the half-width approaches $\pm b\pi$. With the stream function (or velocity potential) known, the velocity components at any point can be obtained. For the half-body, using the stream function given by Eq. 3.89 ,

and

$$v_r = \frac{1}{r}\frac{\partial\psi}{\partial\theta} = U\cos\theta + \frac{m}{2\pi r}$$

$$v_\theta = -\frac{\partial\psi}{\partial r} = -U\sin\theta$$

Thus, the square of the magnitude of the velocity, V, at any point is

$$V^2 = v_r^2 + v_\theta^2 = U^2 + \frac{Um\cos\theta}{\pi r} + \left(\frac{m}{2\pi r}\right)^2$$

and since $b = m/2\pi U$

$$V^2 = U^2\left(1 + 2\frac{b}{r}\cos\theta + \frac{b^2}{r^2}\right) \qquad (3.93)$$

With the velocity known, the pressure at any point can be determined from the Bernoulli equation, which can be written between any two points in the flow field since the flow is irrotational. Thus, applying the Bernoulli equation between a point far from the body, where the pressure is p_0 and the velocity is U, and some arbitrary point with pressure p and velocity V, it follows that

$$p_0 + \tfrac{1}{2}\rho U^2 = p + \tfrac{1}{2}\rho V^2 \qquad (3.94)$$

where elevation changes have been neglected. Equation 6.101 can now be substituted into Eq. 3.94 to obtain the pressure at any point in terms of the reference pressure, p_0, and the upstream velocity, U.

This relatively simple potential flow provides some useful information about the flow around the front part of a streamlined body, such as a bridge pier or strut placed in a uniform stream. An important point to be noted is that the velocity tangent to the surface of the body is not zero; that is, the fluid "slips" by the boundary. This result is a consequence of neglecting viscosity, the fluid property that causes real fluids to stick to the boundary, thus creating a "no-slip" condition. All potential flows differ from the flow of real fluids in this respect and do not accurately represent the velocity very near the boundary. However, outside this very thin boundary layer the velocity distribution will generally correspond to that predicted by potential flow theory if flow separation does not occur. Also, the pressure distribution along the surface will closely approximate that predicted from the potential flow theory, since the boundary layer is thin and there is little opportunity for the pressure to vary through the thin layer. In fact, as discussed in more detail in Part (4) , the pressure distribution obtained from potential flow theory is used in conjunction with viscous flow theory to determine the nature of flow within the boundary layer.

Example 3.8:

The shape of a hill arising from a plain can be approximated with the top section of a half-body as is illustrated in Fig. E3.8. The height of the hill approaches 200 ft as shown. (a) When a 40 mi/hr wind blows toward the hill, what is the magnitude of the air velocity at a point on the hill directly above the origin [point (2)]? (b) What is the elevation of point (2) above the plain and what is the difference in pressure between point (1) on the plain far from the hill and point (2)? Assume an air density of 0.00238 slugs/ft^3.

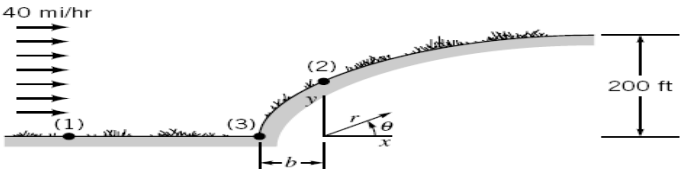

FIGURE E 3.8

Solution

(a) The velocity is given by Eq. 3.93 as $V^2 = U^2\left(1 + 2\frac{b}{r}\cos\theta + \frac{b^2}{r^2}\right)$

At point (2), $\theta = \pi/2$, and since this point is on the surface (Eq. 3.92)

$$r = \frac{b(\pi - \theta)}{\sin\theta} = \frac{\pi b}{2} \tag{1}$$

Thus,

$$V_2^2 = U^2\left[1 + \frac{b^2}{(\pi b/2)^2}\right]$$

$$= U^2\left(1 + \frac{4}{\pi^2}\right)$$

and the magnitude of the velocity at (2) for a 40 mi/hr approaching wind is

$$V_2 = \left(1 + \frac{4}{\pi^2}\right)^{1/2}(40 \text{ mi/hr}) = 47.4 \text{ mi/hr} \quad \textbf{(Ans)}$$

(b) The elevation at (2) above the plain is given by Eq. 1 as $y_2 = \frac{\pi b}{2}$

Since the height of the hill approaches 200 ft and this height is equal to πb, it follows that

$$y_2 = \frac{200 \text{ ft}}{2} = 100 \text{ ft} \quad \textbf{(Ans)}$$

From the Bernoulli equation (with the y axis the vertical axis)

so that

$$\frac{p_1}{\gamma} + \frac{V_1^2}{2g} + y_1 = \frac{p_2}{\gamma} + \frac{V_2^2}{2g} + y_2$$

$$p_1 - p_2 = \frac{\rho}{2}(V_2^2 - V_1^2) + \gamma(y_2 - y_1)$$

and with

$$V_1 = (40 \text{ mi/hr})\left(\frac{5280 \text{ ft/mi}}{3600 \text{ s/hr}}\right) = 58.7 \text{ ft/s}$$

and

$$V_2 = (47.4 \text{ mi/hr})\left(\frac{5280 \text{ ft/mi}}{3600 \text{ s/hr}}\right) = 69.5 \text{ ft/s}$$

it follows that

$$p_1 - p_2 = \frac{(0.00238 \text{ slugs/ft}^3)}{2}[(69.5 \text{ ft/s})^2 - (58.7 \text{ ft/s})^2]$$

$$+ (0.00238 \text{ slugs/ft}^3)(32.2 \text{ ft/s}^2)(100 \text{ ft} - 0 \text{ ft})$$

$$= 9.31 \text{ lb/ft}^2 = 0.0647 \text{ psi} \quad \textbf{(Ans)}$$

This result indicates that the pressure on the hill at point (2) is slightly lower than the pressure on the plain at some distance from the base of the hill with a 0.0533 psi difference due to the elevation increase and a 0.0114 psi difference due to the velocity increase.

The maximum velocity along the hill surface does not occur at point (2) but farther up the hill at $\theta = 63°$. At this point $V_{surface} = 1.26U$ (Problem 6.55). The minimum velocity ($V = 0$) and maximum pressure occur at point (3), the stagnation point.

Some Notes on the case of Rankine Half-body:

If the origin contains a source, a plane half-body is formed with its nose to the left, as in Fig.3.18*a*. If the origin is a *sink*, $m < 0$, the half-body nose is to the right, as in Fig.3.18*c*. In either case the stagnation point is at a position $a = m/U_\infty$ away from the origin.

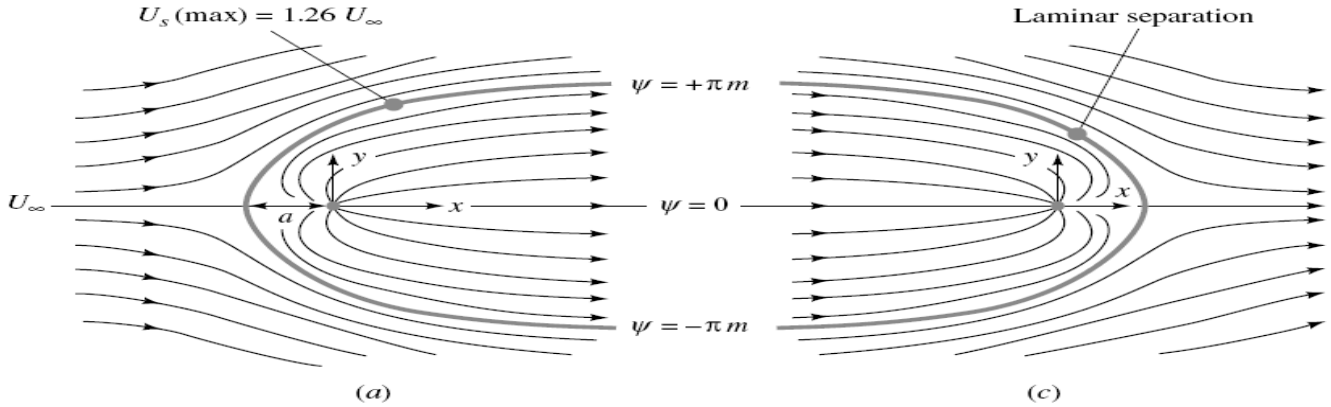

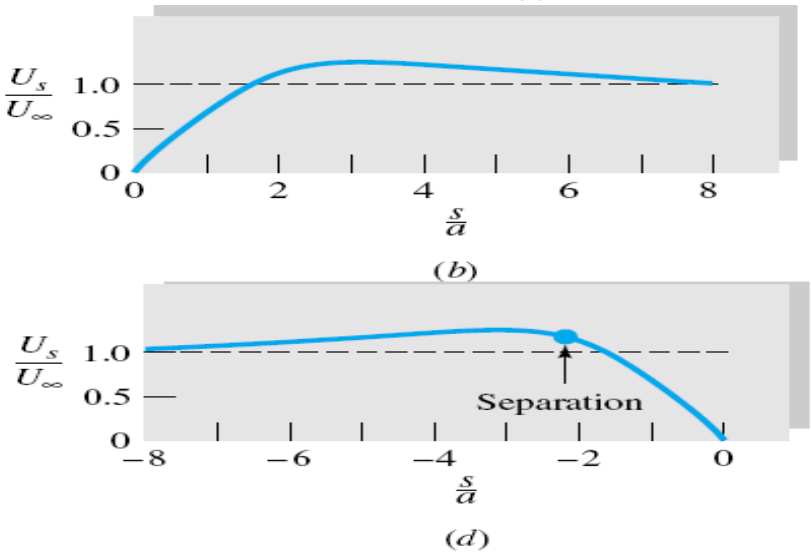

Fig.3.18 The Rankine half-body; pattern (*c*) is not found in a real fluid because of boundary-layer separation: (*a*) uniform stream plus a source equals a half-body; stagnation point at $x = -a = -m/U_\infty$; (*b*) slight adverse gradient for *s/a* greater than 3.0: no separation; (*c*) uniform stream plus a sink equals the rear of a half-body; stagnation point at $x = a = m/U_\infty$; (*d*) strong adverse gradient for $s/a > -3.0$: separation.

Boundary Layer Separation on Rankine half-body:

Although the inviscid-flow patterns, Fig.3.18 a and *c*, are mirror images, their viscous (boundary-layer) behavior is different. The body shape and the velocity along the surface are repeated here

$$V^2 = U_\infty^2\left(1 + \frac{a^2}{r^2} + \frac{2a}{r}\cos\theta\right) \qquad \text{along} \qquad r = \frac{m(\pi - \theta)}{U_\infty \sin\theta} \qquad (3.95)$$

The computed surface velocities are plotted along the half-body contours in Fig.3.18*b* and *d* as a function of arc length *s/a* measured from the stagnation point. These plots are also mirror images. However, if the nose is in front, Fig.3.18*b*, the pressure gradient there is *favorable* (decreasing pressure along the surface). In contrast, the pressure gradient is *adverse* (increasing pressure along the surface) when the nose is in the rear, Fig.3.18*d*, and boundary-layer separation may occur. Application to Fig.3.18*b* of laminar boundary reveals that separation does not occur on the front nose of the half-body. Therefore Fig.3.18*a* is a very realistic picture of streamlines past a half-body nose. In contrast, when applied to the tail, Fig.3.18*c*, Thwaites' method predicts separation at about $s/a \approx -2.2$, or $\theta \approx 110°$. Thus, if a half-body is a solid surface, Fig.3.18*c* is *not* realistic and a broad separated wake will form. However, if the half-body tail is a *fluid line* separating the sink-directed flow from the outer stream, as in Example 3.9 , then Fig.3.18*c* is quite realistic and useful. Computations for turbulent boundary-layer theory would be similar: separation on the tail, no separation on the nose.

Example 3.9:

An offshore power plant cooling-water intake sucks in 1500 ft^3/s in water 30 ft deep, as in Fig. 3.9 . If the tidal velocity approaching the intake is 0.7 ft/s, (*a*) how far downstream does the intake effect extend and (*b*) how much width *L* of tidal flow is entrained into the intake?

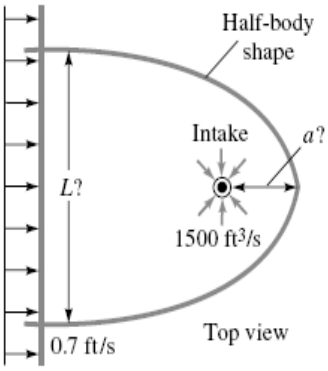

E 3.9

Solution

Recall that the sink strength m is related to the volume flow Q and the depth b into the paper

$$m = \frac{Q}{2\pi b} = \frac{1500\ \text{ft}^3/\text{s}}{2\pi(30\ \text{ft})} = 7.96\ \text{ft}^2/\text{s}$$

Therefore from Fig3.18the desired lengths a and L are

$$a = \frac{m}{U_\infty} = \frac{7.96\ \text{ft}^2/\text{s}}{0.7\ \text{ft/s}} = 11.4\ \text{ft} \qquad \textit{Ans. (a)}$$

$$L = 2\pi a = 2\pi(11.4\ \text{ft}) = 71\ \text{ft} \qquad \textit{Ans. (b)}$$

Example 3.10:

The bottom of a river has a 4-m-high bump which approximates a Rankine half-body, as in Fig. E3.10. The pressure at point *B* on the bottom is 130 kPa, and the river velocity is 2.5 m/s. Use inviscid theory to estimate the water pressure at point *A* on the bump, which is 2 m above point *B*.

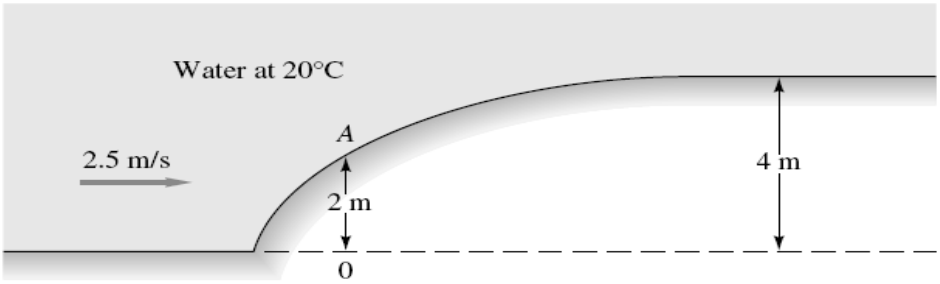

E3.10

Solution

As in all inviscid theories, we ignore the low-velocity boundary layers which form on solid surfaces due to the no-slip condition. From Eq. (3.91) and Fig.3.17 , the downstream bump half-height equals πa. Therefore, for our case, $a = (4\ \text{m})/\pi = 1.27$ m. We have to find the spot where the bump height is half that much, $h = 2\ \text{m} = \pi a/2$. From Eq. (3.91) we may compute

$$r = h_A = \frac{a(\pi - \theta)}{\sin\theta} = \frac{\pi}{2}a \qquad \text{or} \qquad \theta = \frac{\pi}{2} = 90^\circ$$

Thus point *A* in Fig. E3.10 is directly above the (initially unknown) origin of coordinates (labeled *O* in Fig. E3.10) and is 1.27 m to the right of the nose of the bump. With $r = \pi a/2$ and $\theta = \pi/2$ known, we compute the velocity at point *A*:

$$V_A^2 = U^2\left[1 + \frac{a^2}{(\pi a/2)^2} + \frac{2a}{\pi a/2}\cos\frac{\pi}{2}\right] = 1.405U^2$$

or

$$V_A \approx 1.185U = 1.185(2.5\ \text{m/s}) = 2.96\ \text{m/s}$$

For water at 20°C, take $\rho = 998$ kg/m^2 and $\gamma = 9790$ N/m^3. Now, since the velocity and elevation are known at point *A*, we are in a position to use Bernoulli's inviscid, incompressible-flow equation to estimate p_A from the known properties at point *B* (on the same streamline):

$$\frac{p_A}{\gamma} + \frac{V_A^2}{2g} + z_A \approx \frac{p_B}{\gamma} + \frac{V_B^2}{2g} + z_B$$

or

$$\frac{p_A}{9790\ \text{N/m}^3} + \frac{(2.96\ \text{m/s})^2}{2(9.81\ \text{m/s}^2)} + 2\ \text{m} \approx \frac{130{,}000}{9790} + \frac{(2.5)^2}{2(9.81)} + 0$$

Solving, we find

$$p_A = (13.60 - 2.45)(9790) \approx 109{,}200\ \text{Pa} \qquad \textit{Ans.}$$

If the approach velocity is uniform, this should be a pretty good approximation, since water is relatively inviscid and its boundary layers are thin.

3.4.2 A sink plus a Vortex at the Origin:

An interesting flow pattern, approximated in nature, occurs by superposition of a sink and a vortex, both centered at the origin. The composite stream function and velocity potential are

Sink plus vortex: $$\psi = m\theta - K \ln r \qquad \phi = m \ln r + K\theta \qquad (3.96)$$

When plotted, these form two orthogonal families of logarithmic spirals, as shown in Fig. 3.19 . This is a fairly realistic simulation of a tornado (where the sink flow moves up the z-axis into the atmosphere) or a rapidly draining bathtub vortex. At the center of a real (viscous) vortex, where Eq. (3.96) predicts infinite velocity, the actual circulating flow is highly *rotational* and approximates solid-body rotation $v_\theta \approx Cr$.

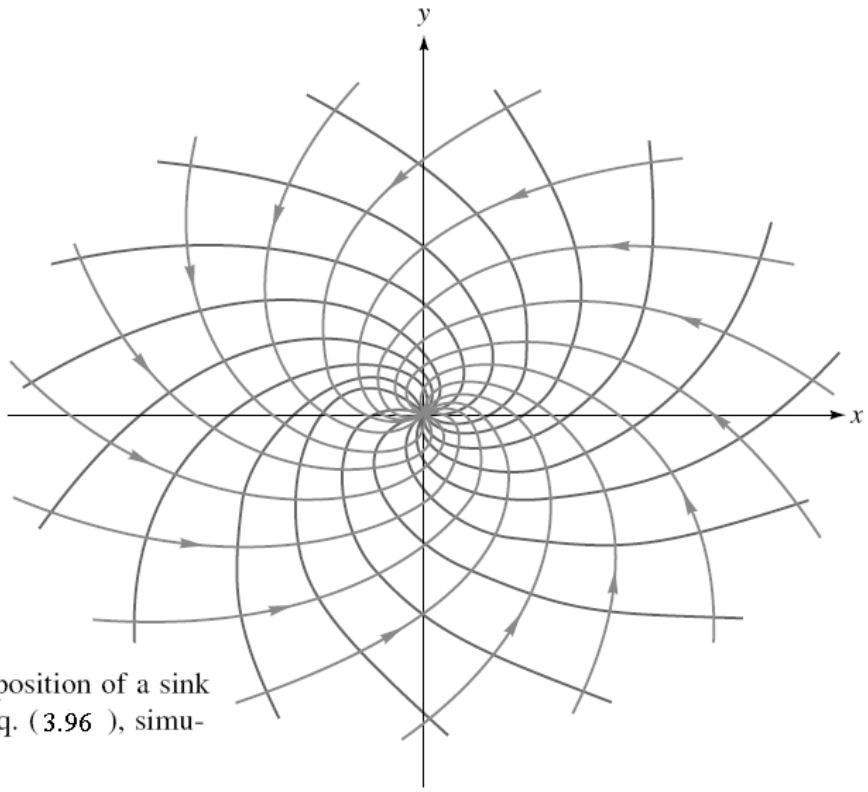

Fig. 3.19 Superposition of a sink plus a vortex, Eq. (3.96), simulates a tornado.

3.4.3 Flow Past a Vortex:

Consider a uniform stream U_∞ in the x direction flowing past a vortex of strength K with center at the origin. By superposition the combined stream function is

$$\psi = \psi_{\text{stream}} + \psi_{\text{vortex}} = U_\infty r \sin\theta - K \ln r \qquad (3.97)$$

The velocity components are given by

$$v_r = \frac{1}{r}\frac{\partial \psi}{\partial \theta} = U_\infty \cos\theta \qquad v_\theta = -\frac{\partial \psi}{\partial r} = -U_\infty \sin\theta + \frac{K}{r} \qquad (3.98)$$

The streamlines are plotted in Fig.3.20 by the graphical method, intersecting the circular streamlines of the vortex with the horizontal lines of the uniform stream.

By setting $v_r = v_\theta = 0$ from (3.98) we find a stagnation point at $\theta = 90°$, $r = a = K/U_\infty$, or $(x, y) = (0, a)$. This is where the counterclockwise vortex velocity K/r exactly cancels the stream velocity U_∞.

Probably the most interesting thing about this example is that there is a nonzero lift force normal to the stream on the surface of any region enclosing the vortex, but we postpone this discussion until the next section.

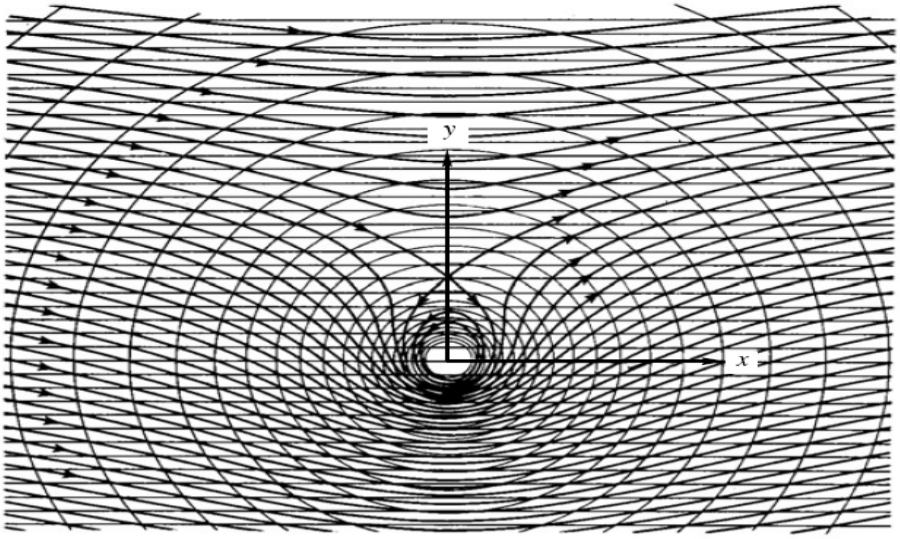

Fig.3.20 Flow of a uniform stream past a vortex constructed by the graphical method.

3.4.4 An Infinite Row of Vortices:

Consider an infinite row of vortices of equal strength K and equal spacing a, as in Fig. 3.21a. This case is included here to illustrate the interesting concept of a *vortex sheet*.

For a single line vortex, the stream function is $= -K \ln r$, where r is measured from the origin.

From this equation, the ith vortex in Fig.3.21a has a stream function $\psi_i = -K \ln r_i$, so that the total infinite row has a combined stream function

$$\psi = -K \sum_{i=1}^{\infty} \ln r_i \qquad (3.99)$$

It can be shown [2, sec. 4.51] that this infinite sum of logarithms is equivalent to a closed-form function

$$\psi = -\tfrac{1}{2}K \ln \left[\frac{1}{2} \left(\cosh \frac{2\pi y}{a} - \cos \frac{2\pi x}{a} \right) \right] \qquad (3.100)$$

Since the proof uses the complex variable $z = x + iy$, $i = (-1)^{1/2}$, we are not going to

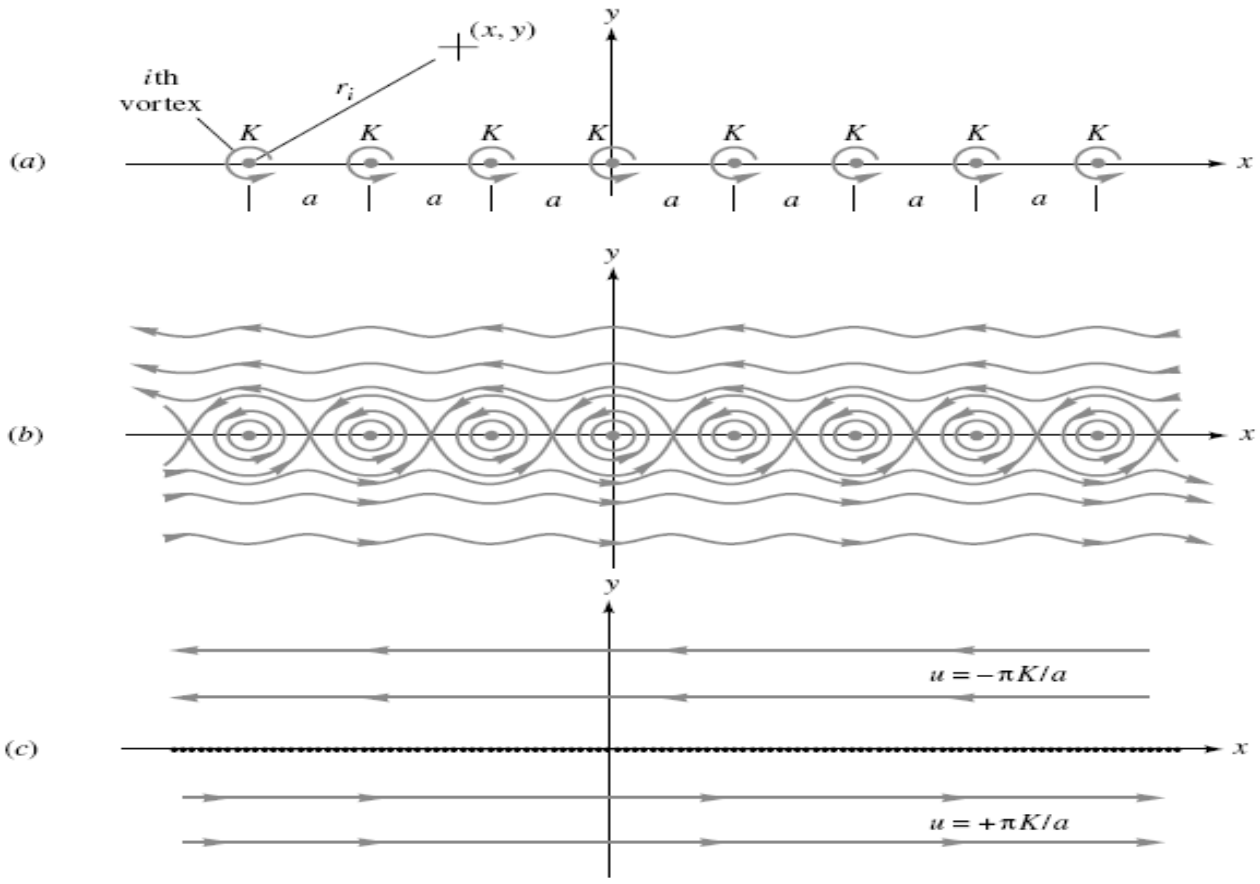

Fig.3.21 Superposition of vortices: (a) an infinite row of equal strength; (b) streamline pattern for part (a); (c) vortex sheet: part (b) viewed from afar.

The streamlines from Eq. (3.100) are plotted in Fig 3.21 *b*, showing what is called a *cat's-eye* pattern of enclosed flow cells surrounding the individual vortices. Above the cat's eyes the flow is entirely to the left, and below the cat's eyes the flow is to the right. Moreover, these left and right flows are uniform if $|y| \gg a$, which follows by differentiating Eq. (3.100)

$$u = \frac{\partial \psi}{\partial y}\bigg|_{|y| \gg a} = \pm \frac{\pi K}{a} \tag{3.101}$$

where the plus sign applies below the row and the minus sign above the row. This uniform left and right streaming is sketched in Fig. 3.21*c*. We stress that this effect is induced by the row of vortices: There is no uniform stream approaching the row in this example.

When Fig. 3.21*b* is viewed from afar, the streaming motion is uniform left above and uniform right below, as in Fig.3.21 *c*, and the vortices are packed so closely together

3.4.5 The Vortex Sheet:

When Fig. 3.21*b* is viewed from afar, the streaming motion is uniform left above and uniform right below, as in Fig. 3.21*c*, and the vortices are packed so closely together that they are smudged into a continuous *vortex sheet*. The strength of the sheet is defined as

$$\gamma = \frac{2\pi K}{a} \tag{3.102}$$

and in the general case γ can vary with x. The circulation about any closed curve which encloses a short length dx of the sheet would be,

$$d\Gamma = u_l\, dx - u_u\, dx = (u_l - u_u)\, dx = \frac{2\pi K}{a}\, dx = \gamma\, dx \tag{3.103}$$

where the subscripts l and u stand for lower and upper, respectively. Thus the sheet strength $\gamma = d\Gamma/dx$ is the circulation per unit length of the sheet. Thus when a vortex sheet is immersed in a uniform stream, γ is proportional to the lift per unit length of any surface enclosing the sheet.

Note that there is no velocity normal to the sheet at the sheet surface. Therefore a vortex sheet can simulate a thin-body shape, e.g., plate or thin airfoil. This is the basis of the thin-airfoil theory mentioned in last section of this part.

3.5 Rankine Ovals:

The half-body described in the previous section is a body that is "open" at one end. To study the flow around a closed body a source and a sink of equal strength can be combined with a uniform flow as shown in Fig. 3.22 *a*. The stream function for this combination is

$$\psi = Ur \sin\theta - \frac{m}{2\pi}(\theta_1 - \theta_2) \tag{3.104}$$

and the velocity potential is

$$\phi = Ur\cos\theta - \frac{m}{2\pi}(\ln r_1 - \ln r_2) \tag{3.105}$$

As discussed in Section 3.3.4 , the stream function for the source-sink pair can be expressed as in Eq. 3.85 and, therefore, Eq. 3.104 can also be written as

$$\psi = Ur\sin\theta - \frac{m}{2\pi}\tan^{-1}\left(\frac{2ar\sin\theta}{r^2 - a^2}\right)$$

or

$$\psi = Uy - \frac{m}{2\pi}\tan^{-1}\left(\frac{2ay}{x^2 + y^2 - a^2}\right) \tag{3.106}$$

The corresponding streamlines for this flow field are obtained by setting ψ = constant. If several of these streamlines are plotted, it will be discovered that the streamline $\psi = 0$ forms a closed body as is illustrated in Fig. 3.22 *b*. We can think of this streamline as forming the surface of a body of length 2ℓ and width $2h$ placed in a uniform stream. The streamlines inside the body are of no practical interest and are not shown. Note that since the body is closed, all of the flow emanating from the source flows into the sink. These bodies have an oval shape and are termed *Rankine ovals*.

Stagnation points occur at the upstream and downstream ends of the body as are indicated in Fig.3.22 *b*. These points can be located by determining where along the x axis the velocity is zero. The stagnation points correspond to the points where the uniform velocity, the source velocity, and the sink velocity all combine to give a zero velocity. The location of the stagnation points depend on the value of a, m, and U. The body half-length, ℓ (the value of $|x|$ that gives $\mathbf{V} = 0$ when $y = 0$), can be expressed as

$$\ell = \left(\frac{ma}{\pi U} + a^2\right)^{1/2} \tag{3.107}$$

or

$$\frac{\ell}{a} = \left(\frac{m}{\pi U a} + 1\right)^{1/2} \tag{3.108}$$

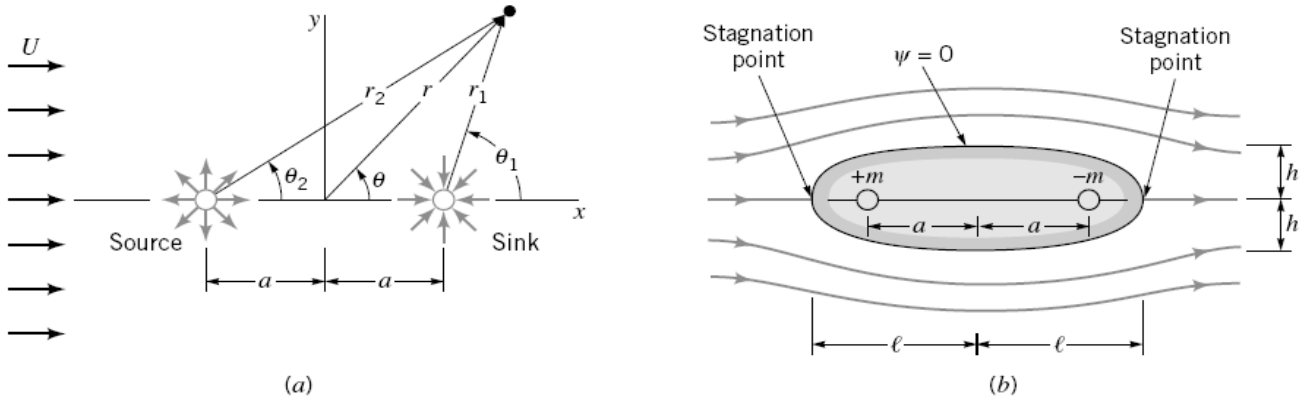

■ **FIGURE 3.22** **The flow around a Rankine oval: (*a*) superposition of source-sink pair and a uniform flow; (*b*) replacement of streamline $\psi = 0$ with solid boundary to form Rankine oval.**

The body half-width, h, can be obtained by determining the value of y where the y axis intersects the $\psi = 0$ streamline. Thus, from Eq. 3.106 with $\psi = 0, x = 0$, and $y = h$, it follows that

$$h = \frac{h^2 - a^2}{2a} \tan \frac{2\pi Uh}{m} \tag{3.109}$$

or

$$\frac{h}{a} = \frac{1}{2}\left[\left(\frac{h}{a}\right)^2 - 1\right] \tan\left[2\left(\frac{\pi Ua}{m}\right)\frac{h}{a}\right] \tag{3.110}$$

Equations 3.108 and 3.110 show that both ℓ/a and h/a are functions of the dimensionless parameter, $\pi Ua/m$. Although for a given value of Ua/m the corresponding value of ℓ/a can be determined directly from Eq. 3.108 , h/a must be determined by a trial and error solution of 3.110 .

A large variety of body shapes with different length to width ratios can be obtained by using different values of Ua/m. As this parameter becomes large, flow around a long slender body is described, whereas for small values of the parameter, flow around a more blunt shape is obtained. Downstream from the point of maximum body width the surface pressure increases with distance along the surface. This condition (called an adverse pressure gradient) typically leads to separation of the flow from the surface, resulting in a large low pressure wake on the downstream side of the body. Separation is not predicted by potential theory (which simply indicates a symmetrical flow) and, therefore, the potential solution for the Rankine ovals will give a reasonable approximation of the velocity outside the thin, viscous boundary layer and the pressure distribution on the front part of the body only.

Table 3.2 Rankine-Oval Parameters

$m/(U_\infty a)$	h/a	L/a	L/h	u_{max}/U_∞
0.0	0.0	1.0	∞	1.0
0.01	0.031	1.010	32.79	1.020
0.1	0.263	1.095	4.169	1.187
1.0	1.307	1.732	1.326	1.739
10.0	4.435	4.583	1.033	1.968
100.0	14.130	14.177	1.003	1.997
∞	∞	∞	1.000	2.000

3.6 Flow Around a Circular Cylinder

As was noted in the previous section, when the distance between the source-sink pair approaches zero, the shape of the Rankine oval becomes more blunt and in fact approaches a circular shape. Since the doublet described in Section 3.3.4 was developed by letting a source-sink pair approach one another, it might be expected that a uniform flow in the positive x direction combined with a doublet could be used to represent flow around a circular cylinder. This combination gives for the stream function

$$\psi = Ur \sin\theta - \frac{K \sin\theta}{r} \tag{3.111}$$

and for the velocity potential

$$\phi = Ur \cos\theta + \frac{K \cos\theta}{r} \tag{3.112}$$

In order for the stream function to represent flow around a circular cylinder it is necessary that ψ = constant for $r = a$, where a is the radius of the cylinder. Since Eq. 3.111 can be written as

$$\psi = \left(U - \frac{K}{r^2}\right) r \sin\theta$$

it follows that $\psi = 0$ for $r = a$ if

$$U - \frac{K}{a^2} = 0$$

which indicates that the doublet strength, K, must be equal to Ua^2. Thus, the stream function for flow around a circular cylinder can be expressed as

$$\psi = Ur\left(1 - \frac{a^2}{r^2}\right) \sin\theta \tag{3.113}$$

and the corresponding velocity potential is

$$\phi = Ur\left(1 + \frac{a^2}{r^2}\right) \cos\theta \tag{3.114}$$

A sketch of the streamlines for this flow field is shown in Fig. 3.23 .

The velocity components can be obtained from either Eq. 3.113 or 3.114 as

$$v_r = \frac{\partial\phi}{\partial r} = \frac{1}{r}\frac{\partial\psi}{\partial\theta} = U\left(1 - \frac{a^2}{r^2}\right)\cos\theta \tag{3.115}$$

and

$$v_\theta = \frac{1}{r}\frac{\partial\phi}{\partial\theta} = -\frac{\partial\psi}{\partial r} = -U\left(1 + \frac{a^2}{r^2}\right)\sin\theta \tag{3.116}$$

On the surface of the cylinder ($r = a$) it follows from Eq. 3.115 and 3.116 that $v_r = 0$ and

$$v_{\theta s} = -2U \sin\theta$$

We observe from this result that the maximum velocity occurs at the top and bottom of the cylinder ($\theta = \pm\pi/2$) and has a magnitude of twice the upstream velocity, U. As we move away from the cylinder along the ray $\theta = \pi/2$ the velocity varies, as is illustrated in Fig. 3.23 .

The pressure distribution on the cylinder surface is obtained from the Bernoulli equation written from a point far from the cylinder where the pressure is p_0 and the velocity is U so that

$$p_0 + \tfrac{1}{2}\rho U^2 = p_s + \tfrac{1}{2}\rho v_{\theta s}^2$$

where p_s is the surface pressure. Elevation changes are neglected. Since $v_{\theta s} = -2U \sin\theta$, the surface pressure can be expressed as

$$p_s = p_0 + \tfrac{1}{2}\rho U^2(1 - 4\sin^2\theta) \tag{3.117}$$

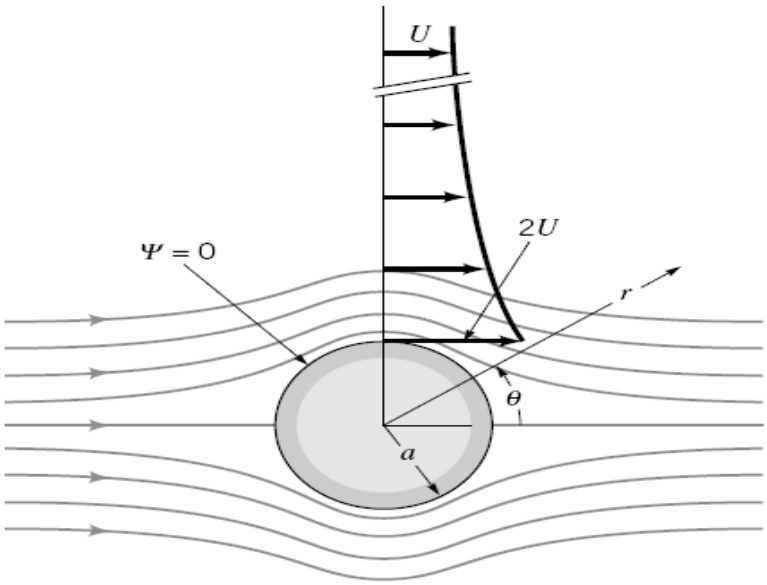

FIGURE 3.23 The flow around a circular cylinder.

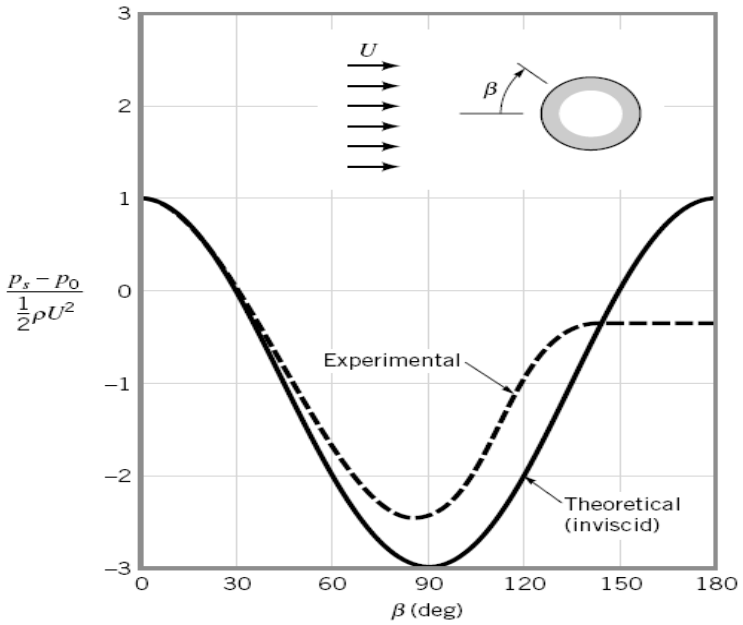

■ **FIGURE 3.24 A comparison of theoretical (inviscid) pressure distribution on the surface of a circular cylinder with typical experimental distribution.**

A comparison of this theoretical, symmetrical pressure distribution expressed in dimensionless form with a typical measured distribution is shown in Fig. 3.24 . This figure clearly reveals that only on the upstream part of the cylinder is there approximate agreement between the potential flow and the experimental results. Because of the viscous boundary layer that develops on the cylinder, the main flow separates from the surface of the cylinder, leading to the large difference between the theoretical, frictionless fluid solution and the experimental results on the downstream side of the cylinder .

The resultant force (per unit length) developed on the cylinder can be determined by integrating the pressure over the surface. From Fig. 3.25 it can be seen that

$$F_x = -\int_0^{2\pi} p_s \cos\theta \, a \, d\theta \tag{3.118}$$

and

$$F_y = -\int_0^{2\pi} p_s \sin\theta \, a \, d\theta \tag{3.119}$$

where F_x is the *drag* (force parallel to direction of the uniform flow) and F_y is the *lift* (force perpendicular to the direction of the uniform flow). Substitution for p_s from Eq. 3.117 into these two equations, and subsequent integration, reveals that $F_x = 0$ and $F_y = 0$ (Problem 3.64). These results indicate that both the drag and left as predicted by potential theory for

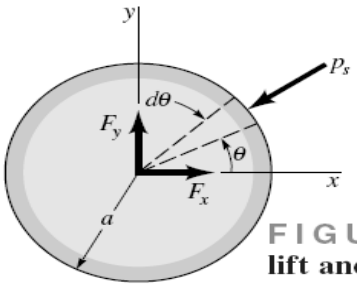

FIGURE 3.25 The notation for determining lift and drag on a circular cylinder.

a fixed cylinder in a uniform stream are zero. Since the pressure distribution is symmetrical around the cylinder, this is not really a surprising result. However, we know from experience that there is a significant drag developed on a cylinder when it is placed in a moving fluid. This discrepancy is known as d'Alembert's paradox. The paradox is named after **Jean le Rond d'Alembert** (1717–1783), a French mathematician and philosopher, who first showed that the drag on bodies immersed in inviscid fluids is zero. It was not until the latter part of the nineteenth century and the early part of the twentieth century that the role viscosity plays in the steady fluid motion was understood and d'Alembert's paradox explained.

Example 3.11:

When a circular cylinder is placed in a uniform stream, a stagnation point is created on the cylinder as is shown in Fig.E3.11*a*. If a small hole is located at this point, the stagnation pressure, p_{stag}, can be measured and used to determine the approach velocity, U. (a) Show how p_{stag} and U are related. (b) If the cylinder is misaligned by an angle α (Fig.E3.11*b*), but the measured pressure still interpreted as the stagnation pressure, determine an expression for the ratio of the true velocity, U, to the predicted velocity, U'. Plot this ratio as a function of α for the range $-20° \le \alpha \le 20°$.

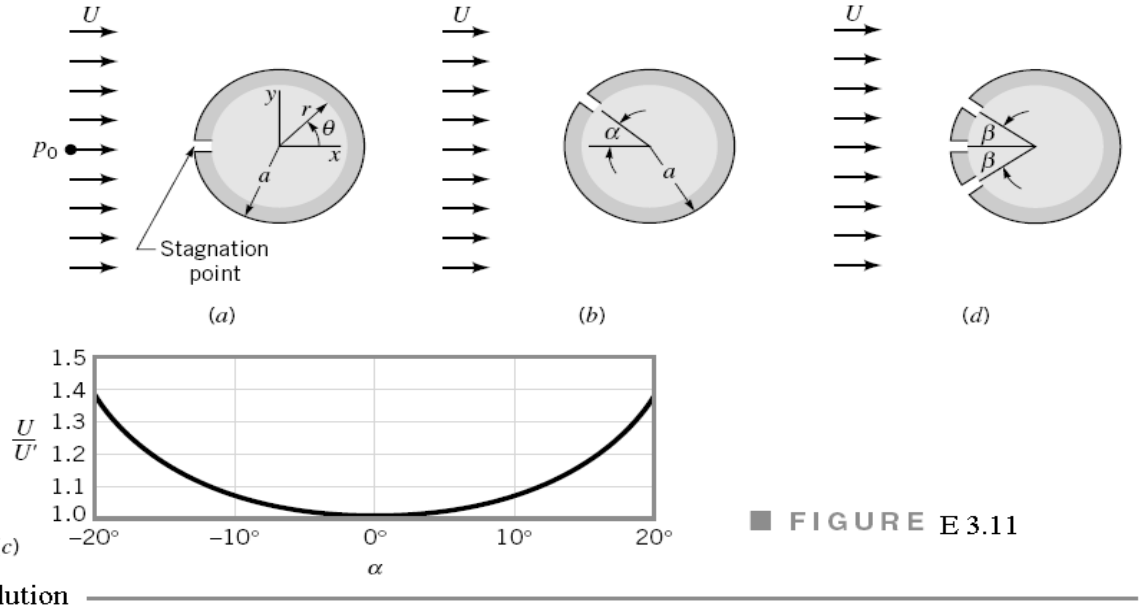

FIGURE E 3.11

Solution

(a) The velocity at the stagnation point is zero so the Bernoulli equation written between a point on the stagnation streamline upstream from the cylinder and the stagnation point gives

$$\frac{p_0}{\gamma} + \frac{U^2}{2g} = \frac{p_{stag}}{\gamma}$$

Thus,

$$U = \left[\frac{2}{\rho}(p_{stag} - p_0)\right]^{1/2} \qquad \text{(Ans)}$$

A measurement of the difference between the pressure at the stagnation point and the upstream pressure can be used to measure the approach velocity. This is, of course, the same result that was obtained for Pitot-static tubes.

(b) If the direction of the fluid approaching the cylinder is not known precisely, it is possible that the cylinder is misaligned by some angle, α. In this instance the pressure actually measured, p_α, will be different from the stagnation pressure, but if the misalignment is not recognized the predicted approach velocity, U', would still be calculated as

Thus,
$$U' = \left[\frac{2}{\rho}(p_\alpha - p_0)\right]^{1/2}$$
$$\frac{U(\text{true})}{U'(\text{predicted})} = \left(\frac{p_{\text{stag}} - p_0}{p_\alpha - p_0}\right)^{1/2} \quad (1)$$

The velocity on the surface of the cylinder, v_θ, where $r = a$, is obtained from Eq. 6.115 as
$$v_\theta = -2U \sin\theta$$
If we now write the Bernoulli equation between a point upstream of the cylinder and the point on the cylinder where $r = a$, $\theta = \alpha$, it follows that
$$p_0 + \frac{1}{2}\rho U^2 = p_\alpha + \frac{1}{2}\rho(-2U \sin\alpha)^2$$
and, therefore,
$$p_\alpha - p_0 = \tfrac{1}{2}\rho U^2(1 - 4\sin^2\alpha) \quad (2)$$
Since $p_{\text{stag}} - p_0 = \frac{1}{2}\rho U^2$ it follows from Eqs. 1 and 2 that
$$\frac{U(\text{true})}{U'(\text{predicted})} = (1 - 4\sin^2\alpha)^{-1/2} \quad \text{(Ans)}$$

This velocity ratio is plotted as a function of the misalignment angle α in Fig. E6.8*c*.

It is clear from these results that significant errors can arise if the stagnation pressure tap is not aligned with the stagnation streamline. As is discussed in Section 3.5, if two additional, symmetrically located holes are drilled on the cylinder, as are illustrated in Fig. E6.8*d*, the correct orientation of the cylinder can be determined. The cylinder is rotated until the pressure in the two symmetrically placed holes are equal, thus indicating that the center hole coincides with the stagnation streamline. For $\beta = 30°$ the pressure at the two holes theoretically corresponds to the upstream pressure, p_0. With this orientation a measurement of the difference in pressure between the center hole and the side holes can be used to determine U.

3.7 Flow Around a Cylinder with Circulation:

An additional, interesting potential flow can be developed by adding a free vortex to the stream function or velocity potential for the flow around a cylinder. In this case we add a vortex at the doublet center, which does not change the shape of the cylinder.

the stream function for flow past a circular cylinder with circulation, centered at the origin, is a uniform stream plus a doublet plus a vortex

$$\psi = U_\infty r \sin\theta - \frac{\lambda \sin\theta}{r} - K \ln r + \text{const} \quad (3.120)$$

The doublet strength λ has units of velocity times length squared. For convenience, let $\lambda = U_\infty a^2$, where a is a length, and let the arbitrary constant in Eq. (3.120) equal $K \ln a$. Then the stream function becomes

$$\psi = U_\infty \sin\theta\left(r - \frac{a^2}{r}\right) - K \ln\frac{r}{a} \quad (3.121)$$

The streamlines are plotted in Fig. 3.26 for four different values of the dimensionless vortex strength $K/(U_\infty a)$. For all cases the line $\psi = 0$ corresponds to the circle $r = a$, that is, the shape of the cylindrical body. As circulation $\Gamma = 2\pi K$ increases, the velocity becomes faster and faster below the cylinder and slower and slower above it. The velocity components in the flow are given by

$$v_r = \frac{1}{r}\frac{\partial\psi}{\partial\theta} = U_\infty \cos\theta\left(1 - \frac{a^2}{r^2}\right)$$
$$v_\theta = -\frac{\partial\psi}{\partial r} = -U_\infty \sin\theta\left(1 + \frac{a^2}{r^2}\right) + \frac{K}{r} \quad (3.122)$$

The velocity at the cylinder surface $r = a$ is purely tangential, as expected

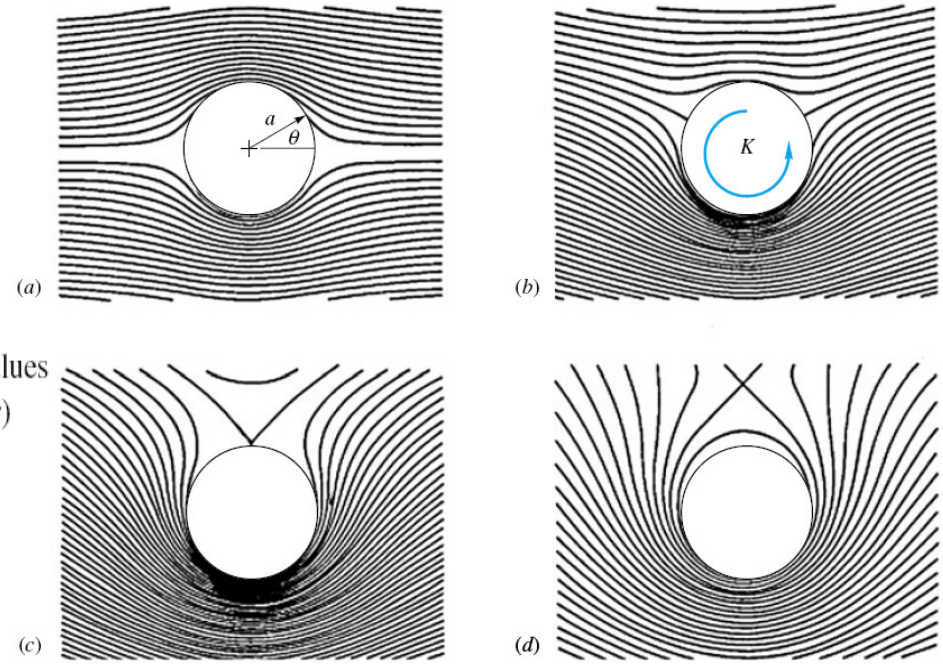

Fig. 3.26 Flow past a circular cylinder with circulation for values of $K/(U_\infty a)$ of (*a*) 0, (*b*) 1.0, (*c*) 2.0, and (*d*) 3.0.

$$v_r(r = a) = 0 \quad v_\theta(r = a) = -2U_\infty \sin\theta + \frac{K}{a} \tag{3.123}$$

For small K, two stagnation points appear on the surface at angles θ_s where $v_\theta = 0$, or, from Eq. (3.123),

$$\sin\theta_s = \frac{K}{2U_\infty a} \tag{3.124}$$

Figure 3.26 *a* is for $K = 0$, $\theta_s = 0$ and 180°, or doubly symmetric inviscid flow past a cylinder with no circulation. Figure 3.26 *b* is for $K/(U_\infty a) = 1$, $\theta_s = 30$ and 150°, and Fig. 3.26 *c* is the limiting case where the two stagnation points meet at the top, $K/(U_\infty a) = 2$, $\theta_s = 90°$.

For $K > 2U_\infty a$, Eq. (3.124) is invalid, and the single stagnation point is above the cylinder, as in Fig. 3.26 *d*, at a point $y = h$ given by

$$\frac{h}{a} = \frac{1}{2}\left[\beta + (\beta^2 - 4)^{1/2}\right] \qquad \beta = \frac{K}{U_\infty a} > 2 \tag{3.125}$$

In Fig. 3.26 *d*, $K/(U_\infty a) = 3.0$, and $h/a = 2.6$.

For the cylinder flows of Fig. 3.26 *b* to *d* there is a downward force, or negative lift, called the *Magnus effect*, which is proportional to stream velocity and vortex strength. We can see from the streamline pattern that the velocity on the top of the cylinder is less and therefore the pressure higher from Bernoulli's equation; this explains the force. There is no viscous force, of course, because our theory is inviscid.

The surface velocity is given by Eq. (3.123). From Bernoulli's equation , neglecting gravity, the surface pressure p_s is given by

$$p_\infty + \frac{1}{2}\rho U_\infty^2 = p_s + \frac{1}{2}\rho\left(-2U_\infty \sin\theta + \frac{K}{a}\right)^2$$

or

$$p_s = p_\infty + \tfrac{1}{2}\rho U_\infty^2(1 - 4\sin^2\theta + 4\beta\sin\theta - \beta^2) \tag{3.126}$$

where $\beta = K/(U_\infty a)$ and p_∞ is the free-stream pressure. If b is the cylinder depth into the paper, the drag D is the integral over the surface of the horizontal component of

pressure force

$$D = -\int_0^{2\pi} (p_s - p_\infty) \cos\theta \, ba \, d\theta$$

where $p_s - p_\infty$ is substituted from Eq. (3.126). But the integral of cos θ times any power of sin θ over a full cycle 2π is identically zero. Thus we obtain the (perhaps surprising) result

$$D(\text{cylinder with circulation}) = 0 \tag{3.127}$$

This is a special case of d'Alembert's paradox,

> According to inviscid theory, the drag of any body of any shape immersed in a uniform stream is identically zero.

D'Alembert published this result in 1752 and pointed out himself that it did not square with the facts for real fluid flows. This unfortunate paradox caused everyone to overreact and reject all inviscid theory until 1904, when Prandtl first pointed out the profound effect of the thin viscous boundary layer on the flow pattern in the rear.

The lift force L normal to the stream, taken positive upward, is given by summation of vertical pressure forces

$$L = -\int_0^{2\pi} (p_s - p_\infty) \sin\theta \, ba \, d\theta$$

The Kutta-Joukowiski Lift Theorem:

Since the integral over 2π of any odd power of sin θ is zero, only the third term in the parentheses in Eq. (3.126) contributes to the lift:

$$L = -\frac{1}{2}\rho U_\infty^2 \frac{4K}{aU_\infty} ba \int_0^{2\pi} \sin^2\theta \, d\theta = -\rho U_\infty (2\pi K) b$$

or

$$\frac{L}{b} = -\rho U_\infty \Gamma \tag{3.128}$$

Notice that the lift is independent of the radius a of the cylinder. Actually, though, as we shall see in Sec. 3.7 , the circulation Γ depends upon the body size and orientation through a physical requirement.

Equation (3.128) was generalized by W. M. Kutta in 1902 and independently by N. Joukowski in 1906 as follows:

> According to inviscid theory, the lift per unit depth of any cylinder of any shape immersed in a uniform stream equals $\rho u_\infty \Gamma$, where Γ is the total net circulation contained within the body shape. The direction of the lift is 90° from the stream direction, rotating opposite to the circulation.

The problem in airfoil analysis, Sec. 3.7 , is thus to determine the circulation Γ as a function of airfoil shape and orientation.

Experimental Lift and Drag of Rotating Cylinder:

It is nearly impossible to test Fig. 3.26 by constructing a doublet and vortex with the same center and then letting a stream flow past them. But one physical realization would be a rotating cylinder in a stream. The viscous no-slip condition would cause the fluid in contact with the cylinder to move tangentially at the cylinder peripheral speed $v_\theta = a\omega$. A net circulation Γ would be set up by this no-slip mechanism, but it turns out to be less than 50 percent of the value expected from inviscid theory, primarily because of flow separation behind the cylinder.

Figure 3.27 shows experimental lift and drag coefficients, based on planform area $2ba$, of rotating cylinders. From Eq. (3.127) the theoretical drag is zero, but the actual C_D is quite large, more even than the stationary cylinder .The theoretical lift follows from Eq. (3.128)

$$C_L = \frac{L}{\frac{1}{2}\rho U_\infty^2 (2ba)} = \frac{2\pi\rho U_\infty K b}{\rho U_\infty^2 ba} = \frac{2\pi v_{\theta s}}{U_\infty} \tag{3.129}$$

where $v_{\theta s} = K/a$ is the peripheral speed of the cylinder.

Figure 3.27 shows that the theoretical lift from Eq. (3.129) is much too high, but the measured lift is quite respectable, much larger in fact than a typical airfoil of the same chord length . Thus rotating cylinders have practical possibilities.

Flettner rotor ship built in Germany in 1924 employed rotating vertical cylinders which developed a thrust due to any winds blowing past the ship. The Flettner design did not

gain any popularity, but such inventions may be more attractive in this era of high energy costs.

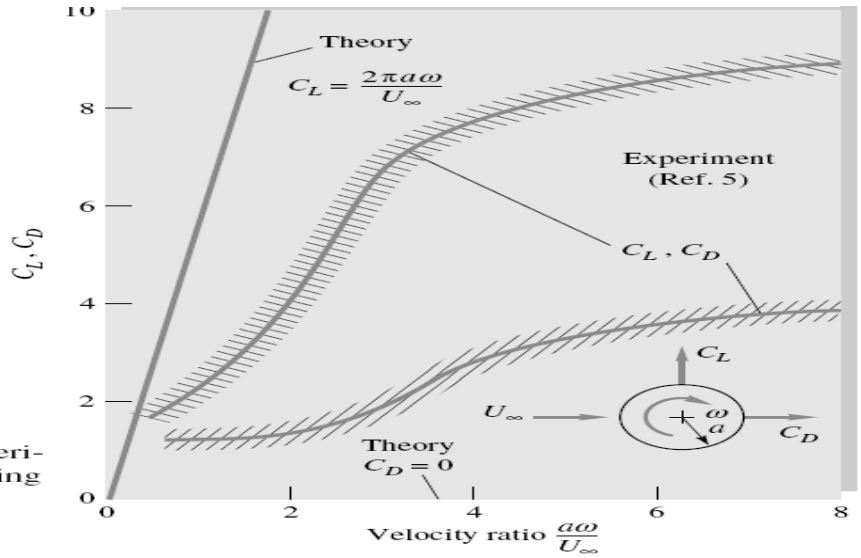

Fig. 3.27 Theoretical and experimental lift and drag of a rotating cylinder. (*From Ref. 22.*)

Example 3.12:

The experimental Flettner rotor sailboat at the University of Rhode Island is shown in Fig. E3.12 The rotor is 2.5 ft in diameter and 10 ft long and rotates at 220 r/min. It is driven by a small lawnmower engine. If the wind is a steady 10 kn and boat relative motion is neglected, what is the maximum thrust expected for the rotor? Assume standard air and water density.

E3.12

(Courtesy of R. C. Lessmann, University of Rhode Island.)

Solution

Convert the rotation rate to $\omega = 2\pi(220)/60 = 23.04$ rad/s. The wind velocity is 10 kn = 16.88 ft/s, so the velocity ratio is $\dfrac{a\omega}{U_\infty} = \dfrac{(1.25\text{ ft})(23.04\text{ rad/s})}{16.88\text{ ft/s}} = 1.71$

Entering Fig. 3.27 , we read $C_L \approx 3.3$ and $C_D \approx 1.2$. From Table , standard air density is 0.002377 slug/ft^3. Then the estimated rotor lift and drag are

$$L = C_L \tfrac{1}{2}\rho U_\infty^2 2ba = 3.3(\tfrac{1}{2})(0.002377)(16.88)^2(2)(10)(1.25)$$

$$= 27.9 \text{ lbf}$$

$$D = C_D \tfrac{1}{2}\rho U_\infty^2 2ba = L\frac{C_D}{C_L} = 27.9\left(\frac{1.2}{3.3}\right) = 10.2 \text{ lbf}$$

The maximum thrust available is the resultant of these two

$$F = [(27.9)^2 + (10.2)^2]^{1/2} = 29 \text{ lbf} \qquad \textit{Ans.}$$

If aligned along the boat's keel, this thrust will drive the boat at a speed of about 5 kn through the water.

3.8 The Kelvin Oval:

A family of body shapes taller than they are wide can be formed by letting a uniform stream flow normal to a vortex pair. If U_∞ is to the right, the negative vortex $-K$ is placed at $y = +a$ and the counterclockwise vortex $+K$ placed at $y = -a$, as in Fig. 3.28 . The combined stream function is

$$\psi = U_\infty y - \frac{1}{2} K \ln \frac{x^2 + (y + a)^2}{x^2 + (y - a)^2} \tag{3.130}$$

The body shape is the line $\psi = 0$, and some of these shapes are shown in Fig. 3.28 . For $K/(U_\infty a) > 10$ the shape is within 1 percent of a Rankine oval (Fig.3.22) turned 90°, but for small $K/(U_\infty a)$ the waist becomes pinched in, and a figure-eight shape occurs at 0.5. For $K/(U_\infty a) < 0.5$ the stream blasts right between the vortices and isolates two more or less circular body shapes, one surrounding each vortex.

A closed body of practically any shape can be constructed by proper superposition of sources, sinks, and vortices. See the advanced work in Refs. 2 to 4 for further details.

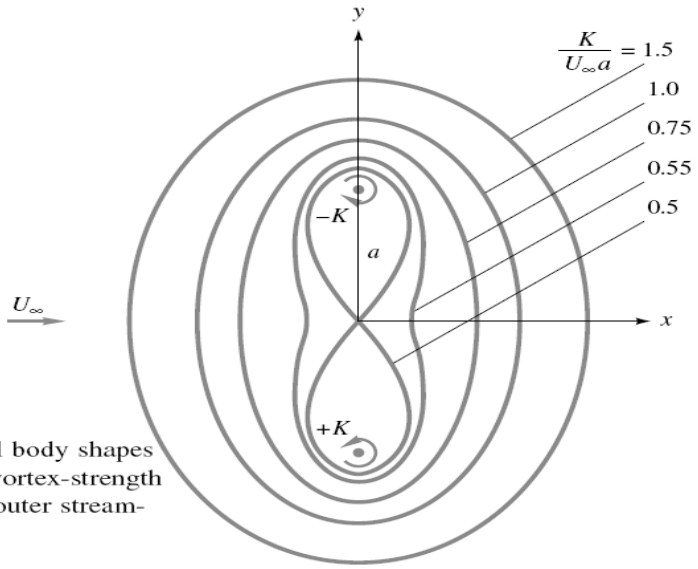

Fig. 3.28 Kelvin-oval body shapes as a function of the vortex-strength parameter $K/(U_\infty a)$; outer streamlines not shown.

3.9 Potential Flow Analogs:

For complicated potential-flow geometries, one can resort to other methods than superposition of sources, sinks, and vortices. There are a variety of devices which simulate solutions to Laplace's equation.

From 1897 to 1900 Hele-Shaw [9] developed a technique whereby laminar flow between very closely spaced parallel plates simulated potential flow when viewed from above the plates. Obstructions simulate body shapes, and dye streaks represent the streamlines. The Hele-Shaw apparatus makes an excellent laboratory demonstration of potential flow [10, pp. 8–10]. Figure 3.29 *a* illustrates Hele-Shaw (potential) flow through an array of cylinders, a flow pattern that would be difficult to analyze just using Laplace's equation. However beautiful this array pattern may be, it is not a good approximation to real (laminar viscous) array flow. Figure 3.29 *b* shows experimental streakline patterns for a similar staggered-array flow at Re ≈ 6400. We see that the interacting wakes of the real flow (Fig. 3.29 *b*) cause intensive mixing and transverse motion, not the smooth streaming passage of the potential-flow model (Fig. 3.29 *a*). The moral is that this is an internal flow with multiple bodies and, therefore, not a good candidate for a realistic potential-flow model.

Other flow-mapping techniques are discussed in Ref. 8. Electromagnetic fields also satisfy Laplace's equation, with voltage analogous to velocity potential and current lines analogous to streamlines. At one time commercial analog field plotters were available, using thin conducting paper cut to the shape of the flow geometry. Potential lines (voltage contours) were plotted by probing the paper with a potentiometer pointer.

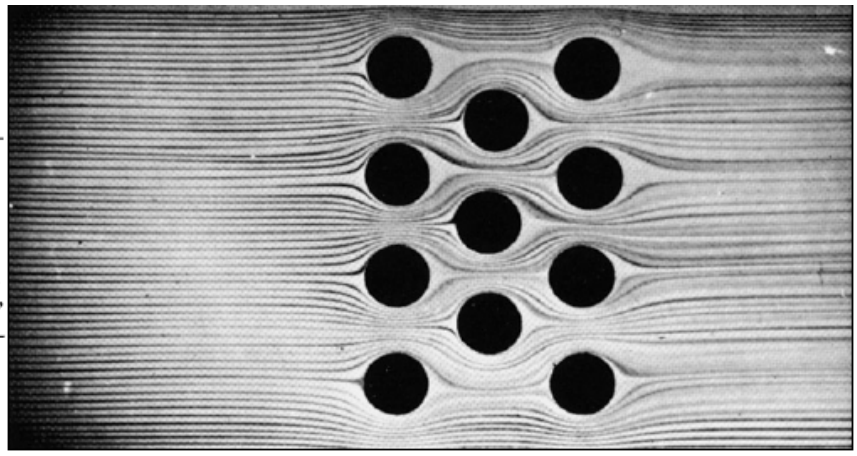

(a)

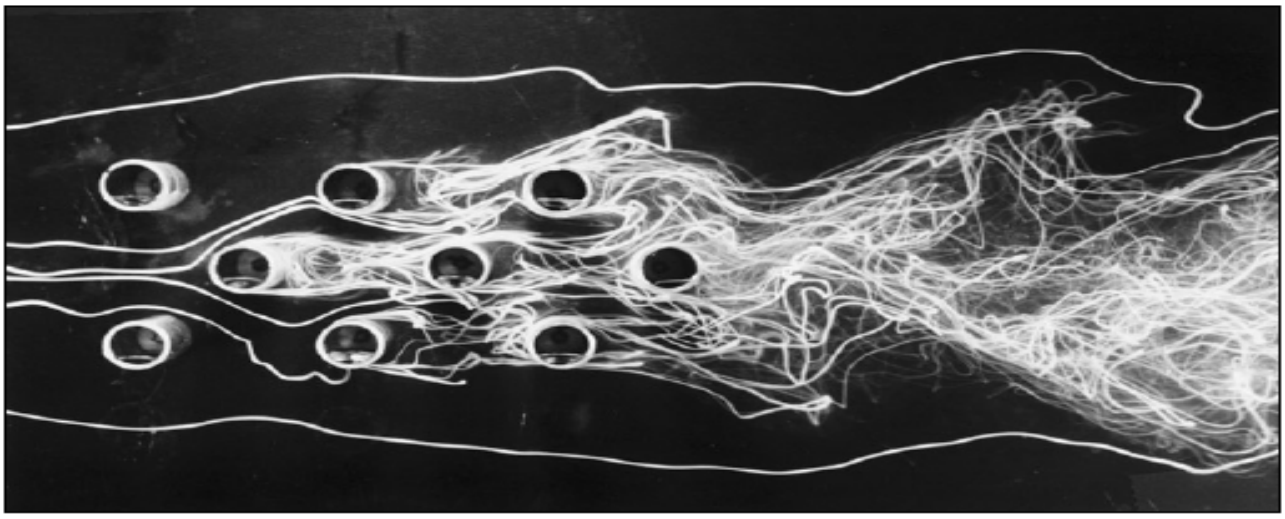

(b)

Fig. 3.29 Flow past a staggered array of cylinders: (*a*) potential-flow model using the Hele-Shaw apparatus *(Tecquipment Ltd., Nottingham, England)*; (*b*) experimental streaklines for actual staggered-array flow at $\mathrm{Re}_D \approx 6400$. *(From Ref. 36, courtesy of Jack Hoyt, with the permission of the American Society of Mechanical Engineers.)*

Hand-sketching "curvilinear square" techniques were also popular. The availability and the simplicity of digital-computer potential-flow methods [5 to 7] have made analog models obsolete.

Example 3.13:

A Kelvin oval from Fig. 3.28 has $K/(U_\infty a) = 1.0$. Compute the velocity at the top shoulder of the oval in terms of U_∞.

Solution

We must locate the shoulder $y = h$ from Eq. (3.130) for $\psi = 0$ and then compute the velocity by differentiation. At $\psi = 0$ and $y = h$ and $x = 0$, Eq. (3.130) becomes

$$\frac{h}{a} = \frac{K}{U_\infty a} \ln \frac{h/a + 1}{h/a - 1}$$

With $K/(U_\infty a) = 1.0$ and the initial guess $h/a \approx 1.5$ from Fig. 3.28 , we iterate and find the location $h/a = 1.5434$.

By inspection $v = 0$ at the shoulder because the streamline is horizontal. Therefore the shoulder velocity is, from Eq. (3.130),

$$u\Big|_{y=h} = \frac{\partial \psi}{\partial y}\Big|_{y=h} = U_\infty + \frac{K}{h-a} - \frac{K}{h+a}$$

Introducing $K = U_\infty a$ and $h = 1.5434a$, we obtain

$$u_{\text{shoulder}} = U_\infty(1.0 + 1.84 - 0.39) = 2.45U_\infty \qquad \textit{Ans.}$$

Because they are short-waisted compared with a circular cylinder, all the Kelvin ovals have shoulder velocity greater than the cylinder result $2.0U_\infty$ from Eq. (3.123).

3.10 Other Plane Potential Flows [The Complex Potential W(z)]:

In principle, any plane potential flow can be solved by the method of *conformal mapping*, by using the complex variable $z = x + iy \qquad i = (-1)^{1/2}$

It turns out that any arbitrary analytic function of this complex variable z has the remarkable property that both its real and its imaginary parts are solutions of Laplace's equation. If $f(z) = f(x + iy) = f_1(x, y) + i f_2(x, y)$

then
$$\frac{\partial^2 f_1}{\partial x^2} + \frac{\partial^2 f_1}{\partial y^2} = 0 = \frac{\partial^2 f_2}{\partial x^2} + \frac{\partial^2 f_2}{\partial y^2} \tag{3.131}$$

We shall assign the proof of this as a problem. Even more remarkable if you have never seen it before is that lines of constant f_1 will be everywhere perpendicular to lines of constant f_2:
$$\left(\frac{dy}{dx}\right)_{f_1=C} = -\frac{1}{(dy/dx)_{f_2=C}} \tag{3.132}$$

We also leave this proof as a problem exercise. This is true for totally arbitrary $f(z)$ as long as this function is analytic; i.e., it must have a unique derivative df/dz at every point in the region.

The net result of Eqs. (3.131) and (3.132) is that the functions f_1 and f_2 can be interpreted to be the potential lines and streamlines of an inviscid flow. By long custom we let the real part of $f(z)$ be the velocity potential and the imaginary part be the stream function
$$f(z) = \phi(x, y) + i\psi(x, y) \tag{3.133}$$

We try various functions $f(z)$ and see whether any interesting flow pattern results. Of course, most of them have already been found, and we simply report on them here.

We shall not go into the details, but there are excellent treatments of this complex-variable technique on both an introductory [4, chap. 5; 10, chap. 5] and a more advanced [2, 3,] level. The method is less important now because of the popularity of digital-computer techniques.

As a simple example, consider the linear function
$$f(z) = U_\infty z = U_\infty x + iU_\infty y$$

It follows from Eq. (3.133) that $\phi = U_\infty x$ and $\psi = U_\infty y$, which, we recall from Eq. (3.70), represents a uniform stream in the x direction. Once you get used to the complex variable, the solution practically falls in your lap.

To find the velocities, you may either separate ϕ and ψ from $f(z)$ and differentiate or differentiate f directly
$$\frac{df}{dz} = \frac{\partial \phi}{\partial x} + i\frac{\partial \psi}{\partial x} = -i\frac{\partial \phi}{\partial y} + \frac{\partial \psi}{\partial y} = u - iv \tag{3.134}$$

Thus the real part of df/dz equals $u(x, y)$, and the imaginary part equals $-v(x, y)$. To get a practical result, the derivative df/dz must exist and be unique, hence the requirement that f be an analytic function. For Eq. (3.134), $df/dz = U_\infty = u$, since it is real, and $v = 0$, as expected.

Sometimes it is convenient to use the polar-coordinate form of the complex variable
$$z = x + iy = re^{i\theta} = r\cos\theta + ir\sin\theta$$

where
$$r = (x^2 + y^2)^{1/2} \qquad \theta = \tan^{-1}\frac{y}{x}$$

This form is especially convenient when powers of z occur.

Summary of Complex Potentials for Elementary Plane Flows:

3.10.1 Uniform Stream at an Angle of Attack:

All the elementary plane flows of Sec. 3.3 have a complex-variable formulation. The uniform stream U_∞ at an angle of attack α has the complex potential

$$f(z) = U_\infty z e^{-i\alpha} \tag{3.135}$$

Compare this form with Eq. (3.72 and 3.73)

3.10.2 Line Source at Point Zo:

Consider a line source of strength m placed off the origin at a point $z_0 = x_0 + iy_0$. Its complex potential is

$$f(z) = m \ln (z - z_0) \tag{3.136}$$

This can be compared with Eq. 3.74&3.75 which is valid only for the source at the origin. For a line sink, the strength m is negative.

3.10.3 Line Vortex at Point Zo:

If a line vortex of strength K is placed at point z_0, its complex potential is

$$f(z) = -iK \ln (z - z_0) \tag{3.137}$$

to be compared with Eq3.77&3.78 Also compare to Eq. (3.136) to see that we reverse the meaning of ϕ and ψ simply by multiplying the complex potential by $-i$.

3.10.4 Flow around a Corner of Arbitrary Angle :

Corner flow is an example of a pattern that cannot be conveniently produced by superimposing sources, sinks, and vortices. It has a strikingly simple complex representation

$$f(z) = Az^n = Ar^n e^{in\theta} = Ar^n \cos n\theta + iAr^n \sin n\theta$$

where A and n are constants.

It follows from Eq. (3.133) that for this pattern

$$\phi = Ar^n \cos n\theta \qquad \psi = Ar^n \sin n\theta \tag{3.138}$$

Streamlines from Eq. (3.138) are plotted in Fig. 3.30 for five different values of n. The flow is seen to represent a stream turning through an angle $\beta = \pi/n$. Patterns in Fig. 3.30 *d* and *e* are not realistic on the downstream side of the corner, where separation will occur due to the adverse pressure gradient and sudden change of direction. In general, separation always occurs downstream of salient, or protruding corners, except in creeping flows at low Reynolds number Re < 1.

Since $360° = 2\pi$ is the largest possible corner, the patterns for $n < \frac{1}{2}$ do not represent corner flow. They are peculiar-looking, and we ask you to plot one as a problem.

If we expand the plot of Fig. 3.30 *a* to *c* to double size, we can represent stagnation flow toward a corner of angle $2\beta = 2\pi/n$. This is done in Fig. 3.31 for $n = 3$, 2, and 1.5. These are very realistic flows; although they slip at the wall, they can be patched to boundary-layer theories very successfully. We took a brief look at corner flows before, in Examples 3.4 and 3.5

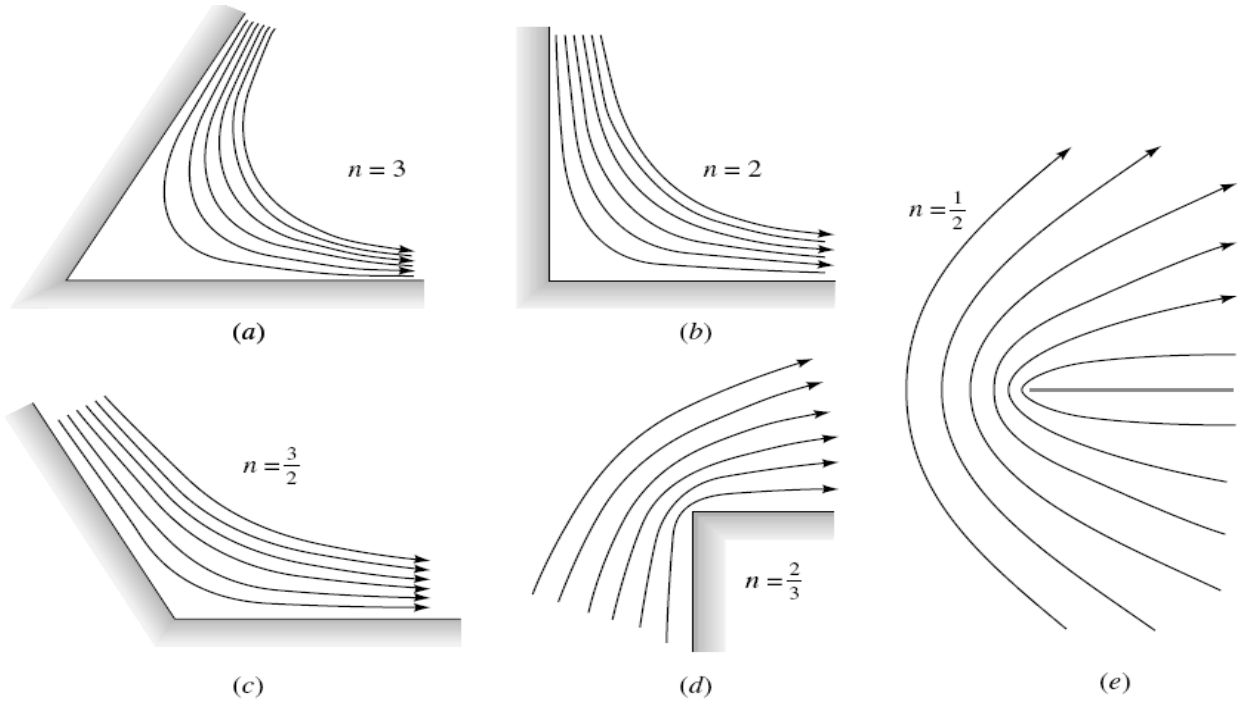

Fig. 3.30 Streamlines for Corner angle β of a) 60° , b) 90° , c) 120° , d) 270°, and e) 360°

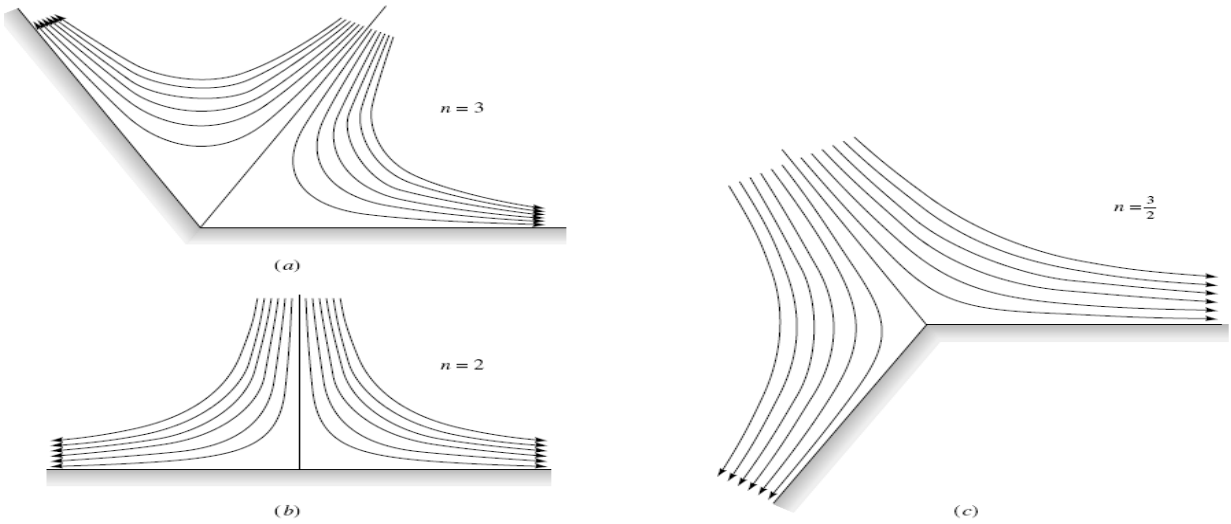

Fig. 3.31 Streamlines for stagnation flow from Eq. 3.138 for corner angle 2β of (*a*) 120°, (*b*) 180°, and (*c*) 240°

3.10.5 Flow Normal to a Flat Plate:

We treat this case separately because the Kelvin ovals of Fig. 3.28 failed to degenerate into a flat plate as K became small. The flat plate normal to a uniform stream is an extreme case worthy of our attention.

Although the result is quite simple, the derivation is very complicated and is given, e.g., in Ref. 2, sec. 9.3. There are three changes of complex variable, or *mappings*, beginning with the basic cylinder-flow solution of Fig. 3.26 *a*. First the uniform stream is rotated to be vertical upward, then the cylinder is squeezed down into a plate shape, and finally the free stream is rotated back to the horizontal. The final result for complex potential is

$$f(z) = \phi + i\psi = U_\infty(z^2 + a^2)^{1/2} \tag{3.139}$$

where $2a$ is the height of the plate. To isolate ϕ or ψ, square both sides and separate real and imaginary parts

$$\phi^2 - \psi^2 = U_\infty^2(x^2 - y^2 + a^2) \qquad \phi\psi = U_\infty^2 xy$$

We can solve for ψ to determine the streamlines

$$\psi^4 + \psi^2 U_\infty^2 (x^2 - y^2 + a^2) = U_\infty^4 x^2 y^2 \tag{3.140}$$

Equation (3.140) is plotted in Fig. 3.32 *a*, revealing a doubly symmetric pattern of streamlines which approach very closely to the plate and then deflect up and over, with very high velocities and low pressures near the plate tips.

The velocity v_s along the plate surface is found by computing df/dz from Eq. (3.139) and isolating the imaginary part

$$\left.\frac{v_s}{U_\infty}\right|_{\text{plate surface}} = \frac{y/a}{(1 - y^2/a^2)^{1/2}} \tag{3.141}$$

Some values of surface velocity can be tabulated as follows:

y/a	0.0	0.2	0.4	0.6	0.71	0.8	0.9	1.0
v_s/U_∞	0.0	0.204	0.436	0.750	1.00	1.33	2.07	∞

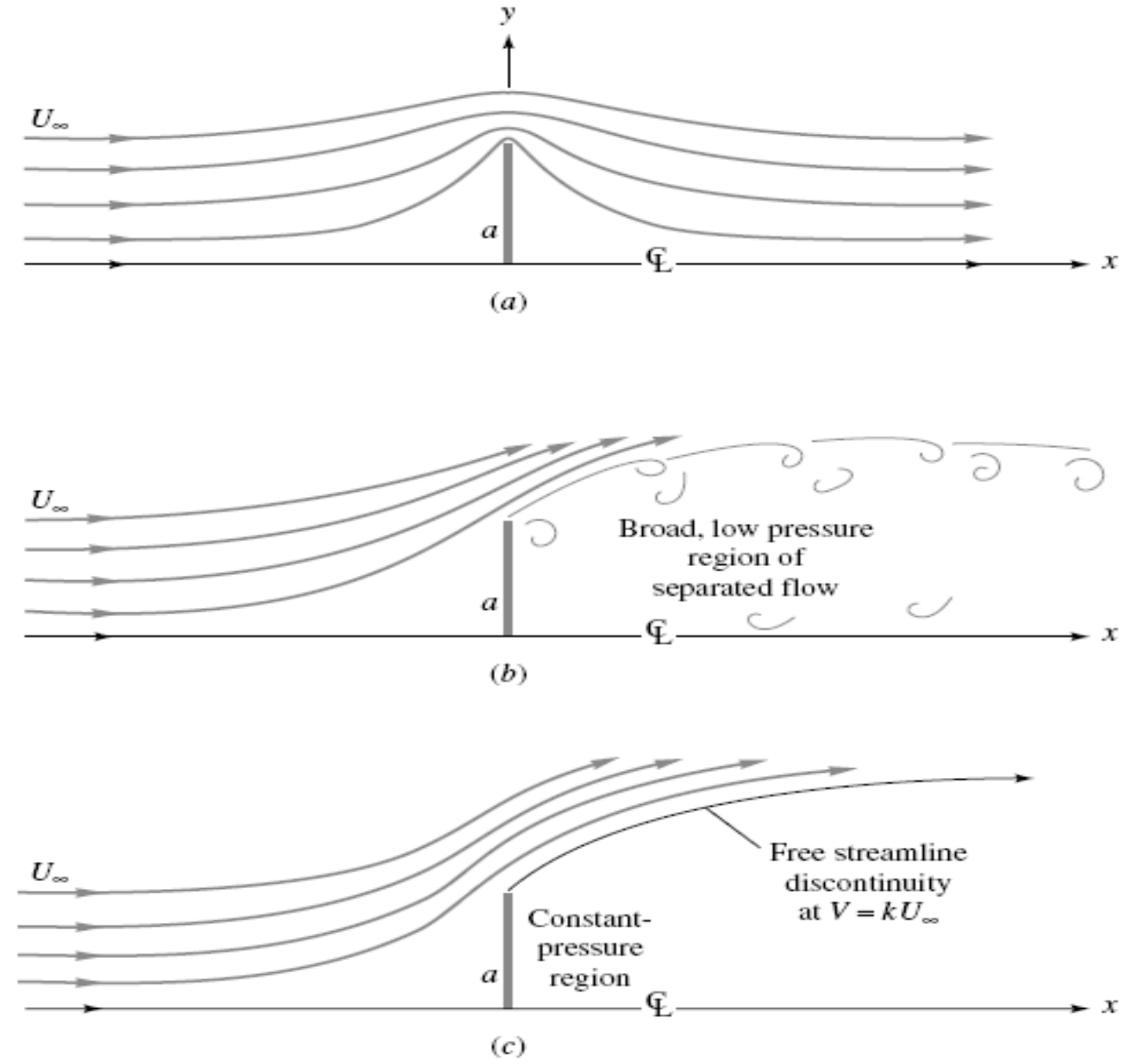

Fig.3.32 Streamlines in upper half-plane for flow normal to a flat plate of height 2a:
a) continuous potential-flow theory; b) actual measured flow pattern;
c) discontinuous potential theory with k ≈ 1.5

The origin is a stagnation point; then the velocity grows linearly at first and very rapidly near the tip, with both velocity and acceleration being infinite at the tip.

As you might guess, Fig. 3.32 *a* is not realistic. In a real flow the sharp salient edge causes separation, and a broad, low-pressure wake forms in the lee, as in Fig. 3.32 *b*. Instead of being zero, the drag coefficient is very large, $C_D \approx 2.0$ from Table 7.2.

A discontinuous-potential-flow theory which accounts for flow separation was devised by Helmholtz in 1868 and Kirchhoff in 1869. This free-streamline solution is shown in Fig. 3.32 *c*, with the streamline which breaks away from the tip having a constant velocity $V = kU_\infty$. From Bernoulli's equation the pressure in the dead-water region behind the plate will equal $p_r = p_\infty + \frac{1}{2}\rho U_\infty^2(1 - k^2)$ to match the pressure along the free streamline. For $k = 1.5$ this Helmholtz-Kirchoff theory predicts $p_r = p_\infty - 0.625\rho U_\infty^2$ and an average pressure on the front $p_f = p_\infty + 0.375\rho U_\infty^2$, giving an overall drag coefficient of 2.0, in agreement with experiment. However, the coefficient k is a priori unknown and must be tuned to experimental data, so free-streamline theory can be considered only a qualified success. For further details see Ref. 2, sec. 11.2.

3.10.6 Complex Potential of The Dipole Flow:

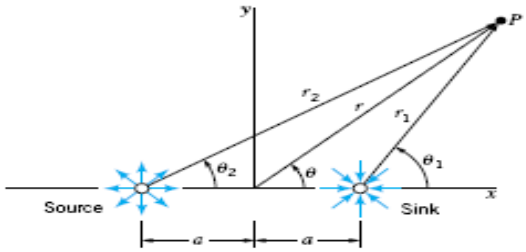

We now analyze the case of the so-called hydrodynamic dipole, which results from the superposition of a source and a sink of equal intensity placed symmetrically with respect to the origin. The analogy with electromagnetism is evident. The magnetic field induced by a wire in which a current flows satisfies equations that are similar to those governing irrotational plane flows. The complex potential of a dipole is (if the source and the sink are

$$W = \frac{m}{2\pi}\ln(z+a) - \frac{m}{2\pi}\ln(z-a) = \frac{m}{2\pi}\ln\left(\frac{z+a}{z-a}\right)$$

positioned in (-*a*,0) and (*a*,0) respectively).

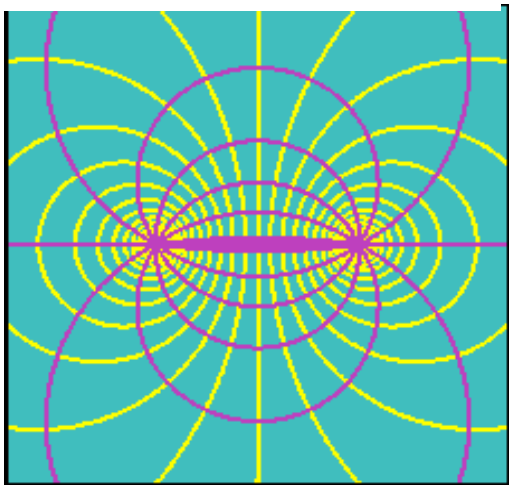

Streamlines are circles, the center of which lie on the *y*-axis and they converge obviously at the source and at the sink. Equipotential lines are circles, the center of which lie on the *x*-axis.

3.10.7 Complex Potential of a Doublet:

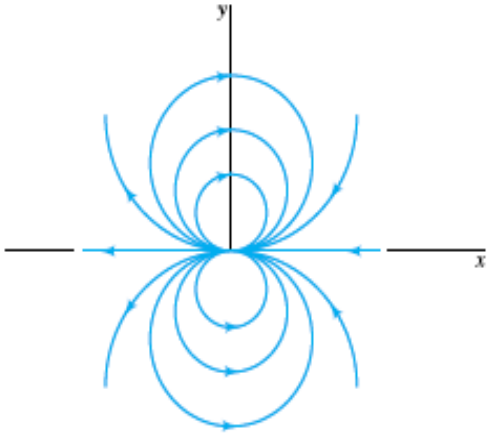

A particular case of dipole is the so-called doublet, in which the quantity *a* tends to zero so that the source and sink both move towards the origin. The complex potential of a doublet is obtained making the limit of the dipole potential for vanishing *a* with the constraint that the intensity of the source and the sink must correspondingly tend to infinity as *a* approaches zero, the quantity $\mu = 2ma$

Being constant (if we just superimpose a source and sink at the origin the resulting potential would be *W*=0)

$$W = \frac{\mu}{2\pi z}$$

Hint: develop ln (z+a) and ln(z-a) in a Taylor series in the neighborhood of the origin, assuming small *a.*

3.10.8 Complex Potential of Flow around A Cylinder:

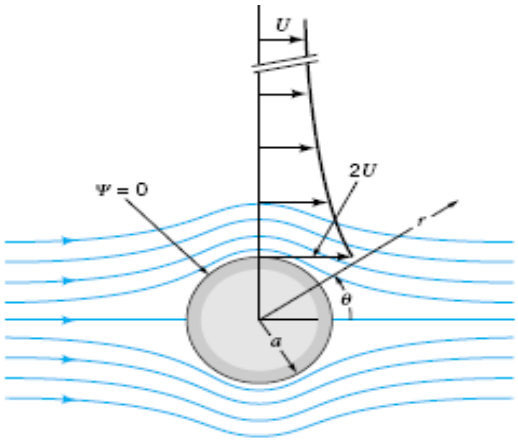

The superposition of a doublet and a uniform flow gives the complex potential

$$W = Uz + \frac{\mu}{2\pi z}$$

That is represented here in terms of streamlines and equipotential lines. Note that one of the streamlines is closed and surrounds the origin at a constant distance equal to

$$R = \sqrt{\left(\frac{\mu}{2\pi U}\right)}$$

Recalling the fact that, by definition, a streamline cannot be crossed by the fluid, this complex potential represents the irrotational flow around a cylinder of radius *R* approached by a uniform flow with velocity *U*. Moving away from the body, the effect of the doublet decreases so that far from the cylinder we find, as expected, the undisturbed uniform flow. In the two intersections of the *x*-axis with the cylinder, the velocity is found to be zero. These two points are thus called stagnation points.

3.10.9 FLOW AROUND A CYLINDER WITH NONZERO CIRCULATION:

In the last example, we superimpose to the complex potential that gives the flow around a cylinder a vortex of intensity γ positioned at the center of the cylinder. The resulting potential is

$$W = Uz + \frac{\mu}{2\pi z} - \frac{i\gamma}{2\pi}\ln(z)$$

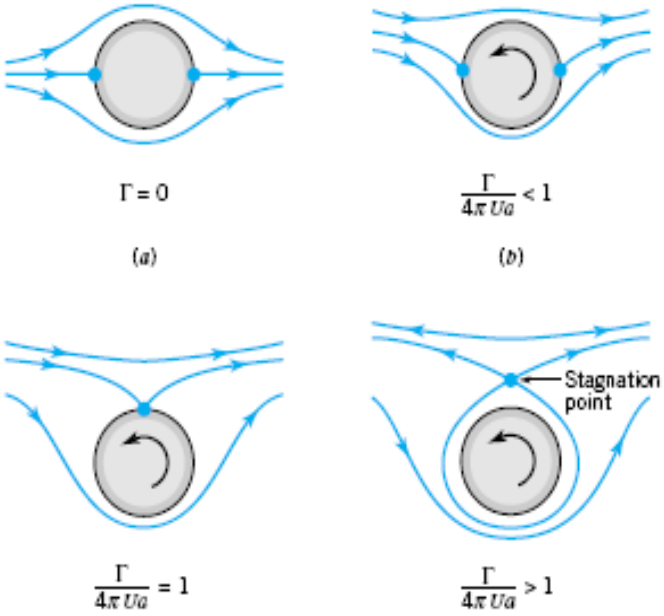

The presence of the vortex does not alter the streamline describing the cylinder, while the two stagnation points below the *x*-axis. The streamlines are closer to each other on the upper part of the cylinder and more distant on the lower part. This indicates that the flow is accelerated on the upper face of the cylinder and decelerated on the lower part, with respect to the zero circulation case. The resulting flow field corresponds to the case of a rotating cylinder, which accelerates (with respect to the case of no circulation) fluid particles on part of the cylinder and decelerates them on the remainder of the cylinder. Note the presence of a discontinuity in the potential function (thick yellow line on the left) that is related to the fact that the vortex potential (as mentioned in a previous section) has a nonzero cyclic constant.

3.11 The Method of Images:

The previous solutions have all been for unbounded flows, such as a circular cylinder immersed in a broad expanse of uniformly streaming fluid, Fig. 3.26*a*. However, many practical problems involve a nearby rigid boundary constraining the flow, e.g., (1) groundwater flow near the bottom of a dam, (2) an airfoil near the ground, simulating landing or takeoff, or (3) a cylinder mounted in a wind tunnel with narrow walls. In such cases the basic unbounded-potential-flow solutions can be modified for wall effects by the method of *images*.

Consider a line source placed a distance a from a wall, as in Fig. 3.33 *a*. To create the desired wall, an image source of identical strength is placed the same distance below the wall. By symmetry the two sources create a plane-surface streamline between them, which is taken to be the wall.

In Fig. 3.33 *b* a vortex near a wall requires an image vortex the same distance below but of *opposite* rotation. We have shaded in the wall, but of course the pattern could also be interpreted as the flow near a vortex pair in an unbounded fluid.

In Fig. 3.33 *c* an airfoil in a uniform stream near the ground is created by an image airfoil below the ground of opposite circulation and lift. This looks easy, but actually it is not because the airfoils are so close together that they interact and distort each other's shapes. A rule of thumb is that nonnegligible shape distortion occurs if the body shape is within two chord lengths of the wall. To eliminate distortion, a whole series of "corrective" images must be added to the flow to recapture the shape of the original isolated airfoil. Reference 2, sec. 7.75, has a good discussion of this procedure, which usually requires digital-computer summation of the multiple images needed.

Figure 3.33 *d* shows a source constrained between two walls. One wall required only one image in Fig. 3.33 *a*, but *two* walls require an infinite array of image sources above and below the desired pattern, as shown. Usually computer summation is necessary, but sometimes a closed-form summation can be achieved, as in the infinite vortex row of Eq. (3.100).

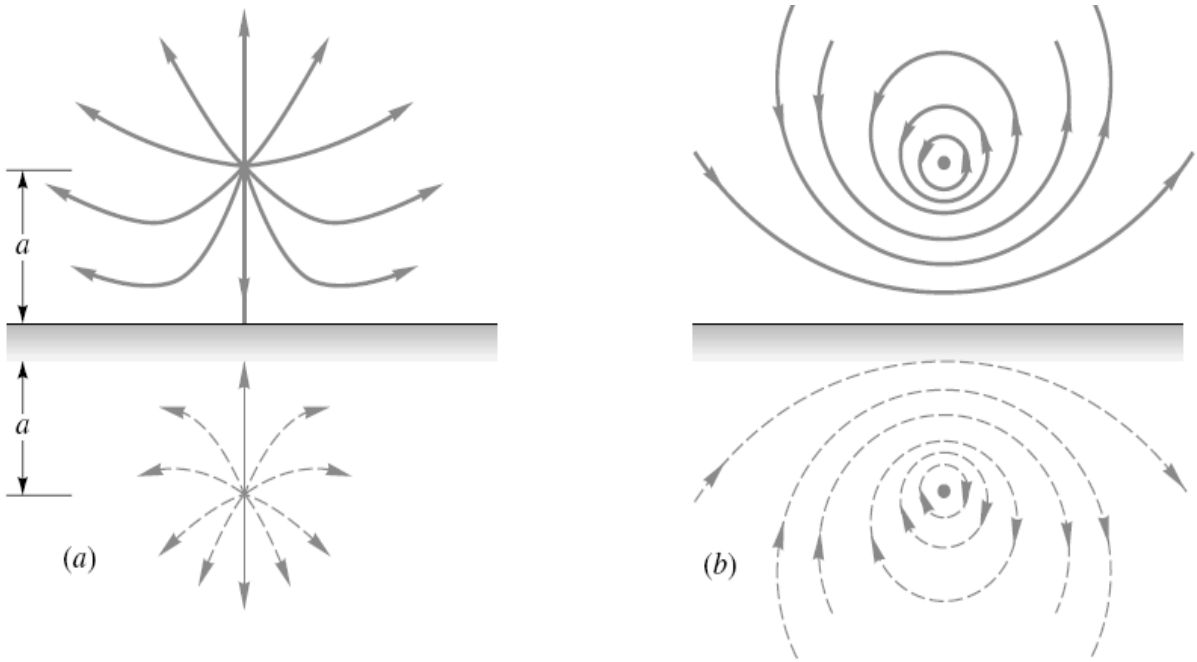

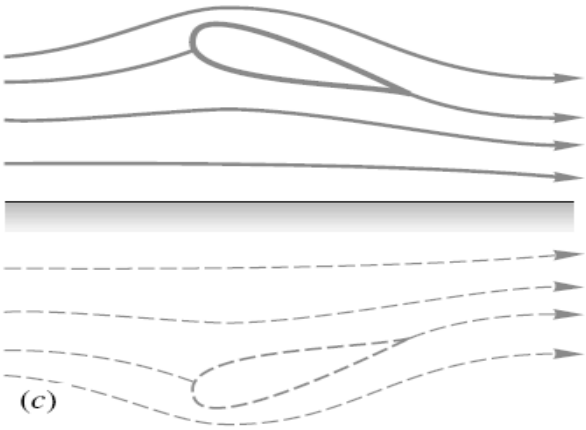

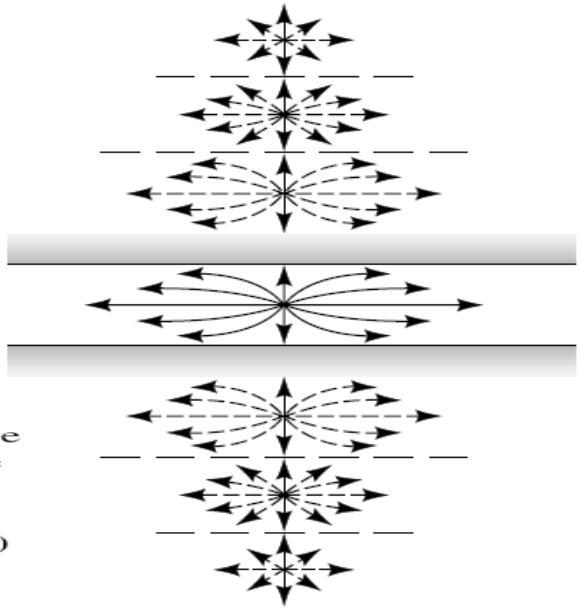

Fig. 3.33 Constraining walls can be created by image flows: (*a*) source near a wall with identical image source; (*b*) vortex near a wall with image vortex of opposite sense; (*c*) airfoil in ground effect with image airfoil of opposite circulation; (*d*) source between two walls requiring an infinite row of images.

Example 3.14:

For the source near a wall as in Fig. 3.33 *a*, the wall velocity is zero between the sources, rises to a maximum moving out along the wall, and then drops to zero far from the sources. If the source strength is 8 m^2/s, how far from the wall should the source be to ensure that the maximum velocity along the wall will be 5 m/s?

Solution

At any point x along the wall, as in Fig. E3.14 each source induces a radial outward velocity $v_r = m/r$, which has a component $v_r \cos\theta$ along the wall. The total wall velocity is thus

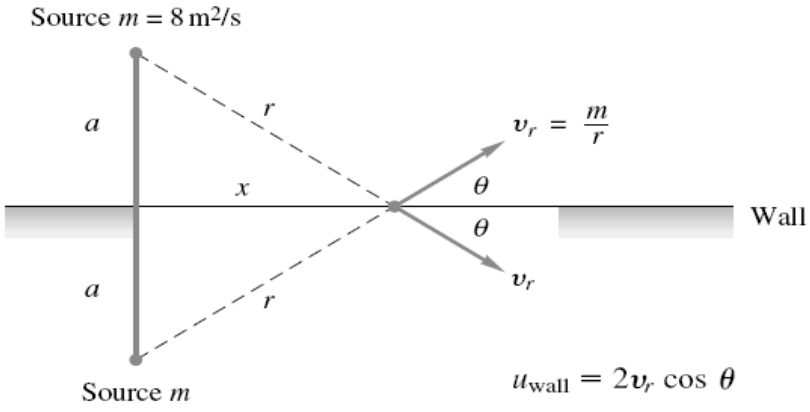

$$v_r = \frac{m}{r}$$

$$u_{\text{wall}} = 2v_r \cos\theta$$

From the geometry of Fig. E3.14, $r = (x^2 + a^2)^{1/2}$ and $\cos\theta = x/r$. Then the total wall velocity can be expressed as

$$u = \frac{2mx}{x^2 + a^2}$$

This is zero at $x = 0$ and at $x \to \infty$. To find the maximum velocity, differentiate and set equal to zero

$$\frac{du}{dx} = 0 \quad \text{at} \quad x = a \qquad \text{and} \qquad u_{\max} = \frac{m}{a}$$

We have omitted a bit of algebra in giving these results. For the given source strength and maximum velocity, the proper distance a is

$$a = \frac{m}{u_{\max}} = \frac{8\ \text{m}^2/\text{s}}{5\ \text{m/s}} = 1.625\ \text{m} \qquad \textit{Ans.}$$

For $x > a$, there is an adverse pressure gradient along the wall, and boundary-layer theory should be used to predict separation.

3.12 Axisymmetric Potential Flows:

The same superposition technique which worked so well for plane flow in Sec. 3.3* is also successful for axisymmetric potential flow. We give some brief examples here.

Most of the basic results carry over from plane to axisymmetric flow with only slight changes owing to the geometric differences. Consider the following related flows:

Basic plane flow	Counterpart axisymmetric flow
Uniform stream	Uniform stream
Line source or sink	Point source or sink
Line doublet	Point doublet
Line vortex	No counterpart
Rankine half-body cylinder	Rankine half-body of revolution
Rankine-oval cylinder	Rankine oval of revolution
Circular cylinder	Sphere
Symmetric airfoil	Tear-shaped body

Since there is no such thing as a point vortex, we must forgo the pleasure of studying circulation effects in axisymmetric flow. However, as any smoker knows, there is an axisymmetric ring vortex, and there are also ring sources and ring sinks, which we leave to advanced texts [for example, 3].

3.12.1 Spherical Polar Coordinates:

Axisymmetric potential flows are conveniently treated in the spherical polar coordinates of Fig. 3.34 . There are only two coordinates (r, θ), and flow properties are constant on a circle of radius $r \sin \theta$ about the x-axis.

The equation of continuity for incompressible flow in these coordinates is

$$\frac{\partial}{\partial r}(r^2 v_r \sin\theta) + \frac{\partial}{\partial \theta}(r v_\theta \sin\theta) = 0 \tag{3.142}$$

where v_r and v_θ are radial and tangential velocity as shown. Thus a spherical polar stream function[6] exists such that

$$v_r = -\frac{1}{r^2 \sin\theta}\frac{\partial \psi}{\partial \theta} \qquad v_\theta = \frac{1}{r \sin\theta}\frac{\partial \psi}{\partial r} \tag{3.143}$$

In like manner a velocity potential $\phi(r, \theta)$ exists such that

$$v_r = \frac{\partial \phi}{\partial r} \qquad v_\theta = \frac{1}{r}\frac{\partial \phi}{\partial \theta} \tag{3.144}$$

These formulas serve to deduce the ψ and ϕ functions for various elementary-axisymmetric potential flows.

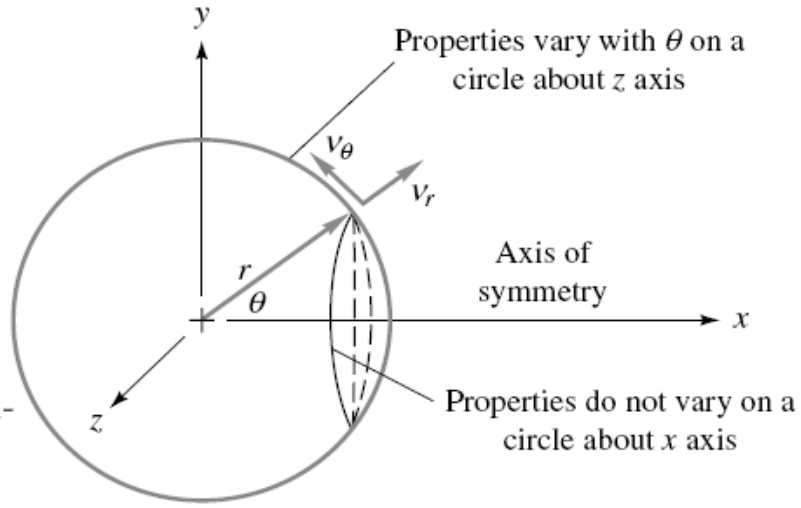

Fig. 3.34 Spherical polar coordinates for axisymmetric flow.

3.12.2 Uniform Stream in the x-direction:

A stream U_∞ in the x direction has components

$$v_r = U_\infty \cos\theta \qquad v_\theta = -U_\infty \sin\theta$$

Substitution into Eqs. (3.143) and (3.144) and integrating give

Uniform stream: $$\psi = -\tfrac{1}{2}U_\infty r^2 \sin^2\theta \qquad \phi = U_\infty r\cos\theta \tag{3.145}$$

As usual, arbitrary constants of integration have been neglected.

3.12.3 Point Source or Sink:

Consider a volume flux Q issuing from a point source. The flow will spread out radially and at radius r will equal Q divided by the area $4\pi r^2$ of a sphere. Thus

$$v_r = \frac{Q}{4\pi r^2} = \frac{m}{r^2} \qquad v_\theta = 0 \tag{3.146}$$

with $m = Q/(4\pi)$ for convenience. Integrating (3.143) and (3.144) gives

Point source $$\psi = m\cos\theta \qquad \phi = -\frac{m}{r} \tag{3.147}$$

For a point sink, change m to $-m$ in Eq. (3.147).

3.12.4 Point Doublet:

Exactly as in Fig. 3.15, place a source at $(x, y) = (-a, 0)$ and an equal sink at $(+a, 0)$, taking the limit as a becomes small with the product $2am = \lambda$ held constant

$$\psi_{\text{doublet}} = \lim_{\substack{a\to 0 \\ 2am=\lambda}} (m\cos\theta_{\text{source}} - m\cos\theta_{\text{sink}}) = \frac{\lambda \sin^2\theta}{r} \tag{3.148}$$

We leave the proof of this limit as a problem. The point-doublet velocity potential

$$\phi_{\text{doublet}} = \lim_{\substack{a\to 0 \\ 2am=\lambda}} \left(-\frac{m}{r_{\text{source}}} + \frac{m}{r_{\text{sink}}}\right) = \frac{\lambda\cos\theta}{r^2} \tag{3.149}$$

The streamlines and potential lines are shown in Fig. 3.35 . Unlike the plane doublet flow of Fig. 3.15, neither set of lines represents perfect circles.

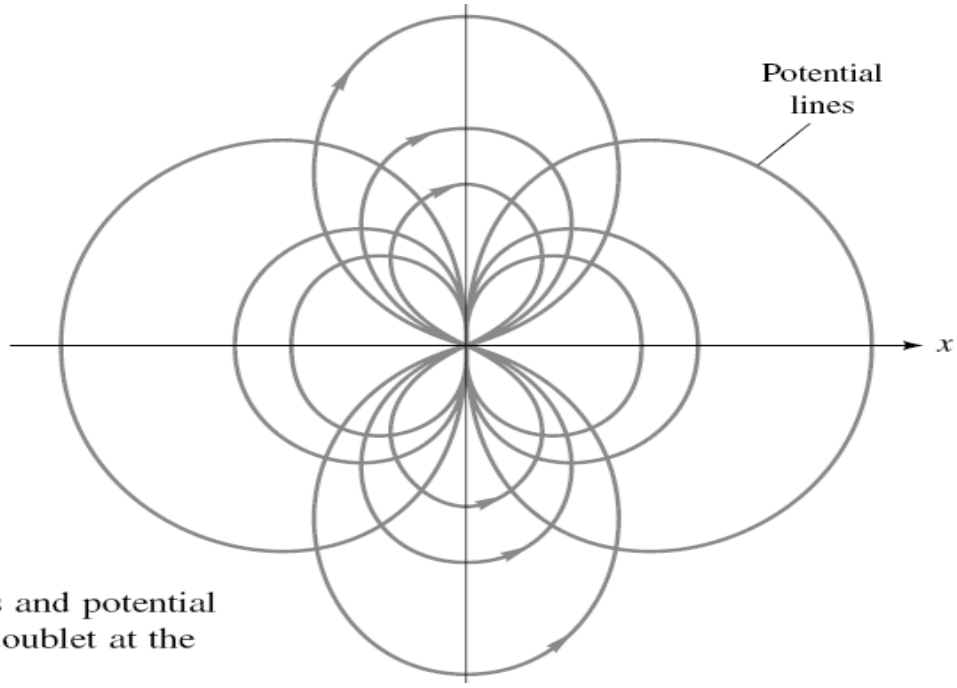

Fig. 3.35 Streamlines and potential lines due to a point doublet at the

3.12.5 Uniform Stream Plus a Point Source:

By combining Eqs. (3.145) and (3.147) we obtain the stream function for a uniform stream plus a point source at the origin

$$\psi = -\tfrac{1}{2}U_\infty r^2 \sin^2\theta + m\cos\theta \tag{3.150}$$

From Eq. (3.143) the velocity components are, by differentiation,

$$v_r = U_\infty \cos\theta + \frac{m}{r^2} \qquad v_\theta = -U_\infty \sin\theta \tag{3.151}$$

Setting these equal to zero reveals a stagnation point at $\theta = 180°$ and $r = a = (m/U_\infty)^{1/2}$, as shown in Fig. 3.36 . If we let $m = U_\infty a^2$, the stream function can be rewritten as

$$\frac{\psi}{U_\infty a^2} = \cos\theta - \frac{1}{2}\left(\frac{r}{a}\right)^2 \sin^2\theta \tag{3.152}$$

The stream surface which passes through the stagnation point $(r, \theta) = (a, \pi)$ has the value $\psi = -U_\infty a^2$ and forms a half-body of revolution enclosing the point source, as shown in Fig. 3.36 . This half-body can be used to simulate a pitot tube. Far downstream the half-body approaches the constant radius $R = 2a$ about the x-axis. The maximum velocity and minimum pressure along the half-body surface occur at $\theta = 70.5°$, $r = a\sqrt{3}$, $V_s = 1.155U_\infty$. Downstream of this point there is an adverse gradient as V_s slowly decelerates to U_∞, but boundary-layer theory indicates no flow separation. Thus Eq. (3.152) is a very realistic simulation of a real half-body flow. But when the uniform stream is added to a sink to form a half-body rear surface, e.g., similar to Fig. 3.18 , separation is predicted and the inviscid pattern is not realistic.

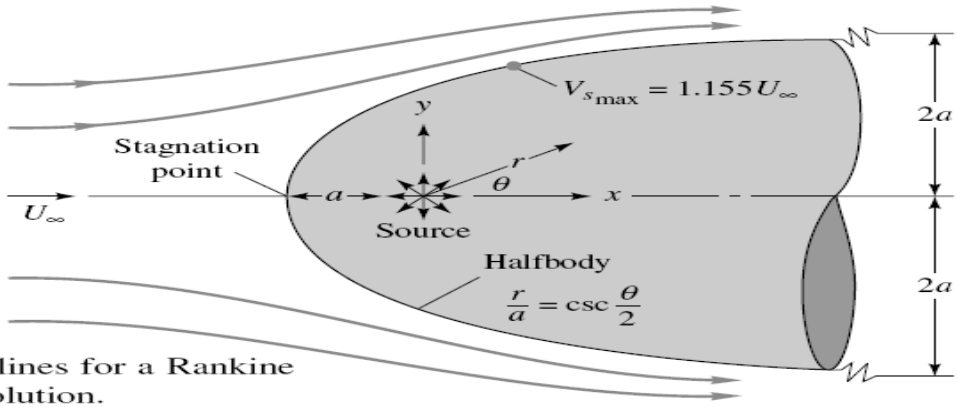

Fig. 3.36 Streamlines for a Rankine half-body of revolution.

3.12.6 Uniform Stream Plus a point Doublet (Flow Around a Sphere):

From Eqs. (3.145) and (3.148), combination of a uniform stream and a point doublet at the origin gives

$$\psi = -\frac{1}{2}U_\infty r^2 \sin^2\theta + \frac{\lambda}{r}\sin^2\theta \tag{3.153}$$

Examination of this relation reveals that the stream surface $\psi = 0$ corresponds to the sphere of radius

$$r = a = \left(\frac{2\lambda}{U_\infty}\right)^{1/3} \tag{3.154}$$

This is exactly analogous to the cylinder flow of Fig. 3.26 *a* formed by combining a uniform stream and a line doublet.

Letting $\lambda = \frac{1}{2}U_\infty a^3$ for convenience, we rewrite Eq. (3.153) as

$$\frac{\psi}{\frac{1}{2}U_\infty a^2} = -\sin^2\theta\left(\frac{r^2}{a^2} - \frac{a}{r}\right) \tag{3.155}$$

The streamlines for this sphere flow are plotted in Fig. 3.37 . By differentiation from Eq. (3.143) the velocity components are

$$v_r = U_\infty \cos\theta\left(1 - \frac{a^3}{r^3}\right) \qquad v_\theta = -\frac{1}{2}U_\infty \sin\theta\left(2 + \frac{a^3}{r^3}\right) \tag{3.156}$$

We see that the radial velocity vanishes at the sphere surface $r = a$, as expected. There is a stagnation point at the front (a, π) and the rear $(a, 0)$ of the sphere. The maximum velocity occurs at the shoulder $(a, \pm\frac{1}{2}\pi)$, where $v_r = 0$ and $v_\theta = -1.5U_\infty$. The surface-velocity distribution is

$$V_s = -v_\theta|_{r=a} = \tfrac{3}{2}U_\infty \sin\theta \tag{3.157}$$

Note the similarity to the cylinder surface velocity equal to $2U_\infty \sin\theta$ from Eq. (3.123) with zero circulation.

Equation (3.157) predicts, as expected, an adverse pressure gradient on the rear ($\theta < 90°$) of the sphere. If we use this distribution with laminar-boundary-layer theory [for example, 15, p. 298], separation is computed to occur at about $\theta = 76°$, so that in the actual flow pattern of Fig. 3.38 a broad wake forms in the rear. This wake interacts with the free stream and causes Eq. (3.157) to be inaccurate even in the front of the sphere. The measured maximum surface velocity is equal only to about $1.3U_\infty$ and occurs at about $\theta = 107°$ (see Ref. 15, sec. 4.10.4, for further details).

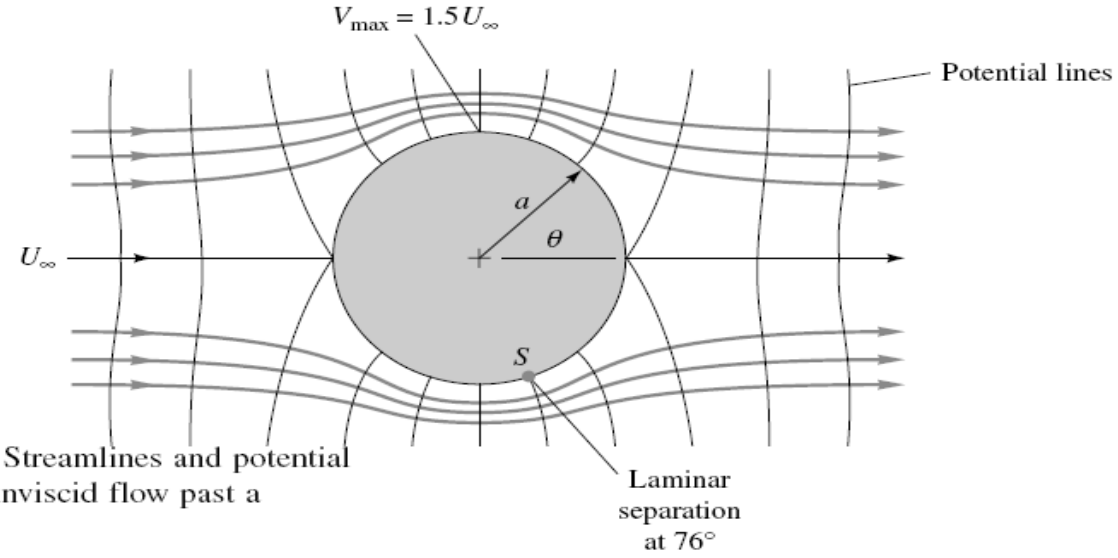

Fig. 3.37 Streamlines and potential lines for inviscid flow past a sphere.

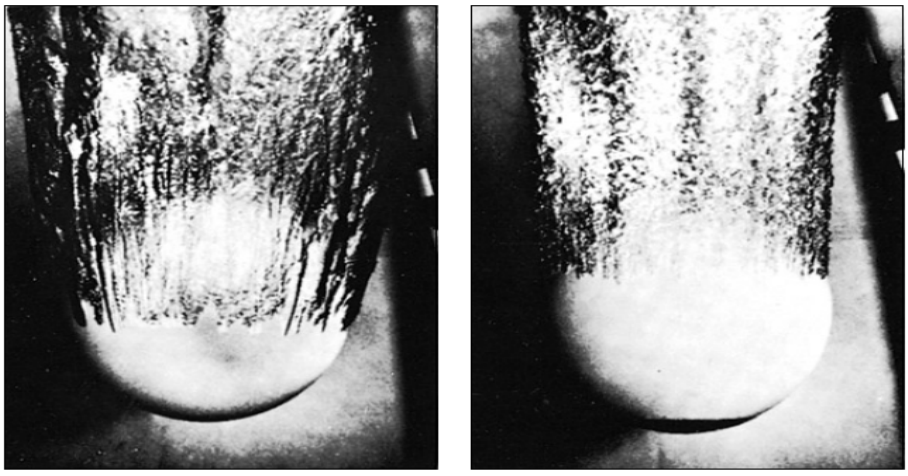

(a) (b)

Fig. 3.38 Strong differences in laminar and turbulent separation on an 8.5-in bowling ball entering water at 25 ft/s: (*a*) smooth ball, laminar boundary layer; (*b*) same entry, turbulent flow induced by patch of nose-sand roughness. (*U.S. Navy photograph, Ordnance Test Station, Pasadena Annex.*)

3.13 The Concept of Hydrodynamic Mass:

When a body moves through a fluid, it must push a finite mass of fluid out of the way. If the body is accelerated, the surrounding fluid must also be accelerated. The body behaves as if it were heavier by an amount called the *hydrodynamic mass* (also called the *added* or *virtual mass*) of the fluid. If the instantaneous body velocity is $\mathbf{U}(t)$, the summation of forces must include this effect

$$\Sigma \mathbf{F} = (m + m_h) \frac{d\mathbf{U}}{dt} \tag{3.158}$$

where m_h, the hydrodynamic mass, is a function of body shape, the direction of motion, and (to a lesser extent) flow parameters such as the Reynolds number.

According to potential theory [2, sec. 6.4; 3, sec. 9.22], m_h depends only on the shape and direction of motion and can be computed by summing the total kinetic energy of the fluid relative to the body and setting this equal to an equivalent body energy

$$\text{KE}_{\text{fluid}} = \int \tfrac{1}{2} dm \; V_{\text{rel}}^2 = \tfrac{1}{2} m_h U^2 \tag{3.159}$$

The integration of fluid kinetic energy can also be accomplished by a body-surface integral involving the velocity potential [16, sec. 11].

Consider the previous example of a sphere immersed in a uniform stream. By subtracting out the stream velocity we can replot the flow as in Fig. 3.39 , showing the streamlines relative to the moving sphere. Note the similarity to the doublet flow in Fig. 3.35 . The relative-velocity components are found by subtracting U from Eqs. (3.156)

$$v_r = -\frac{Ua^3 \cos\theta}{r^3} \qquad v_\theta = -\frac{Ua^3 \sin\theta}{2r^3}$$

The element of fluid mass, in spherical polar coordinates, is

$$dm = \rho(2\pi r \sin\theta) r\, dr\, d\theta$$

When dm and $V_{\text{rel}}^2 = v_r^2 + v_\theta^2$ are substituted into Eq. (3.159), the integral can be evaluated

$$\text{KE}_{\text{fluid}} = \tfrac{1}{3}\rho\pi a^3 U^2$$

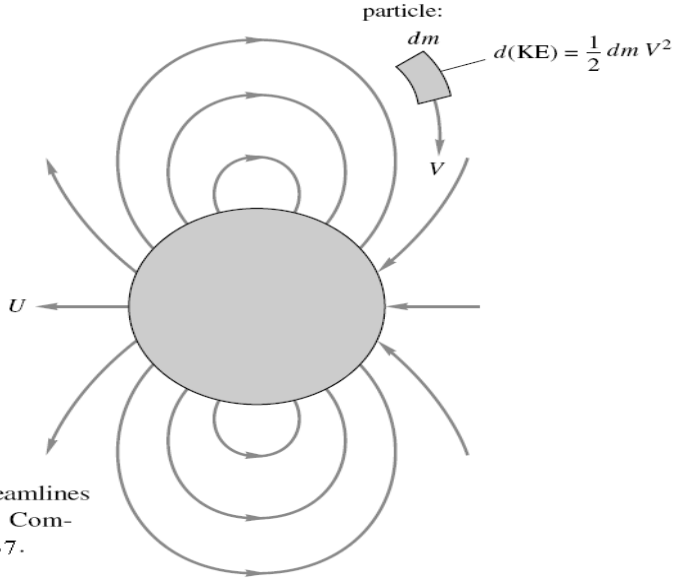

Fig. 3.39 Potential-flow streamlines relative to a moving sphere. Compare with Figs. 3.35 and 3.37.

or

$$m_h(\text{sphere}) = \tfrac{2}{3}\rho\pi a^3 \qquad (3.160)$$

Thus, according to potential theory, the hydrodynamic mass of a sphere equals one-half of its displaced mass, independent of the direction of motion.

A similar result for a cylinder moving normal to its axis can be computed from Eqs. (3.122) after subtracting out the stream velocity. The result is

$$m_h(\text{cylinder}) = \rho\pi a^2 L \qquad (3.161)$$

for a cylinder of length L, assuming two-dimensional motion. The cylinder's hydrodynamic mass equals its displaced mass.

Tables of hydrodynamic mass for various body shapes and directions of motion are given by Patton [17]. See also Ref. 21.

3.14 Other Aspects of Potential Flow Analysis

In the preceding section the method of superposition of basic potentials has been used to obtain detailed descriptions of irrotational flow around certain body shapes immersed in a uniform stream. For the cases considered, two or more of the basic potentials were combined and the question is asked: What kind of flow does this combination represent? This approach is relatively simple and does not require the use of advanced mathematical techniques. It is, however, restrictive in its general applicability. It does not allow us to specify a priori the body shape and then determine the velocity potential or stream function that describes the flow around the particular body. Determining the velocity potential or stream function for a given body shape is a much more complicated problem.

It is possible to extend the idea of superposition by considering a *distribution* of sources and sinks, or doublets, which when combined with a uniform flow can describe the flow around bodies of arbitrary shape. Techniques are available to determine the required distribution to give a prescribed body shape. Also, for plane potential flow problems it can be shown that complex variable theory (the use of real and imaginary numbers) can be effectively used to obtain solutions to a great variety of important flow problems. There are, of course, numerical techniques that can be used to solve not only plane two-dimensional prob-

lems, but the more general three-dimensional problems. Since potential flow is governed by Laplace's equation, any procedure that is available for solving this equation can be applied to the analysis of irrotational flow of frictionless fluids. Potential flow theory is an old and well-established discipline within the general field of fluid mechanics. The interested reader can find many detailed references on this subject, including Refs. 2, 3, 4, 5, and 6 given at the end of this chapter.

An important point to remember is that regardless of the particular technique used to obtain a solution to a potential flow problem, the solution remains approximate because of the fundamental assumption of a frictionless fluid. Thus, "exact" solutions based on potential flow theory represent, at best, only approximate solutions to real fluid problems. The applicability of potential flow theory to real fluid problems has been alluded to in a number of examples considered in the previous section. As a rule of thumb, potential flow theory will usually provide a reasonable approximation in those circumstances when we are dealing with a low viscosity fluid moving at a relatively high velocity, in regions of the flow field in which the flow is accelerating. Under these circumstances we generally find that the effect of viscosity is confined to the thin boundary layer that develops at a solid boundary. Outside the boundary layer the velocity distribution and the pressure distribution are closely approximated by the potential flow solution. However, in those regions of the flow field in which the flow is decelerating (for example, in the rearward portion of a bluff body or in the expanding region of a conduit) the pressure near a solid boundary will increase in the direction of flow. This so-called adverse pressure gradient can lead to flow separation, a phenomenon that causes dramatic changes in the flow field which are generally not accounted for by potential theory. However, as discussed in Chapter 9, in which boundary layer theory is developed, it is found that potential flow theory is used to obtain the appropriate pressure distribution that can then be combined with the viscous flow equations to obtain solutions near the boundary (and also to predict separation). The general differential equations that describe viscous fluid behavior and some simple solutions to these equations are considered in the remaining sections of this chapter.

3.15 Additional Advanced Potential Flows

Up to this point, we do not have any particular convenience in representing the flow in the complex plane. The full potential of this choice will become clear as soon as we introduce *conformal mapping* techniques. Let the following function

$$z' = z'(z)$$

Be an analytic function. It follows that also the inverse function $z\,(z')$ is analytic. Consider the two planes z and

$$z' = x' + iy'$$

The above function creates a link between a point in the z plane and a point in the z' plane. We can state that it maps one plane to the other. This transformation is said to be conformal because it does not affect angles, in the sense that given two lines in the z plane that intersect with some angle, the two transformed lines in the z' plane intersect with the same angle. In particular, two orthogonal families of curves in the z plane map into two other orthogonal families of curves in the z' plane. It follows that a conformal transformation maps equipotential and stream lines of an irrotational flow in the z plane into the corresponding lines of another irrotational flow in the z' plane.

Given a flow field in the z plane with complex potential $W\,(z)$, the function:

$$W'(z') = W(z(z'))$$

Is analytic because both $W\,(z)$ and $z\,(z')$ are analytic. In other words, the derivative

$$\frac{dW'}{dz'} = \frac{dW}{dz}\frac{dz}{dz'}$$

Exists and is unique because the derivatives on the right hand side exist and are unique. Therefore, *W'* is the complex potential of an irrotational inviscid flow in the *z'* plane. If *P* and *P'* are two corresponding points in the *z* and *z'* planes, respectively, $z_P = z(z'_{P'})$

$$W'(z'_{P'}) = W(z(z'_{P'})) = W(z_P)$$

And So that the two complex potentials *W* and *W'* assume the same value in corresponding points of the two domains.Circulation along any (corresponding) closed line has also the same value in the two spaces because it is given by the integrals $\oint_C dW$ $\oint_{C'} dW'$

That are equal because along the two lines *C* and *C'*, the potentials assume the same value.Among the conformal transformations, the Joukowski transformation is relevant for the study of flow around a wing, because it maps the domain around a cylinder into the domain around a wing, whose thickness and curvature can be varied.

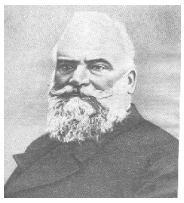

The Joukowski Transformation:

We introduce the conformal transformation due to Joukowski (who is pictured above)

$$z' = z + \frac{\lambda^2}{z}$$

And analyze how a cylinder of radius *R* defined in the *z* plane maps into the *z'* plane:

1. If the circle is centered at (0, 0) and $\lambda = R$ the circle maps into the segment between -2λ and $+2\lambda$ lying on the *x*-axis;
2. If the circle is centered at (x_c ,0) and $\lambda = R - x_c$, the circle maps in an airfoil that is symmetric with respect to the *x'*-axis;
3. If the circle is centered at (0, y_c) and $\lambda = \sqrt{(R^2 - y_c^2)}$, the circle maps into a curved segment;
4. If the circle is centered at (x_c , y_c) and $\lambda = -x_c + \sqrt{(R^2 - y_c^2)}$, , the circle maps into an asymmetric airfoil.

To summarize, moving the center of the circle along the *x*-axis gives thickness to the airfoil, moving the center of the circle along the *y*-axis gives camber to the airfoil. In the following interactive application it is possible to move the center of the circle in the *z* plane and see the resulting transformed airfoil. The site is (http: www.diam.unige.it/) We need to introduce some notations on airfoils.

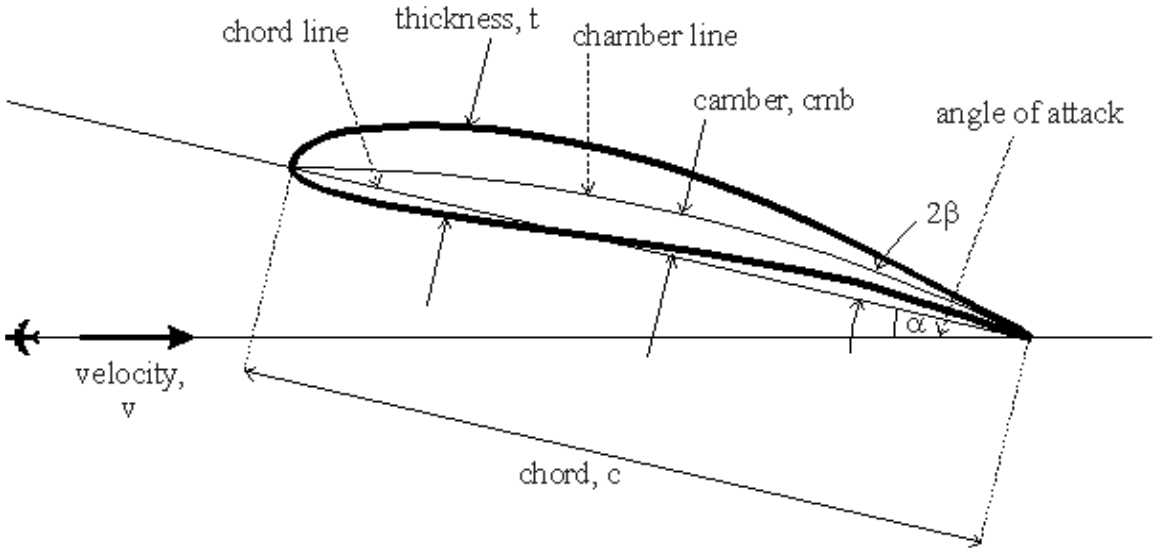

The generic Joukowski airfoil has a rounded leading edge and a cusp at the trailing edge where the camber line forms an angle 2 β with the chord line. In the cylinder plane, β is related to the vertical coordinate of the center of the cylinder so that

$$\beta = \arcsin(y_c)$$

Usually the angle of attack (sometimes called physical) is defined as the angle α that the uniform flow forms with the chord line. More interesting for aerodynamics is the angle

$$\alpha' = \alpha - \beta$$

In fact, when the angle α' is zero, the lift, as will be shown, vanishes. Then the angle α' is often defined as the effective angle of attack.

3.16 Other Aspects of Differential Analysis

In this chapter the basic differential equations that govern the flow of fluids have been developed. The Navier–Stokes equations, which can be compactly expressed in vector notation as

$$\rho\left(\frac{\partial \mathbf{V}}{\partial t} + \mathbf{V}\cdot\nabla\mathbf{V}\right) = -\nabla p + \rho\mathbf{g} + \mu\nabla^2\mathbf{V} \qquad (3.162)$$

along with the continuity equation

$$\nabla\cdot\mathbf{V} = 0 \qquad (3.163)$$

are the general equations of motion for incompressible Newtonian fluids. Although we have restricted our attention to incompressible fluids, these equations can be readily extended to include compressible fluids. It is well beyond the scope of this introductory text to consider in depth the variety of analytical and numerical techniques that can be used to obtain both exact and approximate solutions to the Navier–Stokes equations. Students, however, should be aware of the existence of these very general equations, which are frequently used as the basis for many advanced analyses of fluid motion. A few relatively simple solutions have been obtained and discussed in this chapter to indicate the type of detailed flow information that can be obtained by using differential analysis. However, it is hoped that the relative ease with which these solutions were obtained does not give the false impression that solutions to the Navier–Stokes equations are readily available. This is certainly not true, and as previously mentioned there are actually very few practical fluid flow problems that can be solved by using an exact analytical approach. In fact, there are no known analytical solutions to Eq. 3.162 for flow past any object such as a sphere, cube, or airplane.

Because of the difficulty in solving the Navier–Stokes equations, much attention has been given to various types of approximate solutions. For example, if the viscosity is set equal to zero, the Navier–Stokes equations reduce to Euler's equations. Thus, the frictionless fluid solutions discussed previously are actually approximate solutions to the Navier–Stokes equations. At the other extreme, for problems involving slowly moving fluids, viscous effects may be dominant and the nonlinear (convective) acceleration terms can be neglected. This assumption greatly simplifies the analysis, since the equations now become linear. There are numerous analytical solutions to these "*slow flow*" or "*creeping flow*" problems. Another broad class of approximate solutions is concerned with flow in the very thin boundary layer. L. Prandtl showed in 1904 how the Navier–Stokes equations could be simplified to study flow in boundary layers. Such "boundary layer solutions" play a very important role in the study of fluid mechanics. A further discussion of boundary layers is given in **Chapter 9**.

3.16.1 Numerical Methods:

Numerical methods using digital computers are, of course, commonly utilized to solve a wide variety of flow problems. As discussed previously, although the differential equations that govern the flow of Newtonian fluids [the Navier–Stokes equations (3.162)] were derived many years ago, there are few known analytical solutions to them. With the advent of high-speed digital computers it has become possible to obtain approximate numerical solutions to these (and other fluid mechanics) equations for a wide variety of circumstances.

Of the various techniques available for the numerical solution of the governing differential equations of fluid flow, the following three types are most common: (1) the finite difference method, (2) the finite element (or finite volume) method, and (3) the boundary element method. In each of these methods the continuous flow field (i.e., velocity or pressure as a function of space and time) is described in terms of discrete (rather than continuous) values at prescribed locations. By this technique the differential equations are replaced by a set of algebraic equations that can be solved on the computer.

For the finite element (or finite volume) method, the flow field is broken into a set of small fluid elements (usually triangular areas if the flow is two-dimensional, or small volume elements if the flow is three-dimensional). The conservation equations (i.e., conservation of mass, momentum, and energy) are written in an appropriate form for each element, and the set of resulting algebraic equations is solved numerically for the flow field. The number, size, and shape of the elements are dictated in part by the particular flow geometry and flow conditions for the problem at hand. As the number of elements increases (as is necessary for flows with complex boundaries), the number of simultaneous algebraic equations that must be solved increases rapidly. Problems involving 1000 to 10,000 elements and 50,000 equations are not uncommon. A mesh for calculating flow past an airfoil is shown in Fig. 3.40. Further information about this method can be found in Refs. 10 and 13.

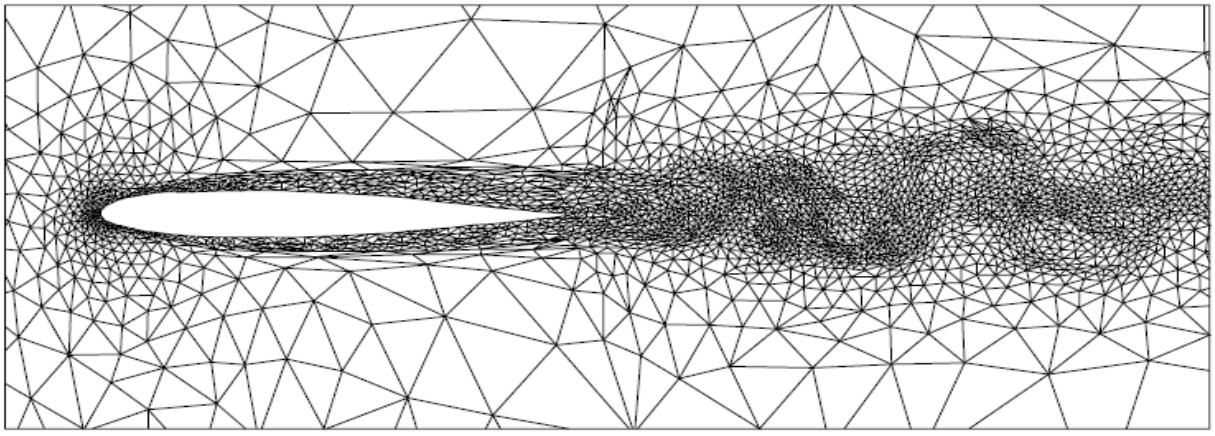

■ FIGURE 3.40 Anisotropic adaptive mesh for the calculation of viscous flow over a NACA 0012 airfoil at a Reynolds number of 10,000, Mach number of 0.755, and angle of attack of 1.5°. (From CFD Laboratory, Concordia University, Montreal, Canada. Used by permission.)

boundary elements. The strength and type of the singularities are chosen so that the appropriate boundary conditions of the flow are obtained on the boundary elements. For points in the flow field not on the boundary, the flow is calculated by adding the contributions from the various singularities on the boundary. Although the details of this method are rather mathematically sophisticated, it may (depending on the particular problem) require less computational time and space than the finite element method.

Typical boundary elements and their associated singularities (vortices) for two-dimensional flow past an airfoil are shown in Fig.3.41 . Such use of the boundary element method in aerodynamics is often termed the *panel method* in recognition of the fact that each element plays the role of a panel on the airfoil surface (Ref. 15).

The finite difference method for computational fluid dynamics is perhaps the most easily understood and widely used of the three methods listed above. For this method the flow field is dissected into a set of grid points and the continuous functions (velocity, pressure, etc.) are approximated by discrete values of these functions calculated at the grid points. Derivatives of the functions are approximated by using the differences between the function values at neighboring grid points divided by the grid spacing. The differential equations are thereby transferred into a set of algebraic equations, which is solved by appropriate numerical techniques. The larger the number of grid points used, the larger the number of equations that must be solved. It is usually necessary to increase the number of grid points (i.e., use a finer mesh) where large gradients are to be expected, such as in the boundary layer near a solid surface.

A very simple two-dimensional example of the finite difference technique is presented in the following example.

In general the governing equations to be solved are partial differential equations [rather than ordinary differential equations and the finite difference method becomes considerably more involved. The following example illustrates some of the concepts involved.

Example 3.15: on Numerical Methods:

Consider steady, incompressible flow of an inviscid fluid past a circular cylinder as shown in Fig. E3.15*a*. The stream function, ψ, for this flow is governed by the Laplace equation (see Section 3.3)

$$\frac{\partial^2 \psi}{\partial x^2} + \frac{\partial^2 \psi}{\partial y^2} = 0 \qquad (1)$$

The exact analytical solution is given in Section 3.6.

Describe a simple finite difference technique that can be used to solve this problem.

Solution

The first step is to define a flow domain and set up an appropriate grid for the finite difference scheme. Since we expect the flow field to be symmetrical both above and below and in front of and behind the cylinder, we consider only one quarter of the entire flow domain as indicated in Fig. E3.15*b*. We locate the upper boundary and right-hand boundary far enough

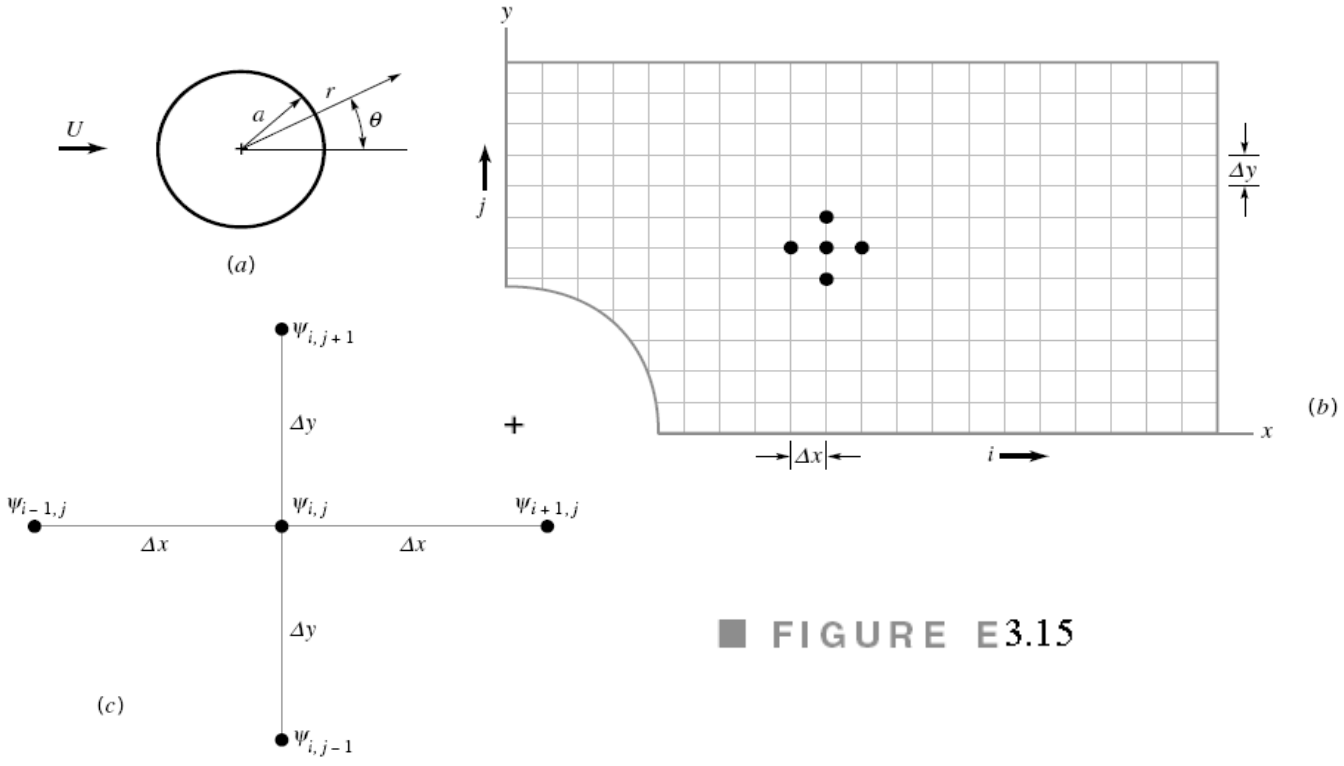

FIGURE E3.15

from the cylinder so that we expect the flow to be essentially uniform at these locations. It is not always clear how far from the object these boundaries must be located. If they are not far enough, the solution obtained will be incorrect because we have imposed artificial, uniform flow conditions at a location where the actual flow is not uniform. If these boundaries are farther than necessary from the object, the flow domain will be larger than necessary and excessive computer time and storage will be required. Experience in solving such problems is invaluable!

Once the flow domain has been selected, an appropriate grid is imposed on this domain (see Fig. E3.15*b*). Various grid structures can be used. If the grid is too coarse, the numerical solution may not be capable of capturing the fine scale structure of the actual flow field. If the grid is too fine, excessive computer time and storage may be required. Considerable work has gone into forming appropriate grids (Ref. 16). We consider a grid that is uniformly spaced in the x and y directions, as shown in Fig. E3.15*b*.

As shown in Eq. 3.113, the exact solution to Eq. 1 (in terms of polar coordinates r, θ rather than Cartesian coordinates x, y) is $\psi = Ur(1 - a^2/r^2)\sin\theta$. The finite difference solution approximates these stream function values at a discrete (finite) number of locations (the grid points) as $\psi_{i,j}$, where the i and j indices refer to the corresponding x_i and y_j locations.

The derivatives of ψ can be approximated as follows:

$$\frac{\partial \psi}{\partial x} \approx \frac{1}{\Delta x}(\psi_{i+1,j} - \psi_{i,j})$$

and

$$\frac{\partial \psi}{\partial y} \approx \frac{1}{\Delta y}(\psi_{i,j+1} - \psi_{i,j})$$

This particular approximation is called a forward-difference approximation. Other approximations are possible. By similar reasoning, it is possible to show that the second derivatives of ψ can be written as follows:

$$\frac{\partial^2 \psi}{\partial x^2} \approx \frac{1}{(\Delta x)^2}(\psi_{i+1,j} - 2\psi_{i,j} + \psi_{i-1,j}) \tag{2}$$

and

$$\frac{\partial^2 \psi}{\partial y^2} \approx \frac{1}{(\Delta y)^2}(\psi_{i,j+1} - 2\psi_{i,j} + \psi_{i,j-1}) \tag{3}$$

Thus, by combining Eqs. 1, 2, and 3 we obtain

$$\frac{\partial^2 \psi}{\partial x^2} + \frac{\partial^2 \psi}{\partial y^2} \approx \frac{1}{(\Delta x)^2}(\psi_{i+1,j} + \psi_{i-1,j}) + \frac{1}{(\Delta y)^2}(\psi_{i,j+1} + \psi_{i,j-1}) - 2\left(\frac{1}{(\Delta x)^2} + \frac{1}{(\Delta y)^2}\right)\psi_{i,j} = 0 \tag{4}$$

Equation 4 can be solved for the stream function at x_i and y_j to give

$$\psi_{i,j} = \frac{1}{2[(\Delta x)^2 + (\Delta y)^2]}[(\Delta y)^2(\psi_{i+1,j} + \psi_{i-1,j}) + (\Delta x)^2(\psi_{i,j+1} + \psi_{i,j-1})] \tag{5}$$

Note that the value of $\psi_{i,j}$ depends on the values of the stream function at neighboring grid points on either side and above and below the point of interest (see Eq. 5 and Fig. E3.15*c*).

To solve the problem (either exactly or by the finite difference technique) it is necessary to specify boundary conditions for points located on the boundary of the flow domain (see Section 3.6). For example, we may specify that $\psi = 0$ on the lower boundary of the domain (see Fig. E3.15*b*) and $\psi = C$, a constant, on the upper boundary of the domain. Appropriate boundary conditions on the two vertical ends of the flow domain can also be specified. Thus, for points interior to the boundary Eq. 5 is valid; similar equations or specified values of $\psi_{i,j}$ are valid for boundary points. The result is an equal number of equations and unknowns, $\psi_{i,j}$, one for every grid point. For this problem, these equations represent a set of linear algebraic equations for $\psi_{i,j}$, the solution of which provides the finite difference approximation for the stream function at discrete grid points in the flow field. Streamlines (lines of constant ψ) can be obtained by interpolating values of $\psi_{i,j}$ between the grid points and "connecting the dots" of ψ = constant. The velocity field can be obtained from the derivatives of the stream function according to Eq. 3.66. That is,

$$u = \frac{\partial \psi}{\partial y} \approx \frac{1}{\Delta y}(\psi_{i,j+1} - \psi_{i,j})$$

and

$$v = -\frac{\partial \psi}{\partial x} \approx -\frac{1}{\Delta x}(\psi_{i+1,j} - \psi_{i,j})$$

Further details of the finite difference technique are beyond the scope of this text but can be found in standard references on the topic (Refs. 11 and 12).

3.16.2 The Finite Difference Method:

Although textbooks on numerical analysis [5, 20] apply finite-difference techniques to many different problems, here we concentrate on potential flow. The idea of FDM is to approximate the partial derivatives in a physical equation by "differences" between nodel values spaced a finite distance apart—a sort of numerical calculus. The basic partial differential equation is thus replaced by a set of algebraic equations for the nodal values. For potential (inviscid) flow, these algebraic equations are linear, but they are generally nonlinear for viscous flows. The solution for nodal values is obtained by iteration or matrix inversion. Nodal spacings need not be equal.

Here we illustrate the two-dimensional Laplace equation, choosing for convenience the stream-function form

$$\frac{\partial^2 \psi}{\partial x^2} + \frac{\partial^2 \psi}{\partial y^2} = 0 \tag{3.164}$$

subject to known values of ψ along any body surface and known values of $\partial\psi/\partial x$ and $\partial\psi/\partial y$ in the free stream.

Our finite-difference technique divides the flow field into equally spaced nodes, as shown in Fig. 8.42 . To economize on the use of parentheses or functional notation, subscripts i and j denote the position of an arbitrary, equally spaced node, and $\psi_{i,j}$ denotes the value of the stream function at that node

$$\psi_{i,j} = \psi(x_0 + i\ \Delta x,\ y_0 + j\ \Delta y)$$

Thus, $\psi_{i+1,j}$ is just to the right of $\psi_{i,j}$, and $\psi_{i,j+1}$ is just above.

An algebraic approximation for the derivative $\partial\psi/\partial x$ is

$$\frac{\partial \psi}{\partial x} \approx \frac{\psi(x + \Delta x,\ y) - \psi(x,\ y)}{\Delta x}$$

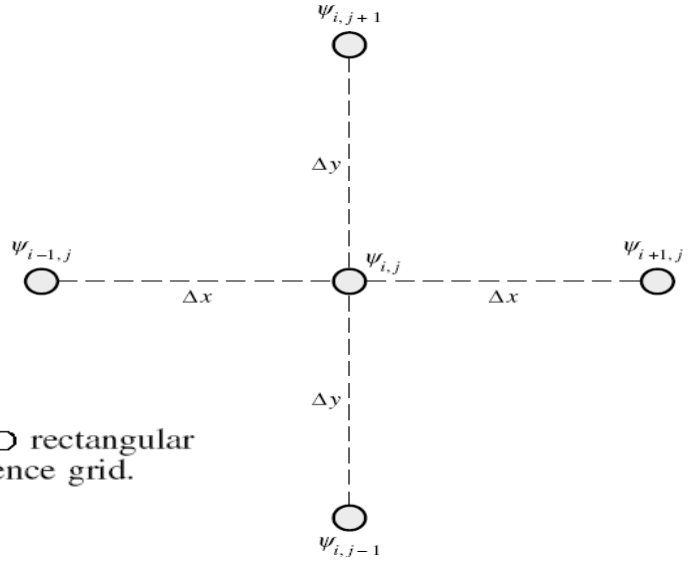

Fig. 3.42 2-D rectangular finite difference grid.

A similar approximation for the second derivative is

$$\frac{\partial^2 \psi}{\partial x^2} \approx \frac{1}{\Delta x}\left[\frac{\psi(x + \Delta x,\ y) - \psi(x,\ y)}{\Delta x} - \frac{\psi(x,\ y) - \psi(x - \Delta x,\ y)}{\Delta x}\right]$$

The subscript notation makes these expressions more compact

$$\frac{\partial \psi}{\partial x} \approx \frac{1}{\Delta x}(\psi_{i+1,j} - \psi_{i,j})$$
$$\frac{\partial^2 \psi}{\partial x^2} \approx \frac{1}{\Delta x^2}(\psi_{i+1,j} - 2\psi_{i,j} + \psi_{i-1,j}) \tag{3.165}$$

These formulas are exact in the calculus limit as $\Delta x \to 0$, but in numerical analysis we keep Δx and Δy finite, hence the term *finite differences*.

In an exactly similar manner we can derive the equivalent difference expressions for the y direction

$$\frac{\partial \psi}{\partial y} \approx \frac{1}{\Delta y}(\psi_{i,j+1} - \psi_{i,j})$$
$$\frac{\partial^2 \psi}{\partial y^2} \approx \frac{1}{\Delta y^2}(\psi_{i,j+1} - 2\psi_{i,j} + \psi_{i,j-1}) \tag{3.166}$$

The use of subscript notation allows these expressions to be programmed directly into a scientific computer language such as BASIC or FORTRAN.

When (3.165) and (3.166) are substituted into Laplace's equation (3.164), the result is the algebraic formula

$$2(1 + \beta)\psi_{i,j} \approx \psi_{i-1,j} + \psi_{i+1,j} + \beta(\psi_{i,j-1} + \psi_{i,j+1}) \qquad (3.167)$$

where $\beta = (\Delta x/\Delta y)^2$ depends upon the mesh size selected. This finite-difference model of Laplace's equation states that every nodal stream-function value $\psi_{i,j}$ is a linear combination of its four nearest neighbors.

The most commonly programmed case is a square mesh ($\beta = 1$), for which Eq. (3.167) reduces to

$$\psi_{i,j} \approx \tfrac{1}{4}(\psi_{i,j+1} + \psi_{i,j-1} + \psi_{i+1,j} + \psi_{i-1,j}) \qquad (3.168)$$

Thus, for a square mesh, each nodal value equals the arithmetic average of the four neighbors shown in Fig. 3.42 . The formula is easily remembered and easily programmed. If P(I, J) is a subscripted variable stream function, the BASIC or FORTRAN statement of (3.168) is

$$\text{P(I, J)} = 0.25 * (\text{P(I, J + 1)} + \text{P(I, J - 1)} + \text{P(I + 1, J)} + \text{P(I - 1, J)}) \qquad (3.169)$$

This is applied in iterative fashion sweeping over each of the internal nodes (I, J), with known values of P specified at each of the surrounding boundary nodes. Any initial guesses can be specified for the internal nodes P(I, J), and the iteration process will converge to the final algebraic solution in a finite number of sweeps. The numerical error, compared with the exact solution of Laplace's equation, is proportional to the square of the mesh size.

Convergence can be speeded up by the *successive overrelaxation* (SOR) method, discussed by Patankar [5]. The modified SOR form of the iteration is

$$\text{P(I, J)} = \text{P(I, J)} + 0.25 * \text{A} * (\text{P(I, J + 1)} + \text{P(I, J - 1)} + \text{P(I + 1, J)} + \text{P(I - 1, J)} - 4 * \text{P(I, J)}) \qquad (3.170)$$

The recommended value of the SOR convergence factor A is about 1.7. Note that the value $A = 1.0$ reduces Eq. (3.170) to (3.169).

Let us illustrate the finite-difference method with an example.

Example 3.16 (Also on Numerical Methods):

Make a numerical analysis, using $\Delta x = \Delta y = 0.2$ m, of potential flow in the duct expansion shown in Fig. 3.43 . The flow enters at a uniform 10 m/s, where the duct width is 1 m, and is assumed to leave at a uniform velocity of 5 m/s, where the duct width is 2 m. There is a straight section 1 m long, a 45° expansion section, and a final straight section 1 m long.

Solution

Using the mesh shown in Fig. 3.43 results in 45 boundary nodes and 91 internal nodes, with i varying from 1 to 16 and j varying from 1 to 11. The internal points are modeled by Eq. (3.169). For convenience, let the stream function be zero along the lower wall. Then since the volume flow is (10 m/s)(1 m) = 10 m^2/s per unit depth, the stream function must equal 10 m^2/s along the upper wall. Over the entrance and exit planes, the stream function must vary linearly to give uniform velocities:

Inlet: $\psi(1, \text{J}) = 2 * (\text{J} - 6)$ for J = 7 to 10

Exit: $\psi(16, \text{J}) = \text{J} - 1$ for J = 2 to 10

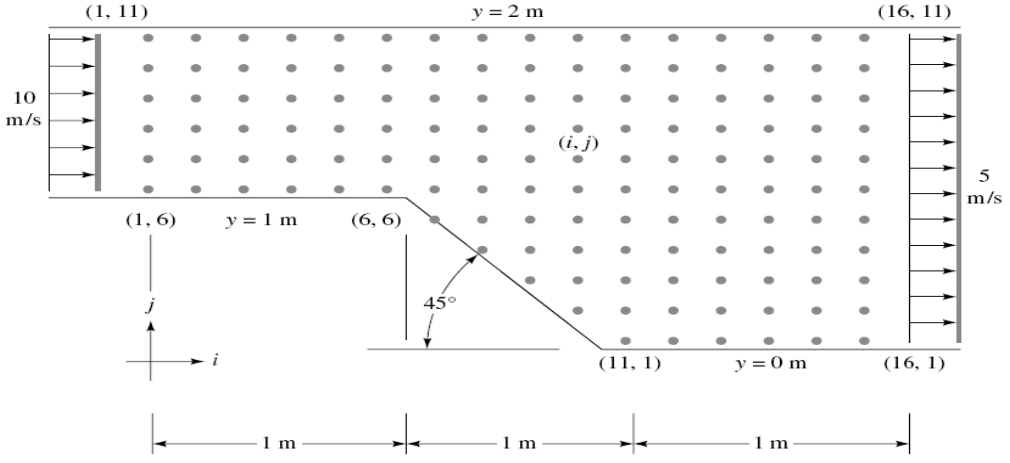

Fig. 3.43 Numerical model of potential flow through a 2-D 45° expansion. The nodal points shown are 20 cm apart There are 45 boundary nodes 91 internal nodes.

All these boundary values must be input to the program and are shown printed in Fig.3.44 .

Initial guesses are stored for the internal points, say, zero or an average value of 5.0 m^2/s. The program then starts at any convenient point, such as the upper left (2, 10), and evaluates Eq. (3.169) at every internal point, repeating this sweep iteratively until there are no further changes (within some selected maximum change) in the nodal values. The results are the finite-difference simulation of this potential flow for this mesh size; they are shown printed in Fig. 3.44 to three-digit accuracy. The reader should test a few nodes in Fig. 3.44 to verify that Eq. (3.169) is satisfied everywhere. The numerical accuracy of these printed values is difficult to estimate, since there is no known exact solution to this problem. In practice, one would keep decreasing the mesh size to see whether there were any significant changes in nodal values.

This problem is well within the capability of a small personal computer. The values shown in Fig.3.44 were obtained after 100 iterations, or 6 min of execution time, on a Macintosh SE personal computer, using BASIC.

ψ = 10.00	10.00	10.00	10.00	10.00	10.00	10.00	10.00	10.00	10.00	10.00	10.00	10.00	10.00	10.00	10.00
8.00	8.02	8.04	8.07	8.12	8.20	8.30	8.41	8.52	8.62	8.71	8.79	8.85	8.91	8.95	9.00
6.00	6.03	6.06	6.12	6.22	6.37	6.58	6.82	7.05	7.26	7.44	7.59	7.71	7.82	7.91	8.00
4.00	4.03	4.07	4.13	4.26	4.48	4.84	5.24	5.61	5.93	6.19	6.41	6.59	6.74	6.88	7.00
2.00	2.02	2.05	2.09	2.20	2.44	3.08	3.69	4.22	4.65	5.00	5.28	5.50	5.69	5.85	6.00
ψ = 0.00	0.00	0.00	0.00	0.00	0.00	1.33	2.22	2.92	3.45	3.87	4.19	4.45	4.66	4.84	5.00
						0.00	1.00	1.77	2.37	2.83	3.18	3.45	3.66	3.84	4.00
							0.00	0.80	1.42	1.90	2.24	2.50	2.70	2.86	3.00
								0.00	0.63	1.09	1.40	1.61	1.77	1.89	2.00
									0.00	0.44	0.66	0.79	0.87	0.94	1.00
										0.00	0.00	0.00	0.00	0.00	0.00

Fig.3.44 Stream-function nodal values for the potential flow of Fig. 3.43. Boundary values are known inputs. Internal nodes are solutions to Eq.3.169

Although Fig. 3.44 is the computer solution to the problem, these numbers must be manipulated to yield practical engineering results. For example, one can interpolate these numbers to sketch various streamlines of the flow. This is done in Fig. 3.45 *a*. We see that the streamlines are curved both upstream and downstream of the corner regions, especially near the lower wall. This indicates that the flow is not one-dimensional.

The velocities at any point in the flow can be computed from finite-difference formulas such as Eqs. (3.165) and (3.166). For example, at the point (I, J) = (3, 6), from Eq. (3.166), the horizontal velocity is approximately

$$u(3,\,6) \approx \frac{\psi(3,\,7) - \psi(3,\,6)}{\Delta y} = \frac{2.09 - 0.00}{0.2} = 10.45 \text{ m/s}$$

and the vertical velocity is zero from Eq. (3.165). Directly above this on the upper wall, we estimate

$$u(3,\,11) \approx \frac{\psi(3,\,11) - \psi(3,10)}{\Delta y} = \frac{10.00 - 8.07}{0.2} = 9.65 \text{ m/s}$$

The flow is not truly one-dimensional in the entrance duct. The lower wall, which contains the diverging section, accelerates the fluid, while the flat upper wall is actually decelerating the fluid.

Another output function, useful in making boundary-layer analyses of the wall regions, is the pressure distribution along the walls. If p_1 and V_1 are the pressure and velocity at the entrance (I = 1), conditions at any other point are computed from Bernoulli's equation, neglecting gravity

$$p + \tfrac{1}{2}\rho V^2 = p_1 + \tfrac{1}{2}\rho V_1^2$$

which can be rewritten as a dimensionless pressure coefficient

$$C_p = \frac{p - p_1}{\frac{1}{2}\rho V_1^2} = 1 - \left(\frac{V}{V_1}\right)^2$$

This determines p after V is computed from the stream-function differences in Fig. 3.44 .

Figure 3.45 *b* shows the computed wall-pressure distributions as compared with the one-dimensional continuity approximation $V_1A_1 \approx V(x)A(x)$, or

$$C_p(\text{one-dim}) \approx 1 - \left(\frac{A_1}{A}\right)^2 \qquad (1)$$

The one-dimensional approximation, which is rather crude for this large (45°) expansion, lies between the upper and lower wall pressures. One-dimensional theory would be much more accurate for a 10° expansion.

Analyzing Fig. 3.45 *b*, we predict that boundary-layer separation will probably occur on the lower wall between the corners, where pressure is strongly rising (highly adverse gradient). There-

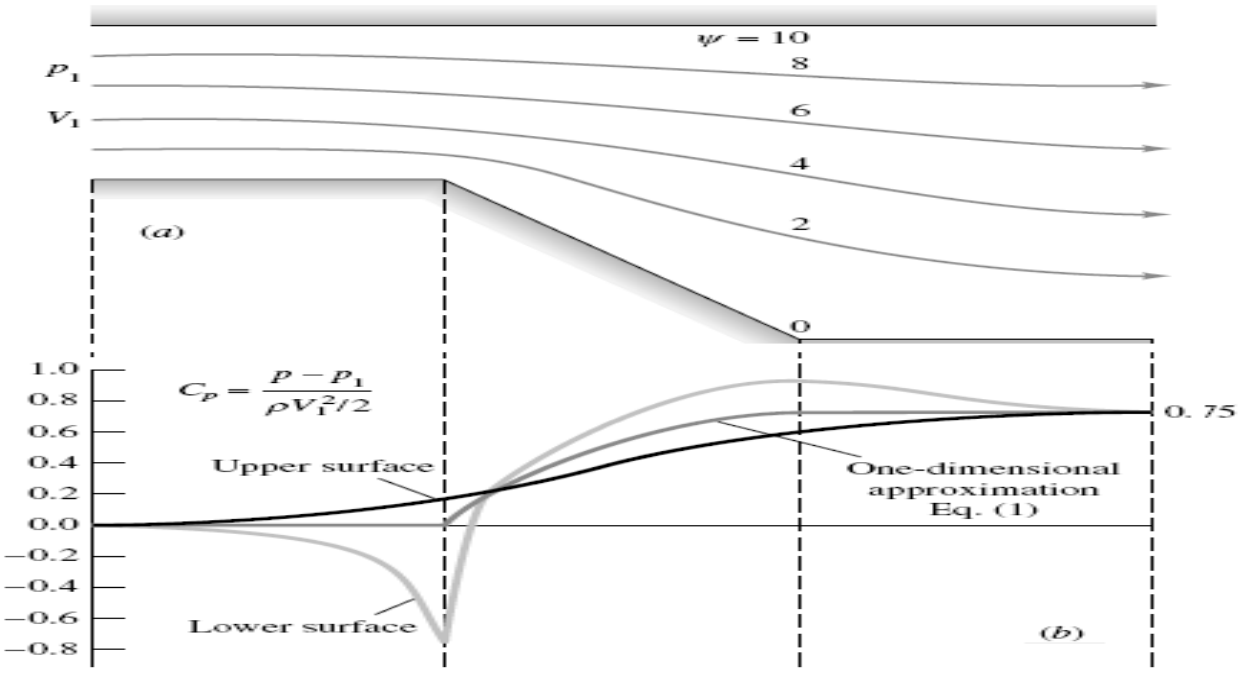

Fig. 3.45 Useful results computed from Fig. 3.44 : (*a*) streamlines of the flow; (*b*) pressure-coefficient distribution along each wall.

fore potential theory is probably not too realistic for this flow, where viscous effects are strong. (as shown in fig.3.46 for the real flow in a diffuser where the current example is half the flow field)

Potential theory is *reversible*; i.e., when we reverse the flow arrows in Fig. 3.45 *a*, then Fig. 3.45*b* is still valid and would represent a 45° *contraction* flow. The pressure would fall on both walls (no separation) from $x = 3$ m to $x = 1$ m. Between $x = 1$ m and $x = 0$, the pressure rises on the lower surface, indicating possible separation, probably just downstream of the corner.

This example should give the reader an idea of the usefulness and generality of numerical analysis of fluid flows.

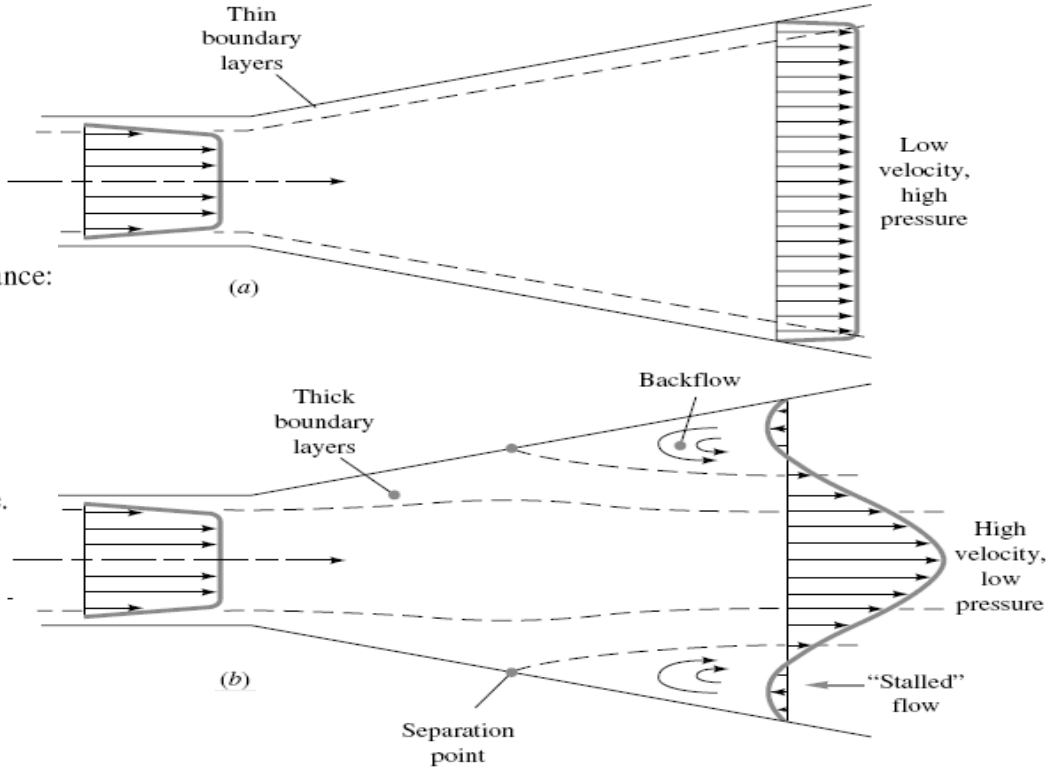

Fig. 3.46 Diffuser performance: (*a*) ideal pattern with good performance; (*b*) actual measured pattern with boundary-layer separation and resultant poor performance.

3.16.3 The Finite Element Method:

The finite-element method [19] is applicable to all types of linear and nonlinear partial differential equations in physics and engineering. The computational domain is divided into small regions, usually triangular or quadrilateral. These regions are delineated with a finite number of *nodes* where the field variables—temperature, velocity, pressure, stream function, etc.—are to be calculated. The solution in each region is approximated by an algebraic combination of local nodal values. Then the approximate functions are integrated over the region, and their error is minimized, often by using a weighting function. This process yields a set of N algebraic equations for the N unknown nodal values. The nodal equations are solved simultaneously, by matrix inversion or iteration. For further details see Ref. 6 or 19.

3.17 Case Study: Numerical Solution of Flow Around a Cylinder***:***

In this section, we will analyze in more detail the irrotational flow field around a cylinder due to a uniform flow. The cylinder is a *bluff* body whereas a wing that is well-oriented (small angle of attack) with respect to flow is a *slender* body. In reality (in the sense of a real viscous fluid) separation of the boundary layer with the formation of a wake will be unavoidable for the cylinder. The irrotational solution cannot predict such phenomenon and the resulting flow field do not resemble the real flow around a cylinder.

Given these, why do we study the irrotational flow around a cylinder? First of all, this flow is a good example of an irrotational flow in a relatively complex geometry. Secondly, and most important, because using conformal mapping we can transform the flow around a cylinder into the flow around a Joukowski wing. If a wing profile is well oriented with respect to the uniform flow, boundary layer separation is negligible and the pressure field obtained by means of the irrotational flow solution can be considered as a good approximation of the actual pressure field. Therefore, the resulting lift is in good agreement with experimental measurements. In the following sections several animations show how the velocity and pressure fields vary as the circulation around the cylinder is changed.

3.17.1 THE STREAMLINES:

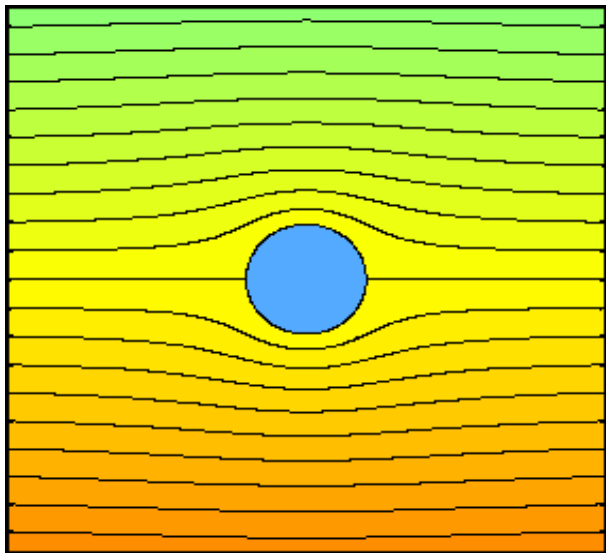

The first animation is for the velocity field, represented here in term of the stream function. For a case of zero circulation, the velocity field is symmetric with respect to the x-axis and the two stagnation points lie at the intersections of the cylinder and the x-axis (left figure). The animation on the right shows the stream function as the circulation increases to a maximum and then decreases to zero. The uniform flow is from right to left and the circulation is counterclockwise. You can see the stagnation points moving towards the lower face of the cylinder as circulation increases. The streamlines become closely packed near the upper face and less packed near the lower face, indicating an acceleration on the upper face and a deceleration on the lower face. In fact, the mass flux in the stream tube defined by two adjacent streamlines is constant. When streamlines get closer to each other, the flow is accelerating and vice versa.

3.17.2 THE STREAKLINES:

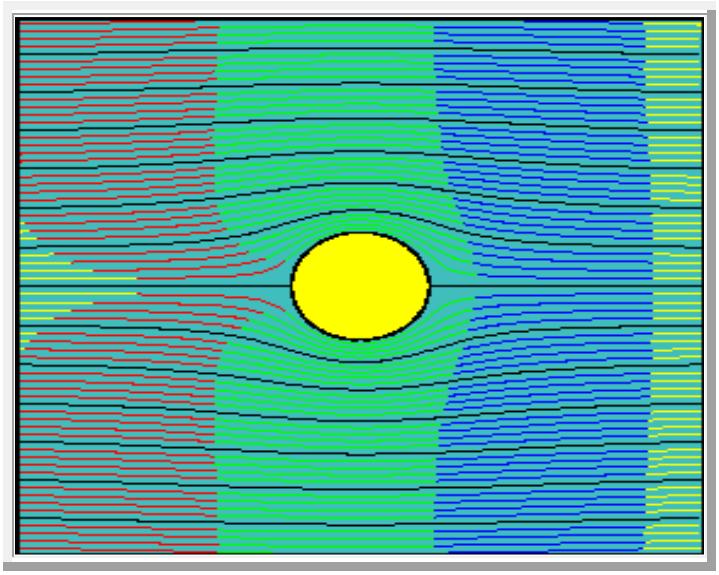

The streaklines displayed in the following animations are the result of an ideal experiment in which a passive tracer (like smoke) is injected in the flow, making the path of ``marked'' fluid particles visible. This allows us to follow, in a Lagrangian sense, the motion of the group of fluid particles that have passed through the same point. Since the flow is steady, the trajectories of such particles (the streaklines) are identical to the streamlines. Changing periodically the color of all the smoke sources allows for a visualization of the time history of subsets of smoke particles injected in the same time interval. When the colored lines become shorter, the marked fluid particles are slowing down and vice versa. The grid of smoke sources is equally spaced in the vertical direction and it is positioned far upstream from the body (at a distance of about 100 times the radius of the cylinder), so that sources are not influenced by the body (uniform flow). Animations have been realized for three increasing values of the circulation around the cylinder. In the first animation, the circulation is zero and the flow is symmetrical with respect to the x-axis. Note how the fluid particles closer to the cylinder are delayed with respect to those passing well above (or below) the cylinder. This delay is not due to friction (we are dealing with an inviscid fluid) but to the fact that near the stagnation points velocity tends to decelerate to zero speed. Due to the symmetry of the flow field, if two particles start symmetrically with respect to the x-axis, they will need the same amount of time to flow around the body.

When circulation is increased, the latter statement is not true anymore. Now, the fluid flowing above the cylinder reaches the downstream section before the fluid flowing below the cylinder. It is possible to demonstrate that the arrival times are the same only for two particles starting slightly above and below the front stagnation point and flowing along the cylinder surface.

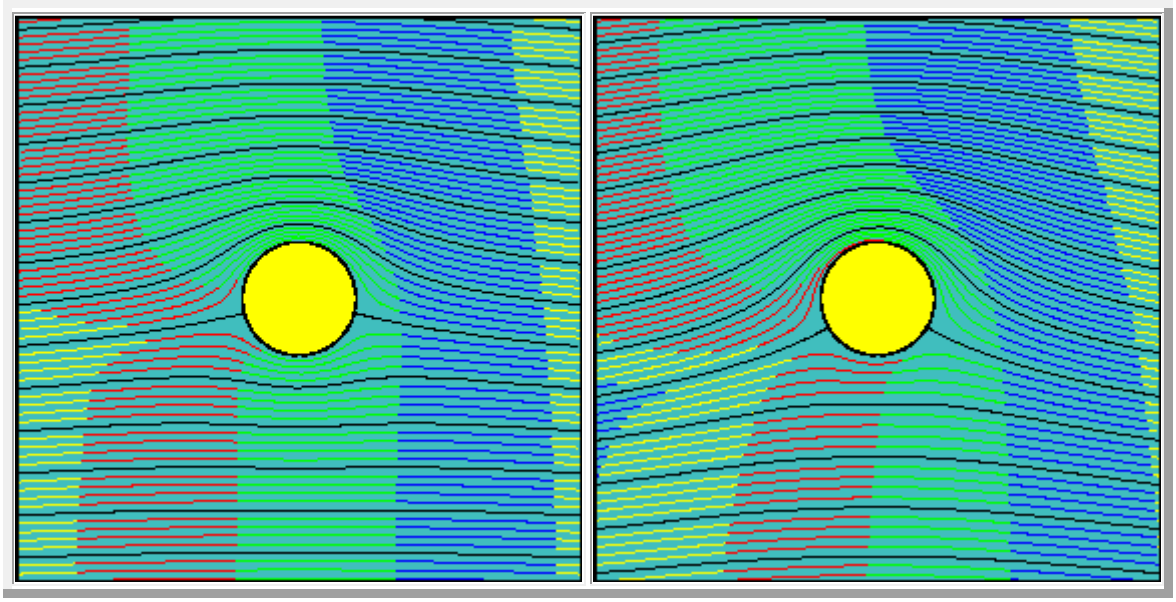

In many elementary aerodynamics textbooks it is stated that, with non-zero circulation, the portion of fluid flowing above the cylinder is accelerated with respect to the one flowing below it ``because it must travel for a longer route to reach downstream in the same amount of time''. In reality there is no physical law imposing that the two fluid portions flowing above and below the cylinder (the interface of which can be identified with the streamline passing through the two stagnation points) must take the same time to travel around the cylinder. Indeed, looking at the second animation, it is evident that far from the body, where the flow is essentially uniform, the ``above-the cylinder'' fluid reaches the left end of the window well before the ``below-the cylinder'' fluid does. If we were allowed to observe what happens far downstream, where the flow is certainly uniform again, we would see that this configuration is somewhat ``frozen'' and the fluid particles which have been delayed do not try in any way to catch up. In the cases examined so far, it is nevertheless still true that two adjacent fluid particles that are separated by the body will become adjacent again once the body is passed, since the arrival times of two particles flowing along the cylinder surface are the same. In the case of flow around an airfoil even the latter statement is true only for a very peculiar case.

3.17.3 THE VELOCITY FIELD:

The animation of the velocity vector field confirms what has been shown in the stream function animation. When circulation is zero, the uniform stream approaching from the right divides into two symmetric flows, one going over the cylinder, the other flowing under it. The two flows connect again downstream of the cylinder. The flow field is symmetric with respect to the *x*-axis. Two fluid particles immediately above and below the upstream stagnation point travel the same distance around the cylinder and then meet again at the downstream stagnation point.

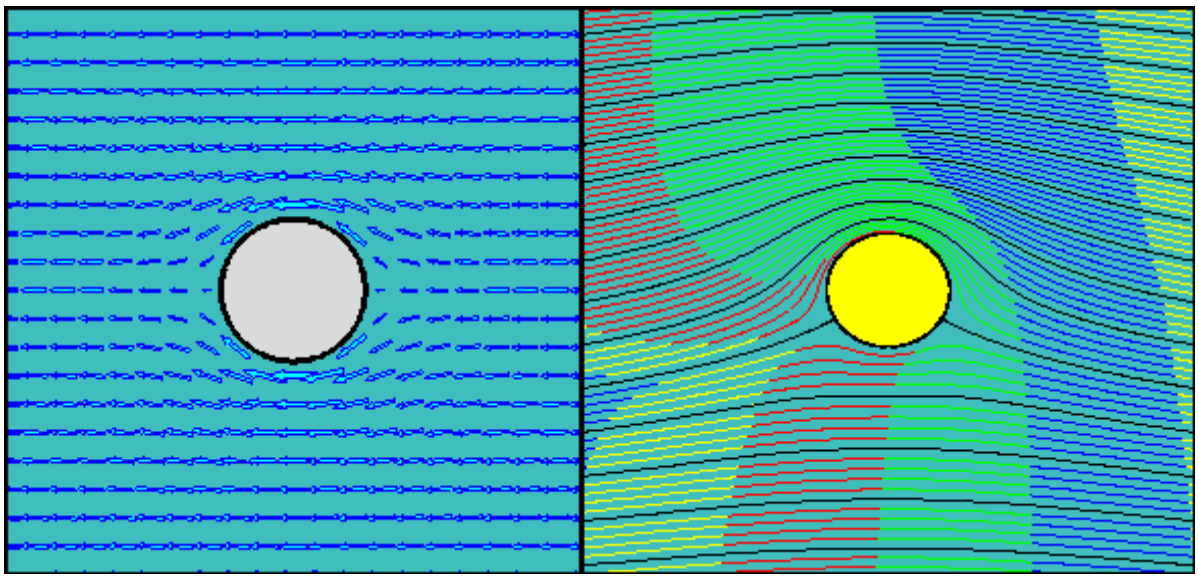

When circulation is increased, the stagnation points move towards the lower half of the cylinder so that the two companion fluid particles follow different routes to reach the downstream stagnation point. In particular the fluid particle that travels above the cylinder makes a longer route with respect to its companion, but it travels fast enough to arrive at the same time at the downstream stagnation point.

3.17.4 THE PRESSURE FIELD:

We can now evaluate the pressure field with the equivalence:

$$\frac{p_{\infty}}{\gamma} + \frac{V_{\infty}^2}{2g} = \frac{p}{\gamma} + \frac{V^2}{2g}$$

Where p_∞ indicates the reference value of the pressure at infinity (where the flow is uniform). In the picture, shown is the excess non-dimensional pressure defined as :

$$\frac{p-p_\infty}{\rho V_\infty^2} = \frac{1}{2}\left(1-\left(\frac{V}{V_\infty}\right)^2\right)$$

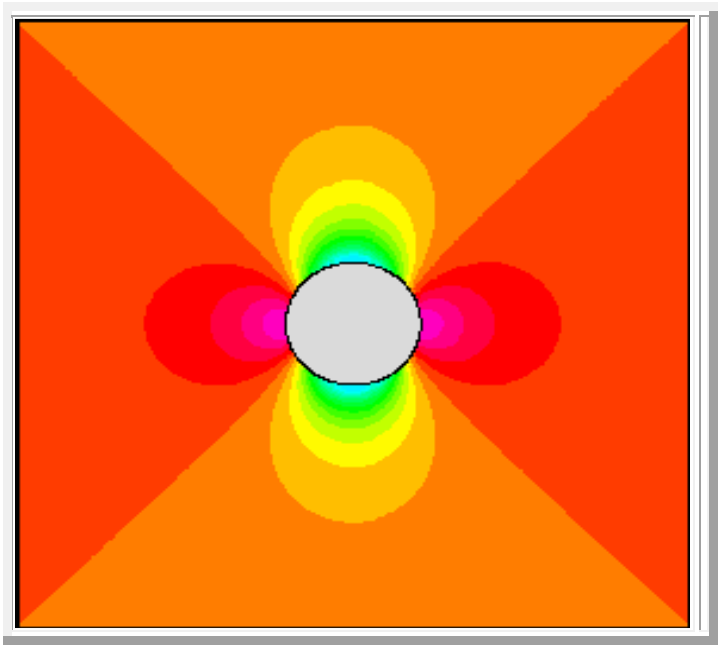

When circulation is absent, the pressure field is symmetric with respect to both the *x* and the *y*-axes. On the stagnation points the excess pressure is positive (which means an action directed **towards** the body) while on the upper and lower points the excess pressure is negative (which means an action directed **away** from the body). As circulation increases the pressure field is still symmetric with respect to the *y*-axis but becomes asymmetric with respect to the *x*-axis.

3.17.5 FORCES ACTING ON THE CYLINDER:

To understand the implication of the asymmetry of the pressure field in terms of the forces acting on the cylinder, the last animation shows the elementary forces as vectors on the cylinder surface. Each elementary force is given by $dF = -pnds$

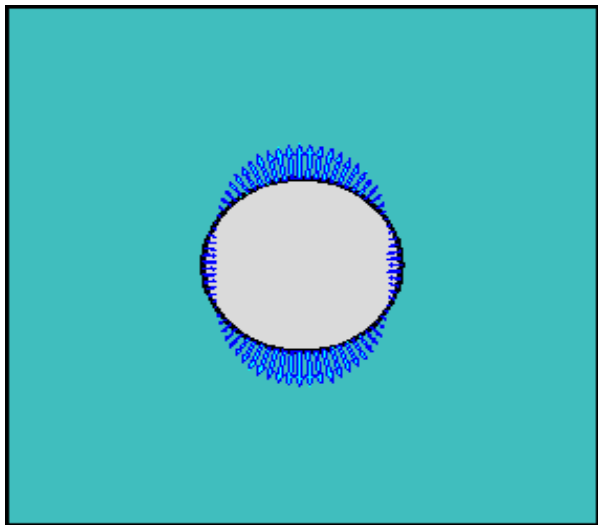

Where *p* is pressure, **n** is the normal unit vector directed away from the surface and *ds* is the surface arc. The resulting force (the vectorial sum of all the elementary forces on the body) is clearly zero when circulation is zero (D'Alambert paradox). As circulation increases the component of the resulting force in the direction of the uniform flow is still zero (no drag), whereas a component in the direction perpendicular to the uniform flow (lift) appears that increases as circulation is enhanced. The modulus of the lift can be evaluated analytically (Kutta-Joukowski theorem) and is $L = \rho U_\infty \gamma$

3.18 FLOW AROUND AN AIRFOIL:

Before analyzing the velocity and pressure field for the case of an airfoil, we need to investigate a little more deeply the role played by circulation. The Kutta-Joukowski theorem shows that lift is proportional to circulation, but apparently the value of the circulation can be assigned arbitrarily. The solution of flow around a cylinder tells us that we should expect to find two stagnation points along the airfoil the position of which is determined by the circulation around the profile. There is a particular value of the circulation that moves the rear stagnation point (V=0) exactly on the trailing edge.

This condition, which fixes a value of the circulation by simple geometrical considerations is the **Kutta condition**. Using Kutta condition the circulation is not anymore a free variable and it is possible to evaluate the lift of an airfoil using the same techniques that were described for the cylinder. Note that the flow fields obtained for a fixed value of the circulation are all valid solutions

of the flow around an airfoil. The Kutta condition chooses one of these fields, one that represents the best actual flow. We can try to give a feasible physical justification of the Kutta condition; to do this we need to introduce a concept that is ignored by the theory for irrotational inviscid flow: the role-played by the viscosity of a real fluid. Suppose we start from a static situation and give a small velocity to the fluid. If the fluid is initially at rest it is also irrotational and, neglecting the effect of viscosity, it must remain irrotational due to Thompson theorem. The flow field around the wing will then have zero circulation, with two stagnation points located one on the lower face of the wing, close to the leading edge, and one on the upper face, close to the trailing edge.

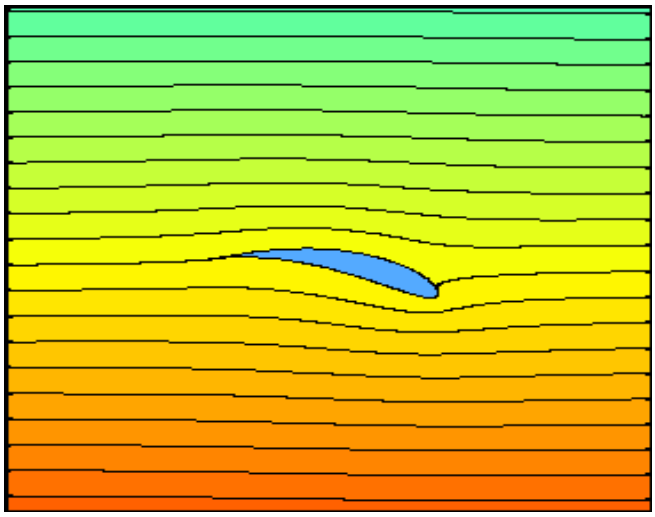

A very unlikely situation is created at the trailing edge: a fluid particle on the lower side of the airfoil should travel along the profile, make a sharp U-turn at the trailing edge, go upstream on the upper face until it reaches the stagnation point and then, eventually, leave the profile. A real fluid cannot behave in this way. Viscosity acts to damp the sharp velocity gradient along the profile causing a separation of the boundary layer and a wake is created with shedding of clockwise vorticity from the trailing edge.

Since the circulation along a curve that includes both the vortex and the airfoil must still be zero, this leads to a counterclockwise circulation around the profile. But if a nonzero circulation is present around the profile, the stagnation points would move and in particular the rear stagnation point would move towards the trailing edge. The sequence vortex shedding -> increase of circulation around the airfoil -> downstream migration of the rear stagnation point continues until the stagnation point reaches the trailing edge. When this happens the sharp velocity gradient disappears and the vorticity shedding stops. This ``equilibrium" situation freezes the value of the circulation around the airfoil, which would not change anymore. Let us now proceed to examine the velocity and pressure fields around an airfoil with the aid of some animations showing how they vary when the (effective) angle of attack is changed. In each shot the flow field is obtained imposing the Kutta condition to determine the circulation. A sequential browsing of the following pages is suggested, at least for first time visitors.

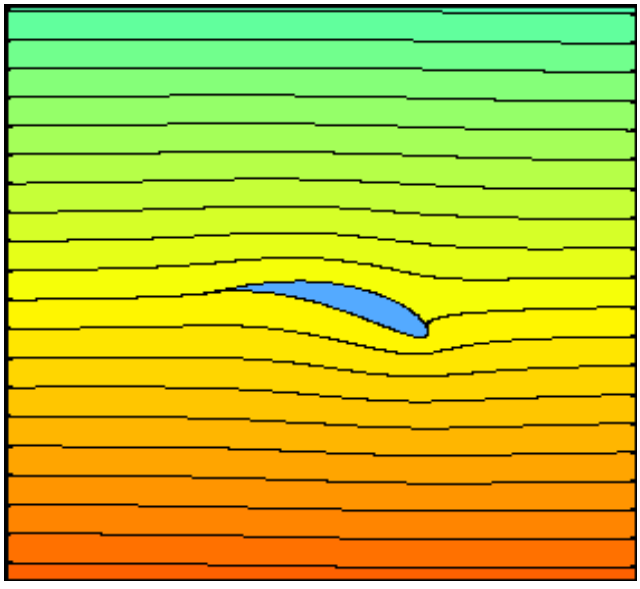

3.18.1 THE STREAMLINES:

In the following animation the stream function is plotted together with the streamlines. Direction of flow is from right to left and the angle of attack is varied by rotating the airfoil. Note that, as the airfoil rotates, a streamline always leaves the trailing edge, indicating that Kutta condition is imposed. Far from the airfoil the streamlines tend to become horizontal, as expected for a uniform flow.

3.18.2 THE STREAKLINES:

In the following animations the streaklines generated by a set of smoke sources equally spaced in the vertical direction and positioned far upstream of the airfoil are presented. The color of the injected smoke has been changed at regular time steps so as to make the time history of the fluid particles that have been ``marked'' passing through each smoke source visible.

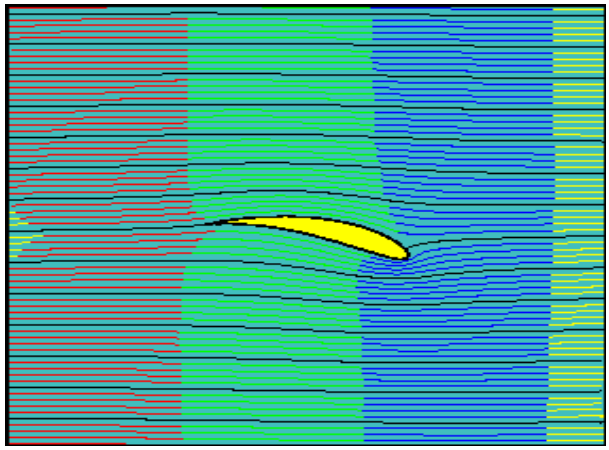

Three increasing values of the effective angle of attack (0, 15 and 30 degrees, respectively) have been chosen for the animations. The first animation shows a smoke pattern similar to that observed for the flow around a cylinder with no circulation. Indeed, in this case the rear stagnation point is naturally coincident with the trailing edge and the Kutta condition is verified with zero circulation around the airfoil. Note how the fluid particles closer to the airfoil are delayed with respect to those passing well above (or below) the airfoil. Friction has no role here and this effect, as for the cylinder, is due to the vanishing of velocity in the neighborhood of the stagnation points. Also note how the two portions of fluid passing above and below the airfoil reach the left end section at the same time. Two fluid particles flowing along the profile need the same time to travel above or below the airfoil.

As the angle of attack, and so the circulation around the airfoil, is increased, the latter statement is not true anymore, in the sense that fluid flowing above the airfoil reach the downstream section earlier than the fluid traveling below it.

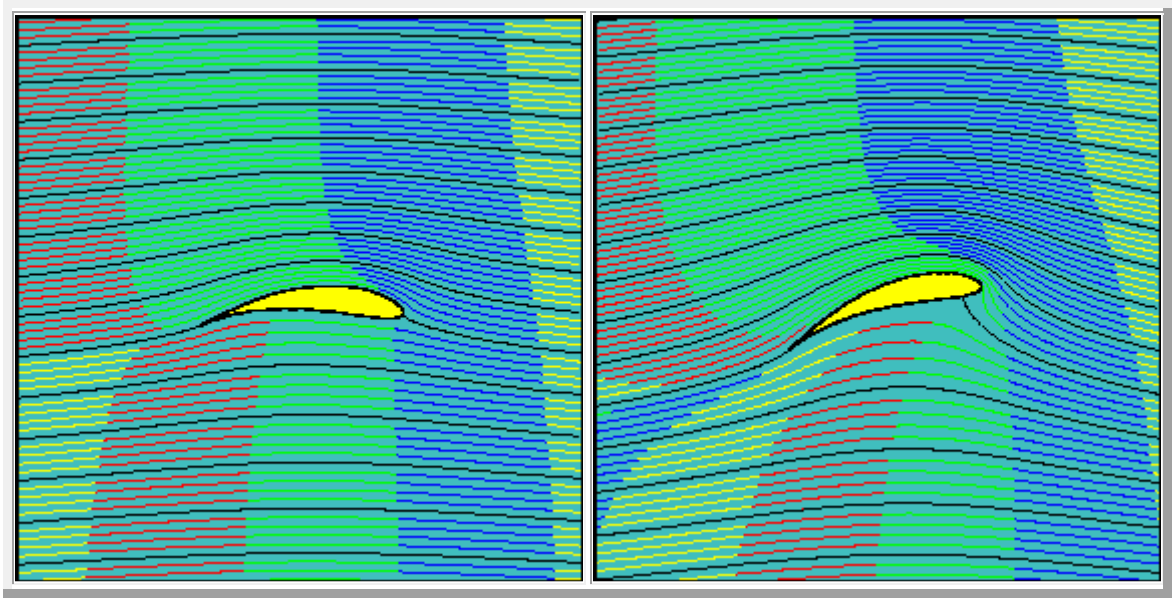

It can be demonstrated that in contrast to what happens for the cylinder, the traveling times are in this case different also for fluid particles flowing along the airfoil surface, as it is evident looking at the animations above and focusing on the neighborhood of the trailing edge. This effect is related to the role played by the conformal transformation, which alters both the length of the path and the velocity but not in a way to keep the traveling times of two particles flowing along the surface of the airfoil equal. The fluid portion flowing below the airfoil is delayed with respect to the portion flowing

above it, and the delay increases as the angle of attack (and so the circulation around the airfoil and, as we will see, the lift) increases. Stating that the fluid flowing above the airfoil is accelerated with respect to the fluid flowing below it ``because it must travel for a longer route in the same time'' is then definitely wrong.

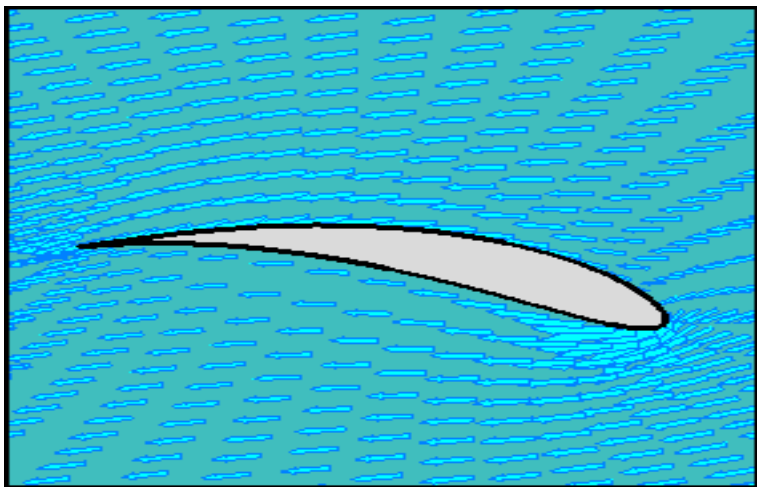

3.18.3 THE VELOCITY FIELD:

This animation shows again the flow field, now described in terms of the velocity vectors.

3.18.4 *THE PRESSURE FIELD:*

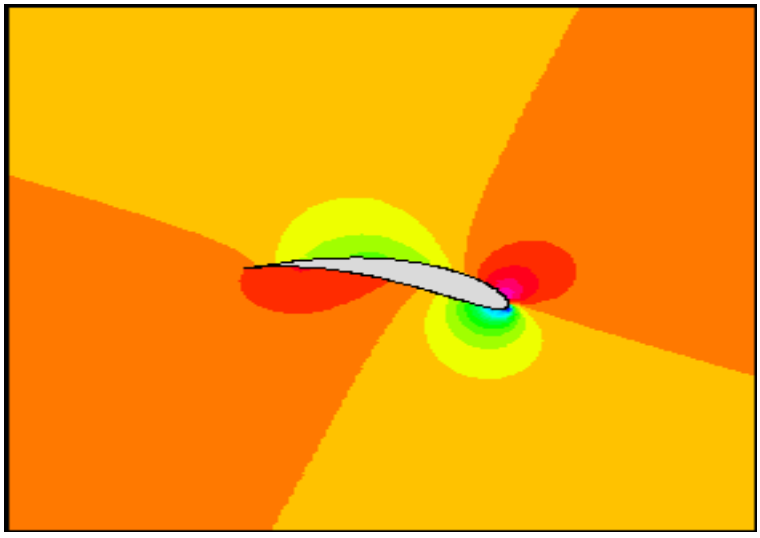

The pressure field shows positive (reddish) values on the lower face of the wing and negative (yellow-green-blue) values on the upper face, thus leading to a lift. Note that for large values of the angle of attack a strong negative (blue) peak of the pressure appears on the upper face of the airfoil close to the leading edge. As this negative peak increases, the positive pressure gradient downstream of it increases, a condition that leads to boundary layer separation on the upper face and consequently to a sudden drop in the lift (stall).

3.18.5 FORCES ON AIRFOIL:

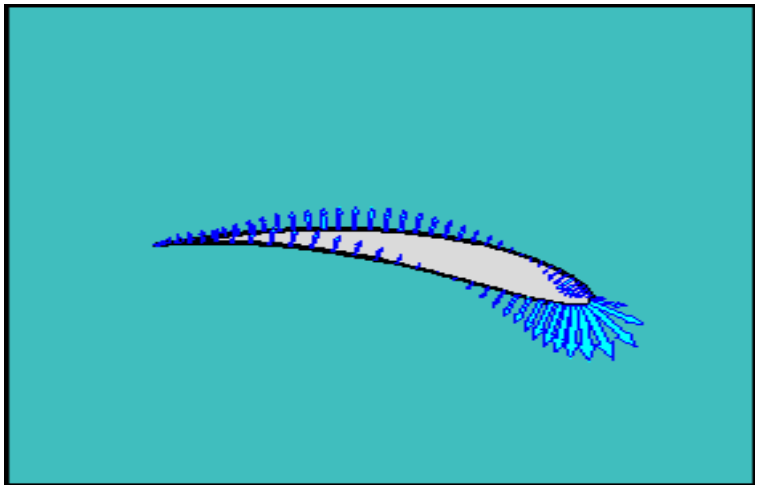

We now examine the forces acting on the airfoil in terms of elementary forces instead of pressure. While it is intuitive that as the angle of attack increases the lift increases, it is not easy to see that the drag is always zero for the airfoil as it was for the cylinder. This is because the unit vector normal to the airfoil is not simply radial as in the cylinder case.

3.19 Tailing and Railing Vortices:

On a clear day, trailing vortices are often seen in the sky following the passage of an airplane. The vortices are formed because the wing develops lift. That is, the pressure on the top of the wing is lower than on the bottom, and near the tips of the wing this pressure difference causes the air to move around the edge from the bottom surface to the top. This results in a roll-up of the fluid, which then forms the trailing vortex. In the sky, the vortex becomes visible when the air has a high

humidity. The velocities inside the vortex can be very high, and the pressure is therefore quite low. Water vapor in the air condenses as water droplets, and the droplets mark the presence of the vortex. In the picture below of a crop-duster flying near the ground, the vortex is made visible by a red flare placed on the ground. The red smoke is wrapped up by the trailing vortex originating near the tip of the wing.

Picture courtesy of DANTEC Measurement Technology.

The strength of the vortex is related to the amount of lift generated by the wing, so they become particularly strong in high-lift conditions such as take-off and landing. They also increase in strength with the size of the airplane, since the lift is equal to the weight of the airplane. For a large transport airplane such as a 747, the vortices are strong enough to flip a small airplane if it gets too close. Trailing vortices are therefore the principal reason for the time delay enforced by the FAA between take-offs and landings at airports.

Railing vortices and downwash phenomenon of an aircraft in flight are seen clearly in the figure below. In this situation, a Cessna Citation VI was flown immediately above the fog bank over Lake Tahoe at approximately 313 km/h or 170 knots (B. Budzowski, Director of Flight Operations, Cessna Aircraft Company, private communication, 1993). Aircraft altitude was about 122 m (400 ft) above the lake, and the weight was approximately 8400 kg. As the trailing vortices descended over the fog layer due to the downwash, the flow field in the wake was made visible by the distortion of the fog layer. The photo was taken by P. Bowen for the Cessna Aircraft Company from the tail gun- ner's position in a B-25 flying in formation slightly above and ahead of the Cessna. The aircraft is seen initiating a gentle climb after a level flight, leaving a portion of the fog layer yet unaffected. The wingspan measured 16.3 m and the wing area was 29 m^2. The Reynolds number based on the mean aerodynamic chord of 2.1 m was 1.1x10^7. The figure below is extract from the Gallery of Fluid Motion, Physics of Fluids A, Vol. 5, September 1993. Contribution by Hiroshi Higuchi (Syracuse University).

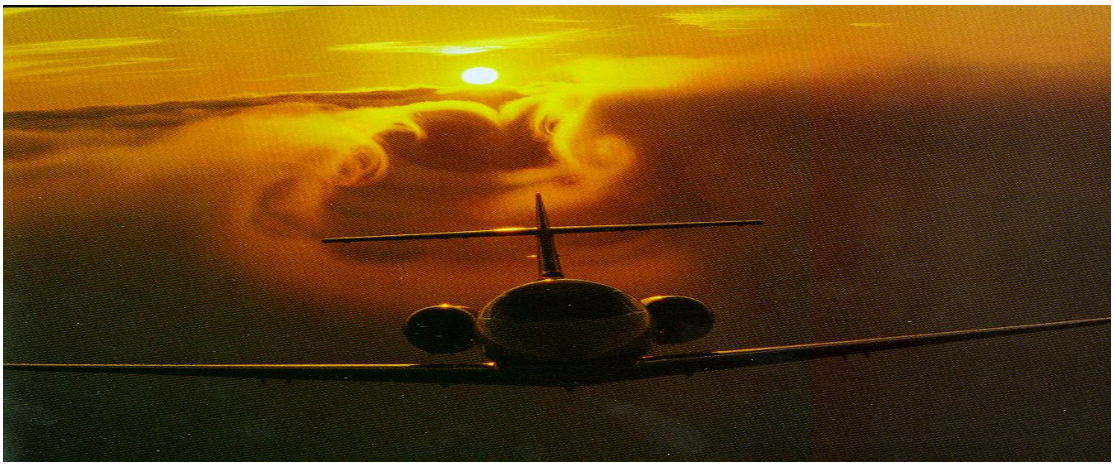

Photo courtesy of Cessna Aircraft Company.

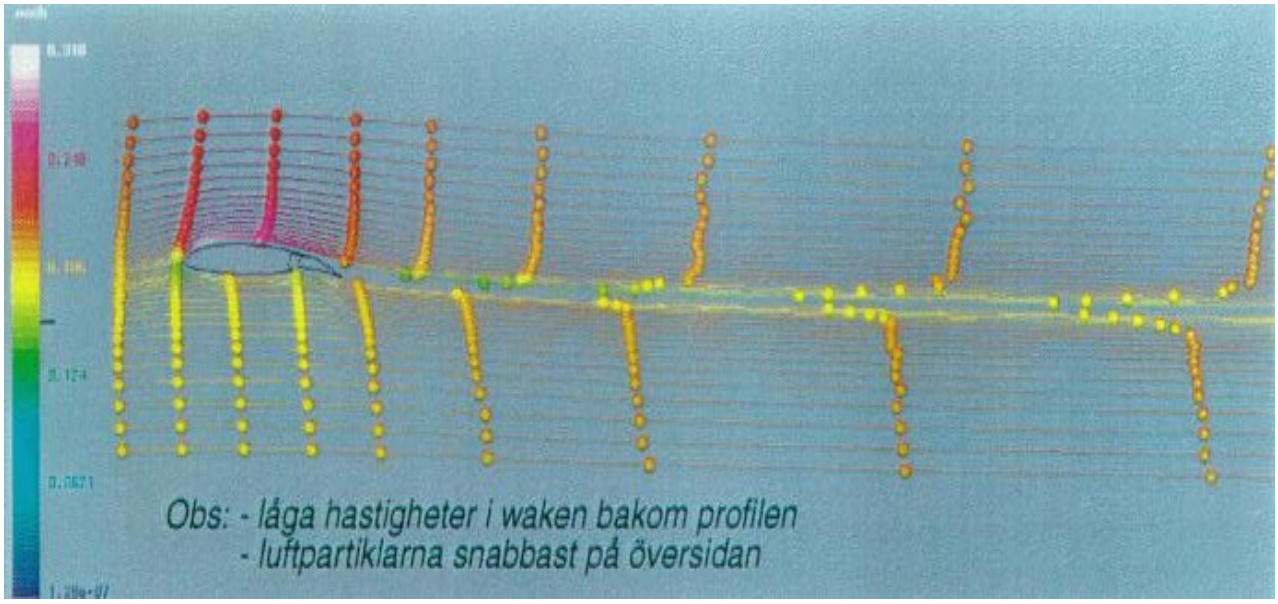

As seen above, fluid simulation from SAAB Aircraft shows phase lag between upper and lower air parcels after an airfoil has passed. Air travels much faster over the top of the airfoil, and then it never rejoins the air, which has traveled below. Note that the airfoil has deflected the air downwards.

Another picture is seen above from the 1993 Aviation Week & Space Technology Photo Contest. This came second in the Military category, and it was taken by James E. Hobbs, from Lockheed Aircraft service Co., Ontario, California. The plane is ejecting flares during a test of an infrared missile warning and self-protection system installed on a C-130 Hercules. The trailing vortices formed in the wake are clearly visible. The size of these vortices is related to the lift produced by the wings, and the photograph suggests that the aircraft was climbing during this maneuver.

This picture shows a SAAB JAS39 Gripen landing on a rainy roadbase. Downwash is made evident by the foggy cloud above the runaway.

Some more downwash ... this is a French Transall deploying flares.

Questions for the Oral Exam

Frictionless Flow (Part 3)

1- If the stream function, Ψ, is defined as $\Psi=f(x,y)$ or $\Psi=g(r,\theta)$. What is the physical and mathematical meaning of these two functions. How can we get the stream function for a given flow field **V**(x,y). What is the relationship between the stream function, Ψ, and the vorticity vector (curl of **V**), linear momentum equations, and the Bernolli's equation in both real and ideal flows. Can we define $\Psi=f(x,y,z)$ or $\Psi=g(r,\theta,z)$ for 3-D, steady, real viscous flow. Give some examples with sketches for Ψ.

2- If an Eulerian velocity flow field is defined as **V**= f(t,x,y,z), Explain the physical and mathematical meaning of this function. What do we mean by the total or substantial derivative? How do we get the acceleration, **a** , of this field? What is the deference between local acceleration and convective acceleration. In a steady flow, can the acceleration of the flow be non-zero? Explain your answer with an example.

3- Discuss what is wrong in the following statements (use sketches if needed):

I. -The stream function, Ψ, represents the mass conservation eqn. 3-D viscous flow.
II. -The value of Ψ function must be constant for all streamlines in 3-D viscous flow.
III. -Values of Ψ function are the difference in the momentum flux between streamlines.
IV. -The Laplace equation, $\nabla^2\Psi=0$ represent the mass conservation equation for a 3-D frictionless flow field and can be solved to get pressure distribution in that flow field.

4- If the potential function, Φ, is defined as $\Phi=f(x,y)$ or $\Phi=g(r,\theta)$. What is the physical and mathematical meaning of these two functions. How can we get the potential function for a given flow field **V**(x,y). What is the relationship between the potential function, Φ, and the vorticity vector (curl of **V**), linear momentum equations, and the Bernolli's equation in both real and ideal flows. Can we define $\Phi=f(x,y,z)$ or $\Phi=g(r,\theta,z)$ for 3-D, steady, real viscous flow. Give some examples with sketches for Φ.

5- What do you know about Euler's equations?. Discuss how can these equation be reduced to Bernoulli's equation along streamline in frictionless flow?. In a frictionless flow field, can we apply Bernoulli's equation everywhere in the flow? How?

6- Discuss what is wrong in the following statements (use sketches if needed)::

I. In 3-D viscous flow, the stream function, Ψ, is parallel to the velocity potential function, Φ, and both of them can be used to get the pressure distribution in the flow.
II. Euler's equations represent the mass conservation for 2-D laminar flow where the no slip condition (zero velocity at the wall) must be valid every where in the flow field.
III. In a 3-D viscous flow, the complex potential function is defined as $W(z) = (\Psi + i\,\Phi)$ where $z = (y + i\,x)$ and the velocity can be obtained from $dW/dz= (v + i\,u)$.

7- Discuss what is wrong in the following statements (use sketches if needed):

I. In a 3-D viscous, rotational flow, the complex potential function for a uniform stream in the –ve x-axis direction is defined as $W(z) = U_\infty\, z\, e^{i\alpha}$
II. In a 3-D viscous, rotational flow, the complex potential function for a point source of strength, Q, located at point z_o is defined as $W(z) = -(Q/2\Pi)\ \ln (z_o - z)$.
III. In a 3-D viscous, rotational flow, the complex potential function for a free, clockwise vortex located at point z_o is defined as $W(z) = -(i\Gamma/2\Pi)\ \ln (z_o - z)$.

8- In our study of Fluid Mechanics, we can use one of the following methods:

a- Differential analysis method

b- Integral analysis method

c- Dimensional analysis method with some experimental work

Explain very briefly those methods showing the main differences between them regarding the reason for, and the output result of each method. Give an example for each method. Do we neglect viscous effects in any of the above methods? Explain your answer.

9- In both real or ideal flow, define the physical meaning and the equation of (a) stream lines, (b) the no-slip condition. Give some examples in both internal flows and external flows. What is the difference between Ideal fluids or Newtonian fluids or Non-Newtonian fluids?.

10- Explain what do we mean by saying that the Eulerian Pressure scalar field is given as $P = f(t,x,y,z)$ or $P = g(t,r,\theta,z)$? What do we mean by the total or substantial derivative d/dt? How do we get dP/dt of the field $P = f(t,x,y,z)$? What is the deference between local pressure derivative and convective pressure derivative. In a steady flow, can the total or substantial pressure derivative of the flow be a non-zero value? Explain your answer with an example.

11- Prove that the time-derivative operator (called total or substantial derivative) following a fluid particle is: $d/dt = \partial / \partial t + (\underline{\mathbf{V}} . \underline{\nabla})$, where $\underline{\nabla}$ is the gradient operator.

12- What do you know about the conservation equations in Fluid Mechanics? Using the differential analysis method, stat and discuss two of the main conservation equations of fluid mechanics. Show all the non-linear terms in those equations. What is the divergence of the velocity vector field?. Can we write the momentum equations for a Non-Newtonian fluid? How.

13- Using the cartesian coordinates, write down and discuss the meaning of each term and show all the differences you know between the Navier-Stoke's equations and the Euler's equations. Can we use Euler's equations to solve the flow in long pipes? Why? What is the relation between Euler's equations and Bernolli's equation?

14- The flow rate is 0.25 m^3/s into a convergent nozzle of 0.6 m height at entrance and 0.3m height at exit. Find the velocity, acceleration and pressure fields through the nozzle. (take the length of the nozzle=1.5m)

15- The flow rate is 0.25 m^3/s into a divergent nozzle of 0.3 m height at entrance and 0.6m height at exit. Find the velocity, acceleration and pressure fields through the nozzle. (take the length of the nozzle=1.5m)

16- Which of the following motions are kinematically possible for incompressible flow (k and Q are constants): i) $u = k x$, $v = k y$, $w = -2k z$ ii) $V_r = - Q/2\pi r$, $V_\theta = k/2\pi r$ iii) $V_r = k \cos\theta$, $V_\theta = -k \sin\theta$

17- For a 2-D flow field in the xy-plane, the y component of the velocity is given by: $v = y^2 - 2x + 2y$. Determine a possible x-component for a steady incompressible flow. Is it also valid for unsteady flow? How many possible x-components are there? Why?.

18- For a 2-D flow field in the xy-plane, the x component of the velocity is given by: $u = y^2 - 2x + 2y$. Determine a possible y-component for a steady incompressible flow. Is it also valid for unsteady flow? How many possible x-components are there? Why?.

19- Prove that the equation of continuity for 2-D incompressible flow in polar coordinates is in the form: $\partial V_r/\partial r + V_r/r + 1/r\ (\partial V_\theta/\partial \theta) = 0$

20- Explain the physical meaning and the mathematical equations for both the divergence operator and the curl operator as applied on a vector field. Take the velocity field $\underline{\mathbf{V}}$ as an example. (hint: prove that the divergence of $\underline{\mathbf{V}}$ = the rate of volume expansion of fluid element per unit initial volume) . Prove also that for an incompressible velocity field, the divergence of $\underline{\mathbf{V}} = 0$. What is the relationship between the curle of $\underline{\mathbf{V}}$ and the rotation in the velocity field.

21- Examine the following functions to determine if they could represent the velocity potential for an incompressible inviscid flow:

a) $\Phi=2x+3y+4z^2$ b) $\Phi = x + xy + xyz$ c) $\Phi = x^2 + y^2 + z^2$

22- The velocity potential of a steady field is given by the expression: $\Phi = 2xy + y$, and the temperature is given by: $T = x^2 + 3xy + 2$. Find both the local and the convective parts of the rate of temperature change in this field.

23- Find the potential function, Φ, of a flow field such that the horizontal component of the velocity varies linearly along the y-axis and has the value U_o on the x-axis. What is the stream function, Ψ, of this field.

24- Find the potential function, Φ, of a flow field such that the vertical component of the velocity varies linearly along the x-axis and has the value V_o on the y-axis. What is the stream function, Ψ, of this field.

25- Velocity components of a 2-D flow are: $u=k(y^2-x^2)$ & $v=2kxy$, find the stream function which has $\Psi=0$ at the origin. Find the potential function Φ, sketch both the Ψ and Φ lines.

26- Velocity components of 2-D flow are: $u=-A(y^2-x^2)$ & $v=-2Axy$, find the stream function which has $\Psi=0$ at the origin. Find the potential function Φ, sketch both the Ψ and Φ lines.

27- The velocity potential of a 2-D flow is: $\Phi=kxy$, Find and sketch the stream lines Ψ.

28- The velocity potential of a 2-D flow is: $\Phi=y+x^2-y^2$, Find and sketch the stream lines Ψ.

29- Show that the 2-D flow: $\Psi = x+2x^2-2y^2$ is irrotational. What is the velocity potential Φ.

30- Find the exact equation for the stream lines Ψ of a flow of water around a 90^o solid corner if the velocity at the point (0,4) = +3 m/s. sketch both the Ψ and Φ lines.

References

1. White, F. M., *Fluid Mechanics*, 2nd Ed., McGraw-Hill, New York, 1986.

2. Streeter, V. L., *Fluid Dynamics*, McGraw-Hill, New York, 1948.

3. Rouse, H., *Advanced Mechanics of Fluids*, Wiley, New York, 1959.

4. Milne-Thomson, L. M., *Theoretical Hydrodynamics*, 4th Ed., Macmillan, New York, 1960.

5. Robertson, J. M., *Hydrodynamics in Theory and Application*, Prentice-Hall, Englewood Cliffs, N.J., 1965.

6. Panton, R. L., *Incompressible Flow*, Wiley, New York, 1984.

7. Li, W. H., and Lam, S. H., *Principles of Fluid Mechanics*, Addison-Wesley, Reading, Mass., 1964.

8. Schlichting, H., *Boundary-Layer Theory*, 7th Ed., McGraw-Hill, New York, 1979.

9. Fuller, D. D., *Theory and Practice of Lubrication for Engineers*, Wiley, New York, 1984.

10. Baker, A. J., *Finite Element Computational Fluid Mechanics*, McGraw-Hill, New York, 1983.

11. Peyret, R., and Taylor, T. D., *Computational Methods for Fluid Flow*, Springer-Verlag, New York, 1983.

12. Tannehill, J. C., Anderson, D. A., and Pletcher, R. H., *Computational Fluid Mechanics and Heat Transfer*, 2nd Ed., Taylor and Francis, Washington, D.C., 1997.

13. Carey, G. F., and Oden, J. T., *Finite Elements: Fluid Mechanics*, Prentice-Hall, Englewood Cliffs, N.J., 1986.

14. Brebbia, C. A., and Dominguez, J., *Boundary Elements: An Introductory Course*, McGraw-Hill, New York, 1989.

15. Moran, J., *An Introduction to Theoretical and Computational Aerodynamics*, Wiley, New York, 1984.

16. Thompson, J. F., Warsi, Z. U. A., and Mastin, C. W., *Numerical Grid Generation: Foundations and Applications*, North-Holland, New York, 1985.

17. Hall, E. J., and Pletcher, R. H., *Simulation of Time Dependent, Compressible Viscous Flow Using Central and Upwind-Biased Finite-Difference Techniques*, Technical Report HTL-52, CFD-22, College of Engineering, Iowa State University, 1990.

---

10 Some velocity measurements in a three-dimensional incompressible flow field indicate that $u = 6xy^2$ and $v = -4y^2z$. There is some conflicting data for the velocity component in the z direction. One set of data indicates that $w = 4yz^2$, and the other set indicates that $w = 4yz^2 - 6y^2z$. Which set do you think is correct? Explain.

11 The velocity components of an incompressible, two-dimensional velocity field are given by the equations

$$u = 2xy$$
$$v = x^2 - y^2$$

Show that the flow is irrotational and satisfies conservation of mass.

12 For each of the following stream functions, with units of m^2/s, determine the magnitude and the angle the velocity vector makes with the x-axis at $x = 1$ m, $y = 2$ m. Locate any stagnation points in the flow field.

(a) $\psi = xy$

(b) $\psi = -2x^2 + y$

13 The stream function for a certain incompressible flow field is

$$\psi = 10y + e^{-y} \sin x$$

Is this an irrotational flow field? Justify your answer with the necessary calculations.

14 The stream function for an incompressible, two-dimensional flow field is

$$\psi = ay^2 - bx$$

where a and b are constants. Is this an irrotational flow? Explain.

15 The velocity components for an incompressible, plane flow are

$$v_r = Ar^{-1} + Br^{-2} \cos\theta$$
$$v_\theta = Br^{-2} \sin\theta$$

where A and B are constants. Determine the corresponding stream function.

16 For a certain two-dimensional flow field

$$u = 0$$
$$v = V$$

(a) What are the corresponding radial and tangential velocity components? **(b)** Determine the corresponding stream function expressed in Cartesian coordinates and in cylindrical polar coordinates.

17 Make use of the control volume shown in Fig. P .17 to derive the continuity equation in cylindrical coordinates

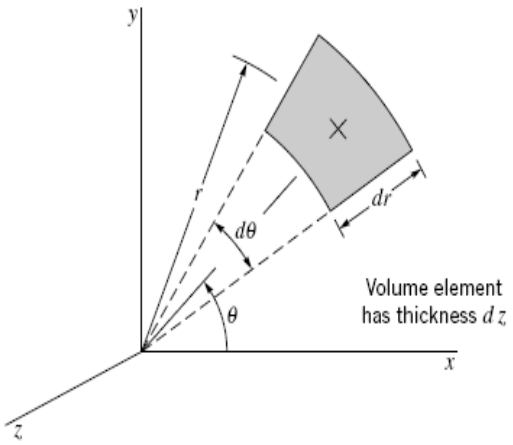

■ FIGURE P .17

18 It is proposed that a two-dimensional, incompressible flow field be described by the velocity components

$$u = Ay$$
$$v = Bx$$

where A and B are both positive constants. **(a)** Will the continuity equation be satisfied? **(b)** Is the flow irrotational? **(c)** Determine the equation for the streamlines and show a sketch of the streamline that passes through the origin. Indicate the direction of flow along this streamline.

19 In a certain steady, two-dimensional flow field the fluid density varies linearly with respect to the coordinate x; that is, $\rho = Ax$ where A is a constant. If the x component of velocity u is given by the equation $u = y$, determine an expression for v.

20 In a two-dimensional, incompressible flow field, the x component of velocity is given by the equation $u = 2x$. **(a)** Determine the corresponding equation for the y component of velocity if $v = 0$ along the x axis. **(b)** For this flow field, what is the magnitude of the average velocity of the fluid crossing the surface OA of Fig. P .20? Assume that the velocities are in feet per second when x and y are in feet.

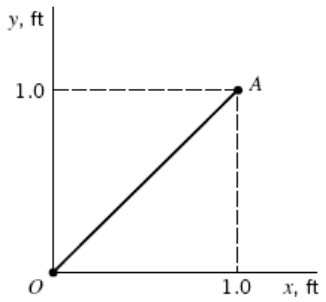

■ FIGURE P .20

21 The radial velocity component in an incompressible, two-dimensional flow field ($v_z = 0$) is

$$v_r = 2r + 3r^2 \sin\theta$$

Determine the corresponding tangential velocity component, v_θ, required to satisfy conservation of mass.

22 The stream function for an incompressible flow field is given by the equation

$$\psi = 3x^2y - y^3$$

where the stream function has the units of m^2/s with x and y in meters. **(a)** Sketch the streamline(s) passing through the origin. **(b)** Determine the rate of flow across the straight path AB shown in Fig. P .22.

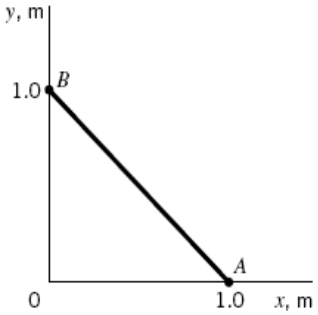

■ FIGURE P .22

23 The streamlines in a certain incompressible, two-dimensional flow field are all concentric circles so that $v_r = 0$. Determine the stream function for **(a)** $v_\theta = Ar$ and for **(b)** $v_\theta = Ar^{-1}$, where A is a constant.

24 The stream function for an incompressible, two-dimensional flow field is

$$\psi = 3x^2y + y$$

For this flow field, plot several streamlines.

25 The stream function for an incompressible, two-dimensional flow field is

$$\psi = 2r^3 \sin 3\theta$$

For this flow field, plot several streamlines for $0 \le \theta \le \pi/3$.

26 A two-dimensional flow field for a nonviscous, incompressible fluid is described by the velocity components

$$u = U_0 + 2y$$
$$v = 0$$

where U_0 is a constant. If the pressure at the origin (Fig. P .26) is p_0, determine an expression for the pressure at **(a)** point A, and **(b)** point B. Explain clearly how you obtained your answer. Assume that the units are consistent and body forces may be neglected.

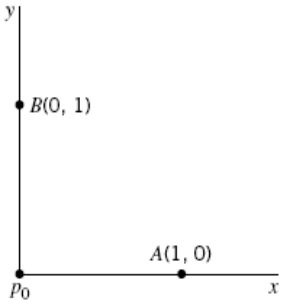

■ FIGURE P .26

27 In a certain two-dimensional flow field, the velocity is constant with components $u = -4$ ft/s and $v = -2$ ft/s. Determine the corresponding stream function and velocity potential for this flow field. Sketch the equipotential line $\phi = 0$ which passes through the origin of the coordinate system.

28 The velocity potential for a given two-dimensional flow field is

$$\phi = (\tfrac{5}{3})x^3 - 5xy^2$$

Show that the continuity equation is satisfied and determine the corresponding stream function.

29 Determine the stream function corresponding to the velocity potential

$$\phi = x^3 - 3xy^2$$

Sketch the streamline $\psi = 0$, which passes through the origin.

30 A certain flow field is described by the stream function

$$\psi = A\,\theta + B\,r\sin\theta$$

where A and B are positive constants. Determine the corresponding velocity potential and locate any stagnation points in this flow field.

31 It is known that the velocity distribution for two-dimensional flow of a viscous fluid between wide parallel plates (Fig. P .31) is parabolic; that is,

$$u = U_c\left[1 - \left(\frac{y}{h}\right)^2\right]$$

with $v = 0$. Determine, if possible, the corresponding stream function and velocity potential.

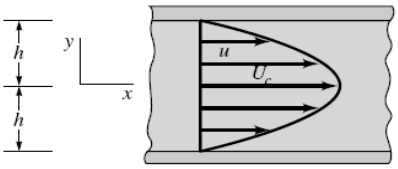

■ FIGURE P .31

32 The velocity potential for a certain inviscid flow field is

$$\phi = -(3x^2y - y^3)$$

where ϕ has the units of ft^2/s when x and y are in feet. Determine the pressure difference (in psi) between the points (1, 2) and (4, 4), where the coordinates are in feet, if the fluid is water and elevation changes are negligible.

6.33 Consider the incompressible, two-dimensional flow of a nonviscous fluid between the boundaries shown in Fig. P 33. The velocity potential for this flow field is

$$\phi = x^2 - y^2$$

(a) Determine the corresponding stream function. **(b)** What is the relationship between the discharge, q (per unit width normal to plane of paper), passing between the walls and the coordinates x_i, y_i of any point on the curved wall? Neglect body forces.

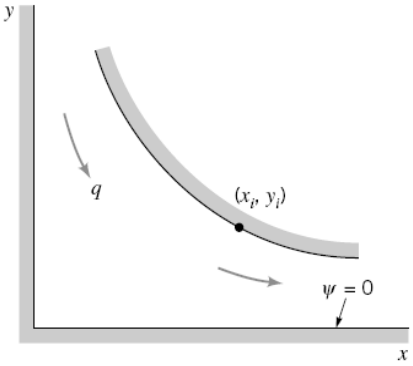

■ FIGURE P .33

34 The stream function for a two-dimensional, nonviscous, incompressible flow field is given by the expression

$$\psi = -2(x - y)$$

where the stream function has the units of ft^2/s with x and y in feet. **(a)** Is the continuity equation satisfied? **(b)** Is the flow field irrotational? If so, determine the corresponding velocity potential. **(c)** Determine the pressure gradient in the horizontal x direction at the point $x = 2$ ft, $y = 2$ ft.

35 In a certain steady, two-dimensional flow field the fluid may be assumed to be ideal and the weight of the fluid (specific weight = 50 lb/ft^3) is the only body force. The x component of velocity is known to be $u = 6x$ which gives the velocity in ft/s when x is measured in feet, and the y component of velocity is known to be a function of only y. The y axis is vertical, and at the origin the velocity is zero. **(a)** Determine the y component of velocity so that the continuity equation is satisfied. **(b)** Can the difference in pressures between the points $x = 1$ ft, $y = 1$ ft and $x = 1$ ft, $y = 4$ ft be determined from the Bernoulli equation? If so, determine the value in lb/ft^2. If not, explain why not.

36 The velocity potential for a certain inviscid, incompressible flow field is given by the equation

$$\phi = 2x^2y - (\tfrac{2}{3})y^3$$

where ϕ has the units of m^2/s when x and y are in meters. Determine the pressure at the point $x = 2$ m, $y = 2$ m if the pressure at $x = 1$ m, $y = 1$ m is 200 kPa. Elevation changes can be neglected, and the fluid is water.

37 **(a)** Determine the velocity potential and the stream function for a steady, uniform, incompressible, inviscid, two-dimensional flow that makes an angle of 30° with the horizontal x-axis. **(b)** Determine an expression for the pressure gradient in the vertical y direction. What is the physical interpretation of this result?

38 The streamlines for an incompressible, inviscid, two-dimensional flow field are all concentric circles, and the velocity varies directly with the distance from the common center of the streamlines; that is

$$v_\theta = Kr$$

where K is a constant. **(a)** For this *rotational* flow, determine, if possible, the stream function. **(b)** Can the pressure difference between the origin and any other point be determined from the Bernoulli equation? Explain.

39 The velocity potential

$$\phi = -k(x^2 - y^2) \qquad (k = \text{constant})$$

may be used to represent the flow against an infinite plane boundary, as illustrated in Fig. P .39. For flow in the vicinity of a stagnation point, it is frequently assumed that the pressure gradient along the surface is of the form

$$\frac{\partial p}{\partial x} = Ax$$

where A is a constant. Use the given velocity potential to show that this is true.

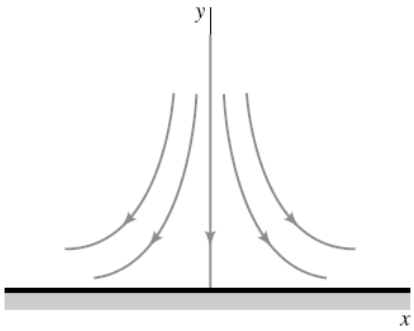

■ FIGURE P .39

40 Water flows through a two-dimensional diffuser having a 20° expansion angle, as shown in Fig. P .40. Assume that the flow in the diffuser can be treated as a radial flow emanating from a source at the origin O. **(a)** If the velocity at the entrance is 20 m/s, determine an expression for the pressure gradient along the diffuser walls. **(b)** What is the pressure rise between the entrance and exit?

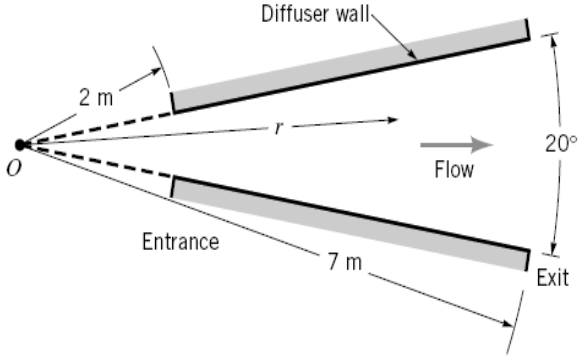

■ FIGURE P .40

41 An ideal fluid flows between the inclined walls of a two-dimensional channel into a sink located at the origin (Fig. P .41). The velocity potential for this flow field is

$$\phi = \frac{m}{2\pi} \ln r$$

where m is a constant. **(a)** Determine the corresponding stream function. Note that the value of the stream function along the wall OA is zero. **(b)** Determine the equation of the streamline passing through the point B, located at $x = 1$, $y = 4$.

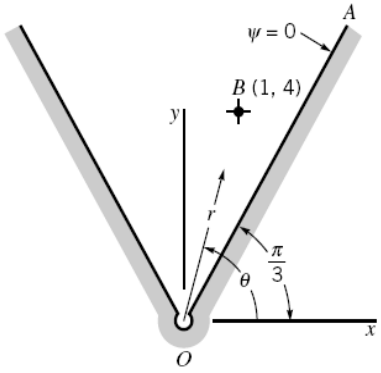

■ FIGURE P .41

42 It is suggested that the velocity potential for the flow of an incompressible, nonviscous, two-dimensional flow along the wall shown in Fig. P .42 is

$$\phi = r^{4/3} \cos \tfrac{4}{3}\theta$$

Is this a suitable velocity potential for flow along the wall? Explain.

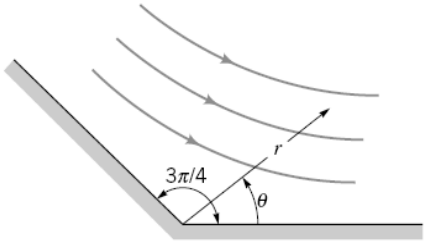

■ FIGURE P .42

43 As illustrated in Fig. P .43, a tornado can be approximated by a free vortex of strength Γ for $r > R_c$, where R_c is the radius of the core. Velocity measurements at points A and B indicate that $V_A = 125$ ft/s and $V_B = 60$ ft/s. Determine the distance from point A to the center of the tornado. Why can the free vortex model not be used to approximate the tornado throughout the flow field ($r \geq 0$)?

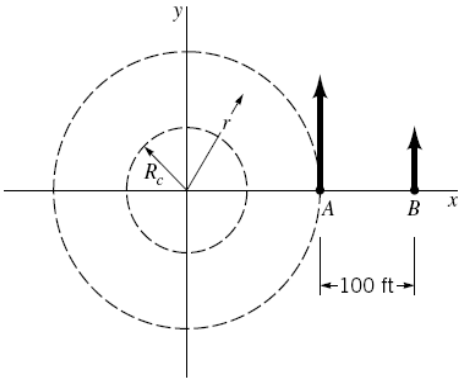

■ FIGURE P .43

44 The velocity distribution in a horizontal, two-dimensional bend through which an ideal fluid flows can be approximated with a free vortex as shown in Fig. P .44. Show how the discharge (per unit width normal to plane of paper) through the channel can be expressed as

$$q = C\sqrt{\frac{\Delta p}{\rho}}$$

where $\Delta p = p_B - p_A$. Determine the value of the constant C for the bend dimensions given.

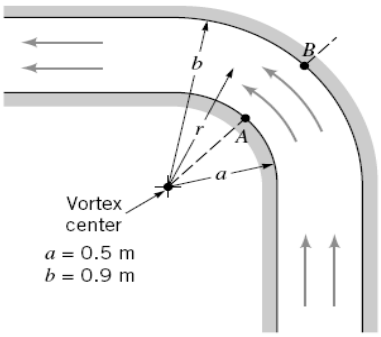

■ FIGURE P .44

45 When water discharges from a tank through an opening in its bottom, a vortex may form with a curved surface profile, as shown in Fig. P .45 and Video V .2. Assume that the velocity distribution in the vortex is the same as that for a free vortex. At the same time the water is being discharged from the tank at point A, it is desired to discharge a small quantity of water through the pipe B. As the discharge through A is increased, the strength of the vortex, as indicated by its circulation, is increased. Determine the maximum strength that the vortex can have in order that no air is sucked in at B. Express your answer in terms of the circulation. Assume that the fluid level in the tank at a large distance from the opening at A remains constant and viscous effects are negligible.

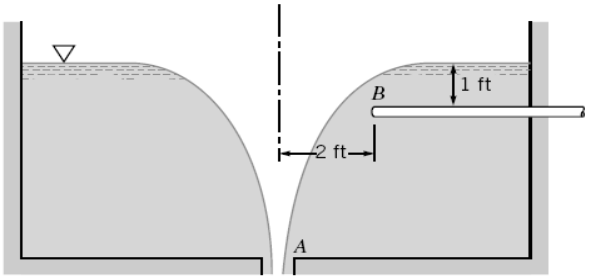

■ FIGURE P .45

46 The streamlines in a particular two-dimensional flow field are all concentric circles, as shown in Fig. P .46. The velocity is given by the equation $v_\theta = \omega r$ where ω is the angular velocity of the rotating mass of fluid. Determine the circulation around the path $ABCD$.

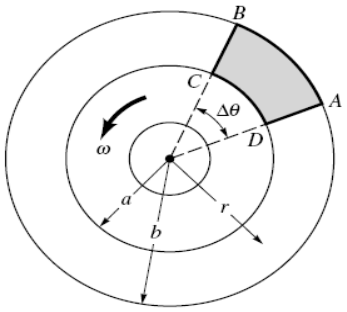

■ FIGURE P .46

47 Water flows over a flat surface at 4 ft/s, as shown in Fig. P .47. A pump draws off water through a narrow slit at a volume rate of 0.1 ft^3/s per foot length of the slit. Assume that the fluid is incompressible and inviscid and can be represented by the combination of a uniform flow and a sink. Locate the stagnation point on the wall (point *A*) and determine the equation for the stagnation streamline. How far above the surface, *H*, must the fluid be so that it does not get sucked into the slit?

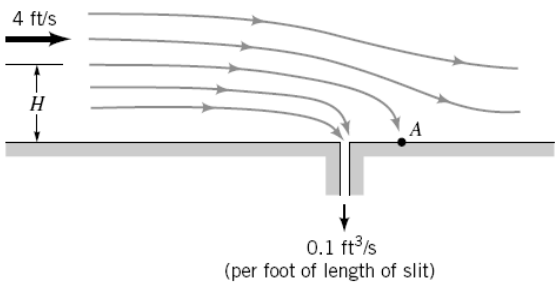

■ FIGURE P .47

48 Consider two sources having equal strengths located along the *x* axis at $x = 0$ and $x = 2$ m, and a sink located on the *y* axis at $y = 2$ m. Determine the magnitude and direction of the fluid velocity at $x = 5$ m and $y = 0$ due to this combination if the flowrate from each of the sources is 0.5 m^3/s per m and the flowrate into the sink is 1.0 m^3/s per m.

49 The velocity potential for a spiral vortex flow is given by $\phi = (\Gamma/2\pi)\,\theta - (m/2\pi)\,\ln r$, where Γ and m are constants. Show that the angle, α, between the velocity vector and the radial direction is constant throughout the flow field (see Fig. P .49).

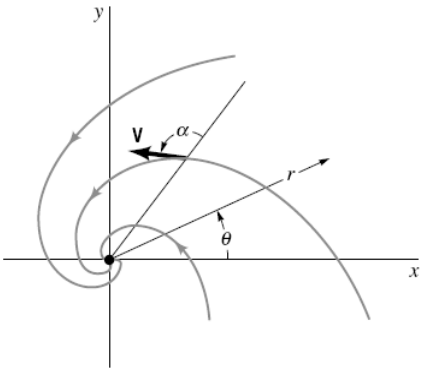

■ FIGURE P .49

50 For a free vortex (see Video V .2) determine an expression for the pressure gradient **(a)** along a streamline, and **(b)** normal to a streamline. Assume that the streamline is in a horizontal plane, and express your answer in terms of the circulation.

51 Potential flow against a flat plate (Fig. P 51*a*) can be described with the stream function

$$\psi = Axy$$

where *A* is a constant. This type of flow is commonly called a "stagnation point" flow since it can be used to describe the flow in the vicinity of the stagnation point at *O*. By adding a source of strength *m* at *O*, stagnation point flow against a flat plate with a "bump" is obtained as illustrated in Fig. P .51*b*. Determine the relationship between the bump height, *h*, the constant, *A*, and the source strength, *m*.

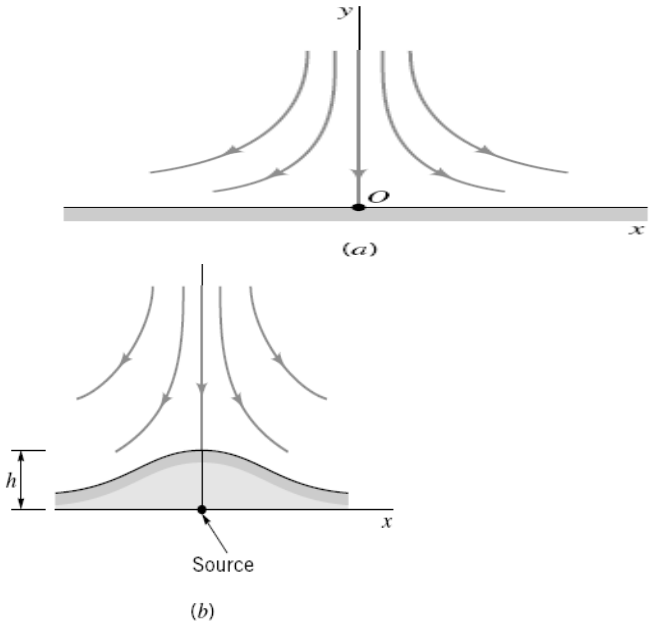

■ FIGURE P .51

52 The combination of a uniform flow and a source can be used to describe flow around a streamlined body called a half-body. (See Video V .3.) Assume that a certain body has the shape of a half-body with a thickness of 0.5 m. If this body is placed in an air stream moving at 15 m/s, what source strength is required to simulate flow around the body?

53 A body having the general shape of a half-body is placed in a stream of fluid. At a great distance upstream the velocity is *U* as shown in Fig. P .53. Show how a measurement of the differential pressure between the stagnation point and point *A* can be used to predict the free-stream velocity, *U*. Express the pressure differential in terms of *U* and fluid density. Neglect body forces and assume that the fluid is nonviscous and incompressible.

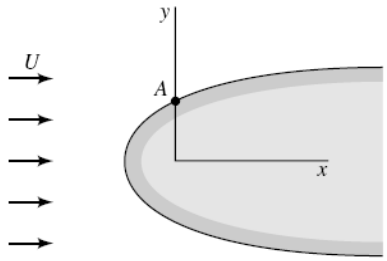

■ FIGURE P 53

54 One end of a pond has a shoreline that resembles a half-body as shown in Fig. P .54. A vertical porous pipe is located near the end of the pond so that water can be pumped out. When water is pumped at the rate of 0.08 m^3/s through a 3-m-long pipe, what will be the velocity at point *A*? *Hint*: Consider the flow *inside* a half-body. (See Video V .3.)

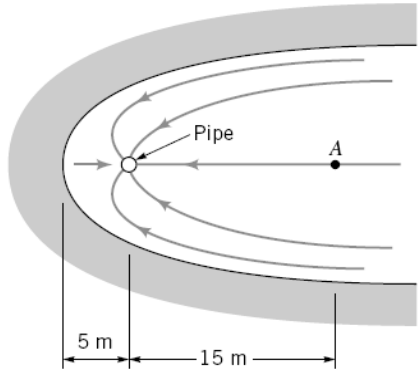

■ FIGURE P .54

55 For the half-body described in Section 3.2, show on a plot how the magnitude of the velocity on the surface, V_s, varies as a function of the distance, s (measured along the surface), from the stagnation point. Use the dimensionless variables V_s/U and s/b where U and b are defined in Fig. 3.24.

56 Consider a uniform flow with velocity U in the positive x direction combined with two free vortices of equal strength located along the y axis. Let one vortex located at $y = a$ be a clockwise vortex ($\psi = K \ln r$) and the other at $y = -a$ be a counterclockwise vortex, where K is a positive constant. It can be shown by plotting streamlines that for $Ua/K < 2$ the streamline $\psi = 0$ forms a closed contour, as shown in Fig. P 56. Thus, this combination can be used to represent flow around a family of bodies (called *Kelvin ovals*). Show, with the aid of a graph, how the dimensionless height, H/a, varies with the parameter Ua/K in the range $0.3 < Ua/K < 1.75$.

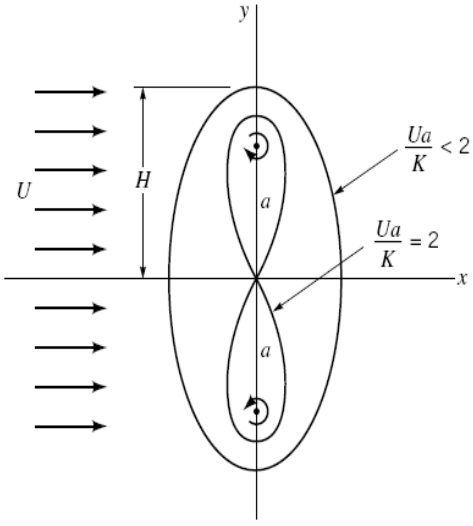

■ FIGURE P 56

57 A Rankine oval is formed by combining a source-sink pair, each having a strength of 36 ft^2/s and separated by a distance of 12 ft along the x axis, with a uniform velocity of 10 ft/s (in the positive x direction). Determine the length and thickness of the oval.

58 Make use of Eqs. 3.108 and 3.110 to construct a table showing how ℓ/a, h/a, and ℓ/h for Rankine ovals depend on the parameter $\pi Ua/m$. Plot ℓ/h versus $\pi Ua/m$ and describe how this plot could be used to obtain the required values of m and a for a Rankine oval having a specific value of ℓ and h when placed in a uniform fluid stream of velocity, U.

6.59 Assume that the flow around the long, circular cylinder of Fig. P .59 is nonviscous and incompressible. Two pressures, p_1 and p_2, are measured on the surface of the cylinder, as illustrated. It is proposed that the free-stream velocity, U, can be related to the pressure difference $\Delta p = p_1 - p_2$ by the equation

$$U = C\sqrt{\frac{\Delta p}{\rho}}$$

where ρ is the fluid density. Determine the value of the constant C. Neglect body forces.

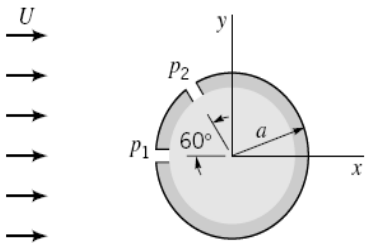

■ FIGURE P .59

60 An ideal fluid flows past an infinitely long, semicircular "hump" located along a plane boundary, as shown in Fig. P 60. Far from the hump the velocity field is uniform, and the pressure is p_0. **(a)** Determine expressions for the maximum and minimum values of the pressure along the hump, and indicate where these points are located. Express your answer in terms of ρ, U, and p_0. **(b)** If the solid surface is the $\psi = 0$ streamline, determine the equation of the streamline passing through the point $\theta = \pi/2$, $r = 2a$.

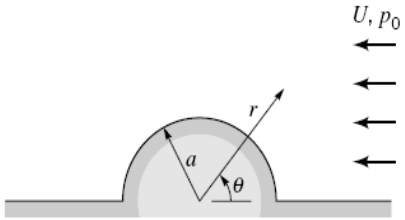

■ FIGURE P .60

61 Water flows around a 6-ft-diameter bridge pier with a velocity of 12 ft/s. Estimate the force (per unit length) that the water exerts on the pier. Assume that the flow can be approximated as an ideal fluid flow around the front half of the cylinder, but due to flow separation (see Video V .4), the average pressure on the rear half is constant and approximately equal to $\frac{1}{2}$ the pressure at point A (see Fig. P 61).

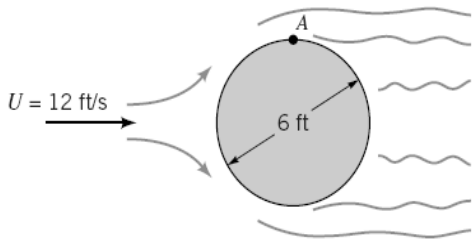

■ FIGURE P .61

62 Consider the steady potential flow around the circular cylinder shown in Fig. 3.23. On a plot show the variation of the magnitude of the dimensionless fluid velocity, V/U, along the positive y axis. At what distance, y/a (along the y axis), is the velocity within 1% of the free-stream velocity?

63 The velocity potential for a cylinder (Fig. P .63) rotating in a uniform stream of fluid is

$$\phi = Ur\left(1 + \frac{a^2}{r^2}\right)\cos\theta + \frac{\Gamma}{2\pi}\theta$$

where Γ is the circulation. For what value of the circulation will the stagnation point be located at: **(a)** point A, **(b)** point B?

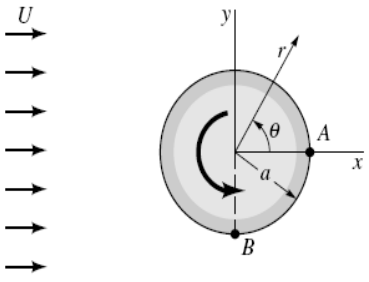

■ FIGURE P .63

64 A fixed circular cylinder of infinite length is placed in a steady, uniform stream of an incompressible, nonviscous fluid. Assume that the flow is irrotational. Prove that the drag on the cylinder is zero. Neglect body forces.

65 Repeat Problem .64 for a rotating cylinder for which the stream function and velocity potential are given by Eqs. 3.121 and 3.122, respectively. Verify that the lift is not zero and can be expressed by Eq. 3.128.

66 A source of strength m is located a distance ℓ from a vertical solid wall as shown in Fig. P 66. The velocity potential for this incompressible, irrotational flow is given by

$$\phi = \frac{m}{4\pi}\{\ln[(x-\ell)^2 + y^2] + \ln[(x+\ell)^2 + y^2]\}$$

(a) Show that there is no flow through the wall. **(b)** Determine the velocity distribution along the wall. **(c)** Determine the pressure distribution along the wall, assuming $p = p_0$ far from the source. Neglect the effect of the fluid weight on the pressure.

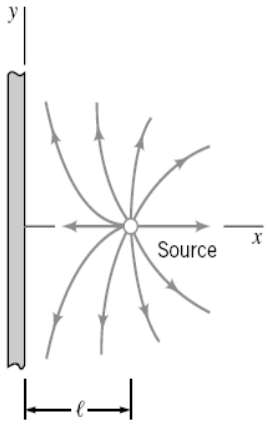

■ FIGURE P .66

67 A long, porous pipe runs parallel to a horizontal plane surface, as shown in Fig. P .67. The longitudinal axis of the pipe is perpendicular to the plane of the paper. Water flows radially from the pipe at a rate of 0.5 π ft^3/s per foot of pipe. Determine the difference in pressure (in lb/ft^2) between point B and point A. The flow from the pipe may be approximated by a two-dimensional source. *Hint*: To develop the stream function or velocity potential for this type of flow, place (symmetrically) another equal source on the other side of the wall. With this combination there is no flow across the x axis, and this axis can be replaced with a solid boundary. This technique is called the *method of images*.

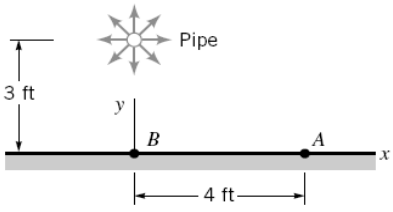

■ FIGURE P .67

68 At a certain point at the beach, the coast line makes a right angle bend, as shown in Fig. P 68*a*. The flow of salt water in this bend can be approximated by the potential flow of an incompressible fluid in a right-angle corner. **(a)** Show that the stream function for this flow is $\psi = A\,r^2 \sin 2\theta$, where A is a positive constant. **(b)** A fresh-water reservoir is located in the corner. The salt water is to be kept away from the reservoir to avoid any possible seepage of salt water into the fresh water (Fig. P 68*b*). The fresh-water source can be approximated as a line source having a strength m, where m is the volume rate of flow (per unit length) emanating from the source. Determine m if the salt water is not to get closer than a distance L to the corner. *Hint:* Find the value of m (in terms of A and L) so that a stagnation point occurs at $y = L$. **(c)** The streamline passing through the stagnation point would represent the line dividing the fresh water from the salt water. Plot this streamline.

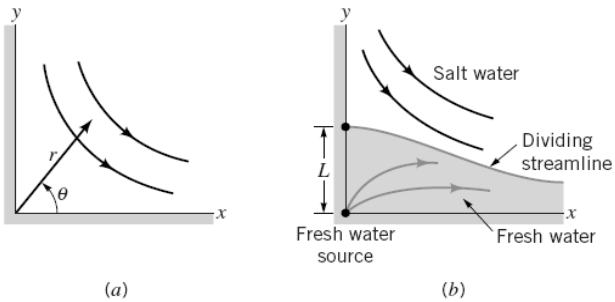

■ FIGURE P .68

69 The two-dimensional velocity field for an incompressible Newtonian fluid is described by the relationship

$$\mathbf{V} = (12xy^2 - 6x^3)\hat{\mathbf{i}} + (18x^2y - 4y^3)\hat{\mathbf{j}}$$

where the velocity has units of m/s when x and y are in meters. Determine the stresses σ_{xx}, σ_{yy}, and τ_{xy} at the point $x = 0.5$ m, $y = 1.0$ m if pressure at this point is 6 kPa and the fluid is glycerin at 20 °C. Show these stresses on a sketch.

70 Typical inviscid flow solutions for flow around bodies indicate that the fluid flows smoothly around the body, even for blunt bodies as shown in Video V .4. However, experience reveals that due to the presence of viscosity, the main flow may actually separate from the body creating a wake behind the body. As discussed in a later section (Section 9.2.6), whether or not separation takes place depends on the pressure gradient along the surface of the body, as calculated by inviscid flow theory. If the pressure decreases in the direction of flow (a *favorable* pressure gradient), no separation will occur. However, if the pressure increases in the direction of flow (an *adverse* pressure gradient), separation may occur. For the circular cylinder of Fig. P .70 placed in a uniform stream with velocity, U, determine an expression for the pressure gradient in the direction flow on the surface of the cylinder. For what range of values for the angle θ will an adverse pressure gradient occur?

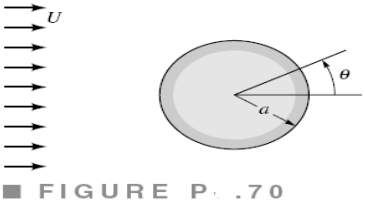

■ FIGURE P .70